FY20 Summary Report on the Received Level Analysis of Satellite Tagged Odontocetes at the Pacific Missile Range Facility

E. Elizabeth Henderson, NIWC Pacific
Cameron R. Martin, NIWC Pacific

Robin W. Baird, Cascadia Research Collective
Michaela A. Kratofil, Cascadia Research Collective

Stephen W. Martin, National Marine Mammal Foundation

Brandon L. Southall, SEA, Inc.

18 November 2021

REPORT DOCUMENTATION PAGE		***Form Approved*** **OMB No. 0704-0188**

Public reporting burden for this collection of information is estimated to average 1 hour per response, including the time for reviewing instructions, searching data sources, gathering and maintaining the data needed, and completing and reviewing the collection of information. Send comments regarding this burden estimate or any other aspect of this collection of information, including suggestions for reducing this burden to Washington Headquarters Service, Directorate for Information Operations and Reports, 1215 Jefferson Davis Highway, Suite 1204, Arlington, VA 22202-4302, and to the Office of Management and Budget, Paperwork Reduction Project (0704-0188) Washington, DC 20503.
PLEASE DO NOT RETURN YOUR FORM TO THE ABOVE ADDRESS.

1. REPORT DATE *(DD-MM-YYYY)* 18-11-2021	**2. REPORT TYPE** Monitoring report	**3. DATES COVERED** *(From - To)* 15 November 2020 - 28 November 2020

4. TITLE AND SUBTITLE FY20 SUMMARY REPORT ON THE RECEIVED LEVEL ANALYSIS OF SATELLITE TAGGED ODONTOCETES AT THE PACIFIC MISSILE RANGE FACILITY	**5a. CONTRACT NUMBER** N62470-15-D-8006
	5b. GRANT NUMBER
	5c. PROGRAM ELEMENT NUMBER

6. AUTHOR(S) E. Elizabeth Henderson Cameron R. Martin Robin W. Baird Michaela A. Kratofil Stephen W. Martin Brandon L. Southall	**5d. PROJECT NUMBER**
	5e. TASK NUMBER
	5f. WORK UNIT NUMBER

7. PERFORMING ORGANIZATION NAME(S) AND ADDRESS(ES) Naval Information Warfare Center, 53560 Hull Street, San Diego, CA 92152 Cascadia Research Collective National Marine Mammal Foundation SEA, Inc.	**8. PERFORMING ORGANIZATION REPORT NUMBER**

9. SPONSORING/MONITORING AGENCY NAME(S) AND ADDRESS(ES) Commander, U.S.Pacific Fleet, 250 Makalapa Dr. Pearl Harbor, HI	**10. SPONSOR/MONITOR'S ACRONYM(S)**
	11. SPONSORING/MONITORING AGENCY REPORT NUMBER

12. DISTRIBUTION AVAILABILITY STATEMENT
Approved for public release; distribution is unlimited

13. SUPPLEMENTARY NOTES

14. ABSTRACT
This report summarizes the development and application of substantially upgraded analytical methods to quantify the movement and diving behavior of satellite tagged odontocetes before, during, and after Submarine Command Course (SCC) training events at the Pacific Missile Range Facility (PMRF) off Kaua'i, Hawai'i, including their predicted exposure and potential response to mid-frequency active sonar (MFAS) during these events. Eleven short-finned pilot whales and seven rough-toothed dolphins were tagged between February 2011 and February 2019. These data had been previously analyzed using simpler, temporally coarser, two-dimensional MFAS received level (RL) estimations. Argos positions typically only occur once every few hours, limiting the number of RL estimates per animal using these earlier methods. In addition, the RLs were estimated for broad "shallow" and "deep" diving depth categories defined for each species, without integrating empirical measurements of diving behavior into the analysis. For this reanalysis effort, satellite tag data were re-processed through the Kalman smoothing algorithm, which compared to the previously used least-squares location data, provides greater temporal resolution in tracks and more robust estimates of positional uncertainty. Available positional data, including Fastloc GPS locations for some recent tags (including one new short-finned pilot whale and two common bottlenose dolphins tagged in 2020), were interpolated every 5-min using

Standard Form 298 (Rev. 8-98)
Prescribed by ANSI-Std Z39-18

the R-package crawl, and using dive data obtained from individual tags, dive depths were estimated at each of those 5-min locations. Further, 95% confidence interval error ellipses were calculated around each 5-min position, with multiple radials running from source locations through error ellipses in order to model transmission loss (TL) values (and thus estimate RLs) from the source to the far edge of the radial and to the seafloor. RL values were then derived for many points in the three-dimensional space within the error ellipse most likely to contain the animal at that time and around the estimated depth value in order to arrive at the most accurate possible modeled RL estimate (with associated variance estimates). A sub-set of data analyzed following the 100-imputed-track method utilized by Schick et al. (2019) yielded comparable results. The error ellipse method was thus applied here.

In addition to these more detailed RL analyses, the movement and dive behavior of the tagged odontocetes were examined relative to both phases of the SCC. Past analyses have focused only on Phase B, which includes the use of hull-mounted MFAS, as well as other sources of MFAS including helo dipping sonar and active sonobuoys. The initial part of the SCC, Phase A, does not include any of these sources or any surface-combatant vessels, but does include other surface and subsurface vessels and other active sonar sources that could potentially cause behavioral responses. Therefore, odontocete behavior herein was examined in five phases: (1) before Phase A; (2) during Phase A; (3) between phases A and B; (4) during Phase B; and (5) after phase B (when all of those periods were applicable for the tagged individual). Movement and dive behavior were also examined in the context of normal patterns, including diel and lunar cycles, in order to put the context of any potential response within the context of baseline behavioral variability. This framework can only be developed because of the high sample size and long-term effort that has been conducted off Kaua'i and the other Hawaiian Islands, and is an essential facet of behavioral response analyses. In this study, while there were statistical differences in dive behavior of all three species across the periods of the SCC, there were no apparent consistent patterns indicating broad, sustained responses to MFAS (e.g., large-scale habitat abandonment). In fact, there were often inter-individual differences in how dive behavior changed across periods, with some instances of behavioral changes more apparently related to the lunar cycle than to training activity.

ii

A quantitative analysis of fine-scale individual responses to evaluate potential behavioral changes as a function of range or RL (as conducted in some dedicated behavioral response studies) was not conducted here. However, there are a few instances where a behavioral response appeared to have occurred at a relatively coarse scale based on the timing of events and apparent movement, as individuals moved towards the region of activity on PMRF and then changed the direction of their travel away during a period of MFAS. However, there were also sharp changes in direction of travel during baseline and non-MFAS periods. A more detailed quantitative analysis may be able to tease apart these differences to determine what may constitute a behavioral response. Statistical methods utilizing comparable satellite-telemetered data such as those collected here are being developed in other studies and would be applicable to these data in the near future.

Although no overt, broadly evident behavioral responses seem to have occurred, there were several instances of animals occurring and apparently continuing to remain quite close to active ships. We estimate that these individuals received some of the higher levels of MFAS exposure yet documented for any marine mammal species. Although vastly improved over previous RL estimates there is still positional uncertainty in these data; while the highest median levels in these close exposure cases were approximately 175 dB re 1µPa, the median levels plus two standard deviations were around 195 dB re 1µPa, and maximum modeled levels exceeded 200 dB re 1µPa. While the probability of reaching those maximum levels was quite low, these results do indicate that in some cases odontocetes at PMRF may be experiencing very high RLs that could approach temporary or potentially even permanent threshold shift levels, provided animals experienced these conditions for some more extended exposure. There are further considerations regarding physiological stress responses even in the absence of behavioral response. All but two of the individuals included in this study have been determined to be part of the resident populations for these species. There is thus likely some degree of habituation that has occurred for these animals to the presence of MFAS, which may lead to a lack of strong behavioral responses. However, additional behavioral samples for most species and the potential for physiological or auditory impacts beyond behavior speaks to the need to continue these detailed tagging, behavior, and received level analyses for all odontocete species at PMRF. Such data will inform not only the short-term MFAS exposure and response questions relevant to U.S. Pacific Fleet monitoring objectives but are also relevant to addressing the long-term population level consequence objectives of understanding potential impacts to these animals.

15. SUBJECT TERMS
Monitoring, marine mammals, toothed whales, satellite tagging, passive acoustic monitoring, received level, Submarine Commanders Course, Hawaii Range Complex, Pacific Missile Range Facility

Submitted in support of the U.S. Navy's 2020 Annual Marine Species Monitoring Report for the Pacific

16. SECURITY CLASSIFICATION OF:			17. LIMITATION OF ABSTRACT UU	18. NUMBER OF PAGES 108	19a. NAME OF RESPONSIBLE PERSON Department of the Navy
a. REPORT Unclassified	b. ABSTRACT Unclassified	c. THIS PAGE Unclassified			19b. TELEPONE NUMBER (*Include area code*) 808-471-6391

STANDARD FORM 298 Back (Rev. 8/98)

Executive Summary

This report summarizes the development and application of substantially upgraded analytical methods to quantify the movement and diving behavior of satellite tagged odontocetes before, during, and after Submarine Command Course (SCC) training events at the Pacific Missile Range Facility (PMRF) off Kaua'i, Hawai'i, including their predicted exposure and potential response to mid-frequency active sonar (MFAS) during these events. Eleven short-finned pilot whales and seven rough-toothed dolphins were tagged between February 2011 and February 2019. These data had been previously analyzed using simpler, temporally coarser, two-dimensional MFAS received level (RL) estimations. Argos positions typically only occur once every few hours, limiting the number of RL estimates per animal using these earlier methods. In addition, the RLs were estimated for broad "shallow" and "deep" diving depth categories defined for each species, without integrating empirical measurements of diving behavior into the analysis. For this reanalysis effort, satellite tag data were re-processed through the Kalman smoothing algorithm, which compared to the previously used least-squares location data, provides greater temporal resolution in tracks and more robust estimates of positional uncertainty. Available positional data, including Fastloc GPS locations for some recent tags (including one new short-finned pilot whale and two common bottlenose dolphins tagged in 2020), were interpolated every 5-min using the R-package *crawl*, and using dive data obtained from individual tags, dive depths were estimated at each of those 5-min locations. Further, 95% confidence interval error ellipses were calculated around each 5-min position, with multiple radials running from source locations through error ellipses in order to model transmission loss (TL) values (and thus estimate RLs) from the source to the far edge of the radial and to the seafloor. RL values were then derived for many points in the three-dimensional space within the error ellipse most likely to contain the animal at that time and around the estimated depth value in order to arrive at the most accurate possible modeled RL estimate (with associated variance estimates). A sub-set of data analyzed following the 100-imputed-track method utilized by Schick et al. (2019) yielded comparable results. The error ellipse method was thus applied here.

In addition to these more detailed RL analyses, the movement and dive behavior of the tagged odontocetes were examined relative to both phases of the SCC. Past analyses have focused only on Phase B, which includes the use of hull-mounted MFAS, as well as other sources of MFAS including helo-dipping sonar and active sonobuoys. The initial part of the SCC, Phase A, does not include any of these sources or any surface-combatant vessels, but does include other surface and subsurface vessels and other active sonar sources that could potentially cause behavioral responses. Therefore, odontocete behavior herein was examined in five phases: (1) before Phase A; (2) during Phase A; (3) between phases A and B; (4) during Phase B; and (5) after phase B (when all of those periods were applicable for the tagged individual). Movement and dive behavior were also examined in the context of normal patterns, including diel and lunar cycles, in order to put the context of any potential response within the context of baseline behavioral variability. This framework can only be developed because of the high sample size and long-term effort that has been conducted off Kaua'i and the other Hawaiian Islands, and is an essential facet of behavioral response analyses. In this study, while there were statistical differences in dive behavior of all three species across the periods of the SCC, there were no apparent consistent patterns indicating broad, sustained responses to MFAS (e.g., large-scale habitat abandonment). In fact, there were often inter-individual differences in how dive behavior changed across periods, with some instances of behavioral changes more apparently related to the lunar cycle than to training activity.

A quantitative analysis of fine-scale individual responses to evaluate potential behavioral changes as a function of range or RL (as conducted in some dedicated behavioral response studies) was not conducted here. However, there are a few instances where a behavioral response appeared to have occurred at a relatively coarse scale based on the timing of events and apparent movement, as individuals moved towards the region of activity on PMRF and then changed the direction of their travel away during a period of MFAS. However, there were also sharp changes in direction of travel during baseline and non-MFAS periods. A more detailed quantitative analysis may be able to tease apart these differences to determine what may constitute a behavioral response. Statistical methods utilizing comparable satellite-telemetered data such as those collected here are being developed in other studies and would be applicable to these data in the near future.

Although no overt, broadly evident behavioral responses seem to have occurred, there were several instances of animals occurring and apparently continuing to remain quite close to active ships. We estimate that these individuals received some of the higher levels of MFAS exposure yet documented for any marine mammal species. Although vastly improved over previous RL estimates there is still positional uncertainty in these data; while the highest median levels in these close exposure cases were approximately 175 dB re 1µPa, the median levels plus two standard deviations were around 195 dB re 1µPa, and maximum modeled levels exceeded 200 dB re 1µPa. While the probability of reaching those maximum levels was quite low, these results do indicate that in some cases odontocetes at PMRF may be experiencing very high RLs that could approach temporary or potentially even permanent threshold shift levels, provided animals experienced these conditions for some more extended exposure. There are further considerations regarding physiological stress responses even in the absence of behavioral response. All but two of the individuals included in this study have been determined to be part of the resident populations for these species. There is thus likely some degree of habituation that has occurred for these animals to the presence of MFAS, which may lead to a lack of strong behavioral responses. However, additional behavioral samples for most species and the potential for physiological or auditory impacts beyond behavior speaks to the need to continue these detailed tagging, behavior, and received level analyses for all odontocete species at PMRF. Such data will inform not only the short-term MFAS exposure and response questions relevant to U.S. Pacific Fleet monitoring objectives but are also relevant to addressing the long-term population level consequence objectives of understanding potential impacts to these animals.

ACRONYMS

ANOVA	Analysis of variance
BARSTUR	Barking Sands Tactical Underwater Range
BSURE	Barking Sands Underwater Range Expansion
CEE	Controlled exposure experiment
CI	Confidence interval
CRC	Cascadia Research Collective
cSEL	Cumulative sound exposure level
DAR	Distance, Angle, Rate filter of the Douglas-Argos Filter
dB	decibel
GMT	Greenwich Mean Time
GPS	Global positioning system
IQR	Interquartile range
km	Kilometer
KS	Kalman smoothing
LC	Location quality class
LIMPET	Low Impact Minimally Percutaneous Electronic Transmitter
LS	Least-squares
m	Meter
MFAS	Mid-frequency active sonar
ONR	Office of Naval Research
PAM	Passive acoustic monitoring
PMRF	Pacific Missile Range Facility
PTS	Permanent threshold shift
RL	Received level
RMS	Root mean square
SCC	Submarine Command Course training event
SD	Standard deviation
SEL	Sound exposure level
SWTR	Shallow Water Training Range
TDR	Time-Depth Recorder tag
TL	Transmission loss
TTS	Temporary threshold shift
ULT	Unit-level training

Contents

Figures

Tables

1 INTRODUCTION

As part of their compliance with multiple Federal environmental laws and regulations (e.g. the Marine Mammal Protection Act and the Endangered Species Act), the U.S. Navy conducts and supports extensive monitoring of marine species across all range complexes. The focus of Navy monitoring efforts includes establishing a baseline of occurrence patterns, understanding the potential for exposure to mid-frequency active sonar (MFAS) or other sounds associated with Navy testing and training activity, and assessing any resulting behavioral responses to those exposures at both the individual level (short-term) and population level (long-term) (Navy ICMP, 2010; Booth et al. 2014). The focus on MFAS as a potential risk for marine mammals stems from multiple strandings of cetacean species (primarily beaked whales) that occurred after several multi-national naval training events near the Bahamas and elsewhere (e.g. Filadelfo et al. 2005; D'Spain et al. 2006; Cox et al. 2006). In Hawaiʻi, the Navy range complex includes the Pacific Missile Range Facility (PMRF), an instrumented underwater range off Kauaʻi that covers over 1100 km^2. Since PMRF is an area with frequent MFAS use, and since Navy scientists can access the underwater hydrophones to record marine mammal and anthropogenic activity, it is an ideal location to conduct opportunistic behavioral response studies of a variety of species exposed to real-world scenarios (e.g. Martin et al. 2015; Manzano-Roth et al. 2016; Henderson et al. 2019; Harris et al. 2019; Durbach et al. 2021). Such monitoring research is intended to better inform regulatory compliance measures specific to this area in particular, but also inform broader assessments of MFAS impacts on protected marine mammals.

Vessel-based field studies of odontocetes first began in the Kaulakahi Channel between Kauaʻi and Niʻihau in 2003 (Baird et al. 2003a) as part of a long-term, multi-species assessment of odontocetes in the main Hawaiian Islands (Baird et al. 2013; Baird 2016) being undertaken by Cascadia Research Collective (CRC). CRC efforts using satellite tags to assess movements and behavior of individual toothed whales on and around PMRF began in June 2008 in association with the Rim-of-the-Pacific naval training event (Baird et al. 2008a). Since 2008, CRC has had 14 additional vessel-based field projects off Kauaʻi. These studies have been focused on odontocete occurrence, potential for exposure to MFAS and associated received levels (RLs), and behavioral responses to MFAS for cetaceans that use all or part of the waters on PMRF. These studies have combined acoustic (e.g., Manzano-Roth et al. 2016) and boat-based methods (Baird et al. 2019a, 2019b). Studies of occurrence revealed the existence of resident populations of four species of odontocetes: rough-toothed dolphins (*Steno bredanensis*), common bottlenose dolphins (*Tursiops truncatus*, hereafter bottlenose dolphins), spinner dolphins (*Stenella longirostris*), and short-finned pilot whales (*Globicephala macrorhynchus*) (Albertson et al. 2016; Baird et al. 2008b, 2009, 2019a; Baird 2016).

Most of the field efforts examining key U.S. Pacific Fleet monitoring questions of marine mammal exposure and response have strategically occurred prior to the start of Submarine Command Courses (SCC), which are typically conducted on PMRF twice a year. Satellite tags that have been deployed on individuals of a number of odontocete species have remained attached and transmitting as designed through all or part of several SCCs. This has also allowed for novel assessments of increasing resolution of both exposure and response to MFAS for these species in this region (Baird et al. 2014, 2017, 2019b), directly addressing key U.S. Pacific Fleet monitoring objectives. Previous integrated occurrence, exposure, and response analyses have been conducted for 21 individuals of five species of odontocetes satellite tagged between 2011 and 2018: one bottlenose dolphin, one false killer whale (*Pseudorca*

crassidens), two melon-headed whales (*Peponocephala electra*), seven rough-toothed dolphins, and 11 short-finned pilot whales (Baird et al. 2014, 2017, 2019b). These assessments have included an integrated analysis of satellite-tag data, information on hull-mounted MFAS use, and acoustic propagation modeling. However, the focus was exclusively on the period of hull-mounted MFAS use, and didn't consider periods of other training activity that did not include hull-mounted MFAS.

In these previous analyses, RLs were estimated using several methods of increasing complexity and 2-D spatial resolution for each Argos satellite-derived location (and, in a few recent cases, Fastloc-GPS positions) of the tagged animals and any MFAS use that had occurred within 1-h of tag transmission from an estimated location. However, potential animal movements over this time difference were not considered. RLs during dives were estimated for discrete depth bins corresponding to "shallow" and "deep" dive categorical depths specific to each species, without applying information based on actual dive data recorded by some of the tags. While useful progressions from single point estimates used in earlier simplistic assessments, these methods, combined with the uncertainty in animal positions associated with Argos satellite telemetry, can lead to greater uncertainty in both estimated RLs and responses to exposure. Further, early analyses examined only exposure to high-power, surface-ship MFAS sources, while other MFAS sources (e.g., mid-power, helicopter-deployed, dipping sonars and sonobuoys), which may influence animal behavior (e.g., Falcone et al. 2017), were not considered.

However, analytical methods to assess animal positions along a satellite tag derived track have improved markedly over the last decade, allowing the track to be interpolated over pre-determined time steps and reducing the positional uncertainty along the track (Hooten et al. 2017). For example, Schick et al. (2019) modeled RLs for satellite tagged short-finned pilot whales and Cuvier's beaked whales (*Ziphius cavirostris*) whose resulting tracks had been interpolated at a five-minute resolution and smoothed using a continuous-time correlated random walk. In that study, in striving to account for the positional uncertainty inherent to satellite location data, 100 possible tracks were imputed for each tagged animal, and RLs were estimated at each imputed location (over depth) and then aggregated.

In our studies, an increasing proportion of satellite tags deployed have also recorded dive depths, allowing an inference of both horizontal and vertical positioning of tagged animals relative to MFAS exposure. Therefore, to begin applying and integrating these data in the 3D space in which the animals exist, a reanalysis was undertaken. Tag data from short-finned pilot whales and rough-toothed dolphins that were tagged with satellite-transmitting sensors on or near the PMRF range before SCC training events between February 2011 and August 2018 were reanalyzed using improved integrative methods in order to better estimate RLs in five-minute intervals and assess potential behavioral responses at this finer resolution. In addition, tags deployed on two bottlenose dolphins and a short-finned pilot whale in February 2020 were included in these analyses, as exposure and response for these individuals had not been previously examined. Data were separated into five periods for analysis: (1) Before any known transmissions; (2) During Phase A; (3) Between Phase A and Phase B; (4) During Phase B; and (4) After Phase B. Phase B is the period that includes surface ship hull-mounted MFAS and was the only focal "during" period in prior analyses. However, Phase A occurs first, and while there are no surface ship combatants with hull-mounted MFAS, there are other range support surface and subsurface vessels present, and other sources of anthropogenic noise that could elicit a behavioral response (e.g. Henderson et al. 2019; Jacobson et al. 2019). It is also important to note that there could be multiple vessels present during the Phase B period; this distinguishes the exposure scenario from single ship Unit Level Training exercises (ULTs) from dedicated Controlled Exposure and Behavioral Response

Experiments, during which a single ship or sonar-dipping helicopter is guided towards a focal animal(s) (e.g., Southall et al. 2019; 2021; Isojunno et al. 2020). Earlier analyses also used least-squared processed location data from Argos, while for this analysis we re-processed all of the earlier data through Kalman-smoothing, which provided increased numbers of locations as well as better estimates of error associated with them (Boyd and Brightsmith 2013; Lopez et al. 2015; Lowther et al. 2015). For one tag, a comparison was undertaken of RLs estimated following the methods developed by Schick et al. (2019) using 100 imputed tracks compared to RLs estimated using the 95% confidence interval error ellipse around each interpolated location. For all tags with available dive depth information, RLs were estimated at the depth predicted by the estimated ascent and descent rates based on the tag dive data, thereby providing more accuracy in the estimated three-dimensional RLs for each interpolated location. By applying these substantially improved and enhanced analytical approaches to not only the most recently collected data but also previously collected results, we now have a substantially robust data set for at least some species (e.g., pilot whales) to begin considering response implications in the context of exposure risk functions.

2 METHODS

2.1 TAG TYPES, PROGRAMMING, AND TAGGED INDIVIDUALS

Tags used during the study period (February 2011 – February 2020 SCC events) were all manufactured by Wildlife Computers (Redmond, Washington) and included Argos location-only tags (SPOT5), Argos location and dive depth transmitting tags (SPLASH10) and Argos location, Fastloc-GPS (Global Positioning System) location, and dive depth transmitting tags (SPLASH10-F). Tags were deployed in the Low Impact Minimally Percutaneous Electronic Transmitter (LIMPET) configuration, using either short (4.4 centimeter) or long (6.8 centimeter) darts (Andrews et al. 2008), depending on the species (e.g., short darts for rough-toothed dolphins and bottlenose dolphins and long darts for short-finned pilot whales). Tags were programmed to optimize the probability of obtaining behavior and location data during the periods spanning SCC events (days before, during, and after the SCC). Prior to each field effort, satellite pass predictions were undertaken using available Argos schedules. These were used to inform programming of daily transmission schedules, such that programmed transmission hours corresponded to those with greatest Argos satellite coverage, with hours spread throughout the 24-hour period to reduce temporal gaps between locations. In general, tags were programmed to transmit from 10 to 18 hours per day, although programming regimes varied by tag type, species tagged, and over the years as information accrued from successive deployments.

For instance, SPLASH10 tags were programmed to transmit for longer periods to maximize the likelihood of obtaining dive behavior data. Similarly, SPLASH10-F (Argos-GPS location tags) were programmed to transmit 17 hours/day and up to 900 times per day to optimize the opportunity for transmission of high-quality GPS locations. For SPLASH10-F tags, transmission of GPS locations were set as high priority and dive behavior was set as low priority, with a 6-day buffer. Dive behavior data and GPS locations were only collected up to 3-3.5 days following the scheduled end of the SCC in order to maximize throughput of both location and behavior data during the period of interest (i.e., before, during, and after the SCC). For tags that continued to transmit after these periods, this programming regime allowed prioritization of transmission of existing data rather than collection of new data, thereby minimizing gaps in location

and dive records during the periods of interest. SPLASH10 tags recorded the start and end time, maximum depth (with minimum/maximum estimates, taking into account the depth sensor accuracy of +/-1% of the reading), and minimum/maximum duration for any dive greater than the user-defined dive depth threshold, with depth readings of 3 meters (m) being used to indicate start/end times. The dive depth threshold value was increased over the years (2011, 2013: 20 m; 2014, 2015, 2016: 30 m; 2018, 2020: 50 m) to reduce gaps in the behavioral records (Quick et al. 2019). Because dive start/end times are bound by the 3 m depth setting, recorded dive durations are slightly negatively biased. Considering typical odontocete dive descent and ascent rates of 1 to 2 meters per second (m/s), recorded dive durations are likely only biased by 3 to 6 seconds. In addition to dive statistics, SPLASH10 tags transmitted the duration of "surface" periods (i.e., any period where the animal remained shallower than the specified dive depth value).

One (2013 through 2016) or two (2017 through 2020) shore-based Argos receiver stations were used to increase throughput of dive behavior data and GPS positions collected by SPLASH10 and SPLASH10-F tags. From 2013 through 2015, this included one (2013, 2014) to three (2015) Telonics TGA-100 7-element antennas, each connected to a Telonics TSUR-400 uplink receiver, connected to a laptop with data recorded using Telonics Uplink Logger v. 1.00. In 2016 (one) and from 2017 through 2020 (two), Wildlife Computers MOTEs (i.e. land-based receiving station) (Jeanniard-du-Dot et al. 2017) were used, which could subsequently be accessed by a Wildlife Computers interface. One system was at 456 m elevation on Mākaha Ridge, Kaua'i (22.13°N, 159.72°W), with directional antennas oriented to the north and southwest (2013 through 2020), and one system (2017, 2018, 2020) was at approximately 365 m elevation on the east side of Ni'ihau (21.95°N, 160.08°W), with one directional antenna oriented to the north and one omnidirectional antenna. In 2020, an Argos Goniometer was used onboard the research vessel when near tagged individuals to record tag transmissions for obtaining additional behavior data.

2.2 LOCATION DATA PROCESSING

Satellite-tag data streams obtained from the Argos System and shore-based receivers were processed through the Wildlife Computers Portal to generate diving and surfacing time series data as well as GPS locations from SPLASH10-F tags. Any messages detected by the Argos Goniometer during the February 2020 effort were decoded using the package *parsegonio* (Cioffi 2020) within the program R v4.0.1 (R Core Team 2020), and incorporated into tag datasets where applicable. Location data for all tags included in the study (short-finned pilot whale, n = 12; rough-toothed dolphin, n = 7; bottlenose dolphin, n =2) were processed through the Kalman smoothing algorithm (Lopez et al. 2015) via the Argos Data Collection and Location System to: (1) increase the number of locations (relative to previously least-squares processed location data used in Baird et al. 2014, 2017, 2019b); (2) generate more robust estimates of positional uncertainty (i.e., error ellipse measures); and (3) increase location accuracy relative to Kalman filtered positions (Lopez et al. 2015).

For the two GPS tags in this study (GmTag214, GmTag231), GPS locations were restricted to those with a residual error less than 35 (Dujon et al. 2014) and/or time error less than 10 seconds. GPS locations calculated from only four satellites tend to have poorer location accuracy than those calculated using at least five satellites (Bryant 2007; Dujon et al. 2014; Hazel 2009), and some studies have restricted analyses to GPS locations obtained from at least five or six satellite acquisitions (Lowether et al. 2015; Witt et al. 2010). However, applying this additional quality control criterion with the current dataset removes around 50% of GPS locations for both tags. Therefore, restricted GPS positions (residual < 35,

time error < 10 sec) were filtered through a general-purpose speed filter accessed through Movebank (Kranstauber et al. 2011), and increased error associated with locations generated from four satellites was accounted for in subsequent analyses (see movement modeling methods). The speed filter applied uses a 'simple outlier' method that tests the filter settings for each location against the previous position and subsequent positions. If neighboring locations require an implausible speed, then the location is marked as an outlier (Kranstauber et al. 2011). Speed filter parameters include maximum plausible speed (m/s) and maximum likely location error for tag type (m); parameters were set to 5 m/s (18 kilometers per hour, km/hr) and 1000 m, informed by travel speeds noted during field observations of short-finned pilot whales and GPS accuracy studies (Bryant 2007; Dujon et al. 2014; Hazel 2009), respectively.

Kalman-smoothed Argos locations were filtered to remove erroneous locations through the Distance, Angle, Rate (DAR) filter of the Douglas-Argos Filter (Douglas et al. 2012) accessed through Movebank (Kranstauber et al. 2011). The DAR filter identifies implausible locations based on extreme movement rates and unrealistic movement patterns (Douglas et al. 2012). User-defined settings were specified as follows: positions with a location quality class (LC) of 2 or 3 (highest quality) were exempt from filtering (KEEPLC); maximum redundant distance between successive locations (MAXREDUN) was set to 3 kilometers; rate coefficient or tolerance level for turning angles (RATECOEF) set to 25 (the default for marine mammals); and maximum sustainable movement rate (MINRATE) was set to 15 km/hr for short-finned pilot whales and 20 km/hr for rough-toothed dolphins and bottlenose dolphins based on travel speeds noted during field observations for each species, respectively. For the GPS tags, Kalman-smoothed positions were merged with restricted GPS positions and processed through the DAR. The DAR requires each position to have an assigned LC, and because GPS locations do not have traditional Argos LCs, these locations were assigned an LC of 3 (i.e., highest quality). Because DAR user settings were defined to automatically retain location classes 2 and 3, all GPS locations were exempt from removal.

For all dive depth transmitting tags (short-finned pilot whale, n = 8; rough-toothed dolphin, n = 4; bottlenose dolphin, n = 2), we examined behavior and tag status files to ensure the tags operated as intended and to check for any indication of pressure transducer failures that may have occurred during the deployment. Specifically, for validated status messages (i.e., those with "CRC" in the Type field) we reviewed the depth value recorded for each status message, which represents the last depth value recorded immediately prior to the tag transmitting a location. Depth values within 1-2 m of zero would be indicative of proper tag function because the animal must surface for a location to be transmitted, although some cases of extreme linear drift have been observed where a range of up to 10 m may be considered acceptable (R.D. Andrews, Marine Ecology and Telemetry Research, pers. comm.) Thus, we considered depth values exceeding ±10 m as a possible indication of pressure transducer failure. We also assessed values reported in the ZeroDepthOffset column, which represents the offset value that the tag applies to the depth sensor readings. We considered values that exceeded ± 9 m as instances of possible transducer failures. Lastly, we calculated minimum rates of ascent and descent, where extreme ascent/descent rates may be indicative of a pressure transducer failure. Ascent/descent rates were calculated by dividing twice the dive depth by the dive duration, and an average value of 2 m/s was used as a proxy for potential transducer issues.

Where multiple tags were deployed on the same species during the same field effort, we assessed whether individuals were acting in concert during the period of overlap by calculating the straight-line

distance between pairs of individuals for locations transmitted during a common satellite pass (approximately 15 minutes). Following Schorr et al. (2009) and Baird et al. (2010), we used both the mean distances and maximum distances between pairs of individuals to inform whether individuals were acting independently.

2.3 TRACK FITTING AND INTERPOLATION

After applying quality control measures, location data were projected (UTM 4N projection) and fit to a continuous-time correlated random walk model using the R package *crawl* v2.2.3 (Johnson et al. 2008; Johnson and London, 2018). By using this model, we were able to directly incorporate Argos error ellipse measures generated by the Kalman smoothing algorithm into location estimation, thereby accounting for positional uncertainty to better predict an animal's movement path (McClintock et al. 2014; Schick et al. 2019). This model also allowed us to estimate locations at regular time intervals.

In order to formulate the error model component of the *crawl* model, all observed locations must include some characterization of positional uncertainty (i.e., Argos LC or error ellipse). For the error model, we used Argos error ellipse metrics rather than Argos location quality classes, as they provide a more robust estimate of error specific to each location (McClintock et al. 2014). However, this information is not available for GPS positions; therefore, where applicable, GPS locations were assigned an error radius of 50 m if they were obtained from at least five satellites and 500 m if they were obtained from four satellites (Bryant 2007; Dujon et al. 2014; Hazel 2009).

Fitted models were used to predict each tagged individuals' location at 5-minute (min) intervals (also chosen by Schick et al. (2019)), to provide a better match with the temporal scale of sonar pulses during SCCs. Locations were predicted starting at the time of the first location of each individuals' deployment rounded to the nearest minute, as the exact timing of sonar pulses within each SCC is classified. Standard error values were estimated in the *x*, *y* plane oriented about each predicted position such that each position had a modeled error ellipse. To evaluate RL estimation methods with respect to effectively incorporating and representing positional uncertainty, we also imputed 100 tracks for GmTag081 such that each 5-min interval included 100 estimated locations (following Schick et al. 2019), as opposed to each location having a model-estimated error ellipse (see below for further details on these analyses methods). We then highlighted twelve sets of 5-min locations from the 100 imputed track data set in relation to the estimated crawl error ellipse (from single track) that represented a variety of ship-whale geometries and distances and for which we estimated RLs.

Due to the nearshore nature of the two bottlenose dolphins tagged during the February 2020 effort and the inherent accuracy of Argos locations, a number of locations were on land (TtTag034, 27 (12%) Douglas-filtered locations on land; TtTag035, 22 (6%) Douglas-filtered locations on land). Although the *crawl* modeled error ellipses for these land locations often extended into areas in-water, and hence would be viable for RL estimation, to ensure that more of the RL estimates would be usable from the error ellipse radials, we re-routed segments on land using the fix_path() function within the *crawl* package (Johnson et al. 2008; Johnson and London 2018). Briefly, this function identifies segments of a predicted trajectory intersecting with land (polygon), and then applies a least-cost algorithm and model-fitted parameters to generate new segments around the land area. This function defaults to re-routing tracks directly along the coastline; consequently, re-routed segments were often in waters much shallower than what we would expect these dolphins to use. In order to better suit the purposes of this

study and increase the number of locations successfully re-routed around land, the function's source code was modified to push crawl tracks farther offshore from the coastline (barrier buffer value = 1000 m for both tags; see https://github.com/NMML/crawl for source code). It should be noted that this function is still in beta-development, and outcomes of this function may generate brief segments requiring artificial high speeds or other unlikely movement patterns. Nevertheless, we deemed this approach more appropriate for our study purposes as locations on land were known to be incorrect.

2.4 SOURCE-RECEIVER GEOMETRY DEVELOPMENT

Overlap between tagged animal locations modeled with *crawl* and surface ship hull-mounted MFAS transmissions were determined by utilizing classified ship positional information (updated every 1 second) and classified passive acoustic monitoring (PAM) localized MFAS transmissions. As a note, ship activity most frequently occurred on the Barking Sands Underwater Range Expansion (BSURE) portion of the PMRF range (Figure 2.5.1-1). The methods to systematically determine geometries between ships (even when not transmitting MFAS) and animals has been previously utilized to investigate exposures for passive acoustically derived baleen whale tracks for U.S. Pacific Fleet monitoring efforts (e.g. Martin et al. 2020), with a focus on minke whale (*Balaenoptera acutorostrata*) movement behavior before and during Navy training activity (Durbach et al. 2021).

Ship positional data and localized MFAS transmissions that occurred closest in time with a maximum time difference less than or equal to 1 second, were less than or equal to 400 m apart, and met frequency thresholds were linked. Times from these exposure data were then examined relative to animal location times to determine overlap. An MFAS transmission that occurred closest in time to an animal location time was linked to a specific animal location only once, thus preventing estimating RLs more than once per animal from a single unique ping. These data were then summarized in 5-min intervals based on the time of the first and last animal tag position. In each 5-min interval, the distance and the animal's orientation relative to the angle off the bow is known for each overlapping ship (both with and without sonar), and the RL from each MFAS transmission can be estimated. However, due to security considerations and the appreciable amount of time required for propagation modeling, the exposure data in each 5-min interval were down sampled. Down sampling was done by determining the first MFAS transmission from each ship closest in time to each 5-min animal position, and only utilizing the one closest in distance (i.e. highest RL) to the animal for further analysis and RL estimation. While this MFAS transmission may not be the absolute closest in distance to each 5-min animal position, the biases to the estimated RLs (which vary based on the ship's speed, distance from the animal, and difference in ping time relative to the animal update time) are negligible unless a ship is within a few hundred meters of an animal.
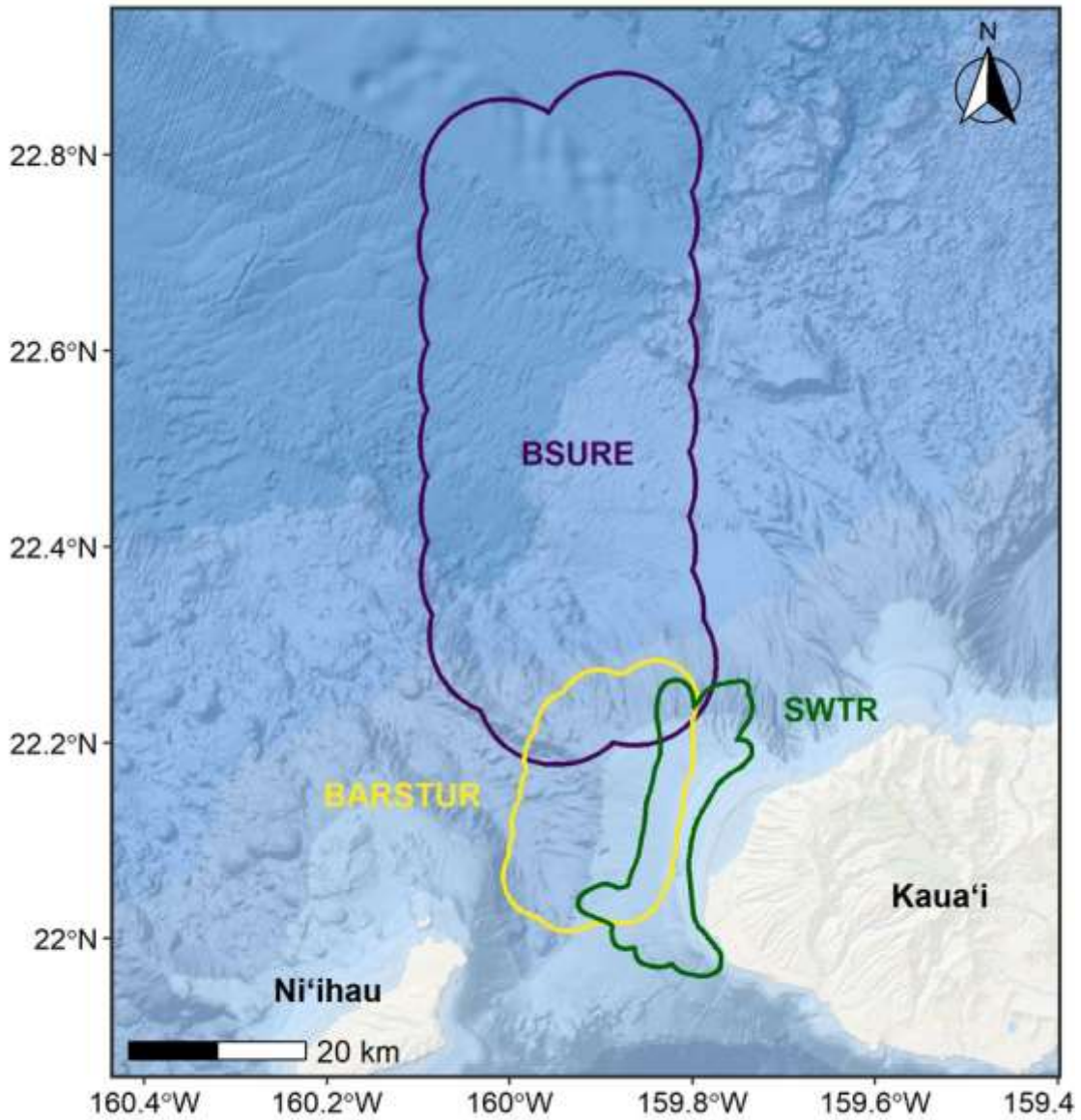
Figure 2.5.1-1. Map of the Pacific Missile Range Facility's three regions of the underwater range outlined. The Barking Sands Underwater Range Expansion (BSURE) is outlined in purple, the Barking Sands Tactical Underwater Range (BARSTUR) is outlined in yellow, and the Shallow Water Training Range (SWTR) is outlined in green. Ship activity primarily occurs on BSURE, but animals are considered to be on the range if they overlap with any portion of the range.

2.5 RECEIVED LEVEL ESTIMATION

To estimate RLs from a single MFAS exposure from U.S. Navy MFAS training at PMRF requires the location of the source at the time of sonar transmission (known accurately as previously described) and the location of the animal (estimated with error), characteristics of the acoustic source, and a robust acoustic propagation model utilizing environmental factors (e.g. bathymetry, surface conditions, sound velocity profiles) to estimate the transmission loss (TL) from the source to the animal location. We utilized the *crawl* 5-min tag locations and estimated the RL for each exposure using 3D (depth, range and azimuth angle) information. The use of *crawl*-derived tracks with 5-min resolution provided fixed time intervals over the duration of the track, which provided the fourth (time) dimension for the estimated exposure levels. Unlike previous analyses of RL for satellite tagged cetaceans at PMRF, for which we estimated RLs along a single radial with a fixed radius around the animal's position, in the current analysis we utilized the positional error generated by the *crawl* model for each 5-min interpolated position. The error at each interpolated position is less than what is typically associated with Argos locations, since the *crawl* model can take into account both previous and future Argos locations (and associated errors) when developing the smoothed track.

The Peregrine propagation model utilized is a range dependent parabolic equation-based model developed by Oasis Ltd (Heany and Campbell 2016) coded in the C programming language and is based upon the Range-dependent Acoustic Model (Collins 1993). The estimated RLs are derived from the MFAS source level and the propagation modelled TL from the source to the whale locations. Surface ducted propagation is common in the PMRF area, where the TL is lower in the near surface regions due to the sound velocity profile effectively trapping some sound in the near surface duct. This surface duct is explicitly accounted for in this propagation model.

The propagation model was run for radial (azimuthal) slices from the source location to animal locations over the full depth regime using 10 log-spaced frequencies to both reduce single frequency constructive/destructive interference effects as well as better representing the bandwidth of the MFAS transmissions. Full depth was considered 5400 m for the majority of the study area near the PMRF range, and is represented by 600 depth bins of 9 m each in the Peregrine outputs. The maximum ranges for each exposure in the propagation modelling were defined as the maximum distance of the animals' potential locations from the source, and were represented in the Peregrine model outputs as 1000 range bins with each bin being 1/1000th of the maximum range. One propagation model run is required for each azimuth angle utilized and provides a 2D (depth vs. range) estimated TL. Combining multiple 2D azimuthal slices to potential animal locations provides a 3D representation of the sound field (depth/range/azimuth angle). The 3D data were further refined by utilizing animal depth information, either provided by the tag or as two depth regimes when no dive depth can be inferred from the tag data. Each species was assigned a maximum and typical dive depth (short-finned pilot whales 1700 m/500 m; bottlenose dolphins 800 m/300 m; and rough-toothed dolphins 500 m/100 m). When tag dive depth data were available, a band for that depth was utilized based on either being near the surface (< 54 m depth) or at the dive depth with a ± percentage of the dive depth when deeper than 54 m. When no animal depth was available, two regimes of depths were utilized: a shallow depth consisting of depths from the surface to 54 m; and the region past 54 m to the species' typical dive depths. Tags with dive depth sensors can have periods with no dive data available, and tags without dive sensors can provide times animals were at the surface based upon the tags' Argos satellite acquisition attempts or times when transmissions were received on the Motes.

2.5.1   3D Received Level Estimation Method Comparison

Two different methods were considered to take into account the location uncertainty of the interpolated animal track positions. Both methods made use of the Peregrine propagation model as described above and the *crawl* 5-min tracks. The first was based upon Schick et al.'s (2019) method of generating 100 imputed tracks and then using a propagation model to estimate the RL over depth at each of the 100 imputed positions for every 5-min location with an MFAS exposure. This method is analogous to dropping 100 pins at each location and then estimating the RL over depth at each pin to sample the RLs for a single sonar transmission. We treated each imputed location independently and ran the propagation model regardless of how close in azimuth angle the imputed locations were, resulting in this method being computationally expensive, requiring us to model the sound propagation along 100 radials for every 5-min track location. This method also only utilizes a small percentage of the propagation modeled TLs, which are utilized to estimate the RL at each animal's imputed location. The model computes the full field (depth vs. distance) from the source to the animal location, of which only the single distance bin at each of the 100 imputed points is utilized, along with the vector of RLs for each depth bin, to derive the estimated RL (i.e. 100 sets of RL vectors over depth).

Therefore, we also explored a new method, taking advantage of each single crawl track with accompanying standard errors in the x and y dimensions to define a 95% confidence interval error ellipse to represent the animal location uncertainty. The animal location uncertainty area was then sampled with radial slices taken systematically in azimuth across the error ellipse for each 5-min location error ellipse area with a sonar exposure. We utilized both methods for representative samples of the various relative geometries of twelve, 5-min positions from one pilot whale track (GmTag081) in order to compare resulting RL estimates and computation time, with the plan to move forward with the remainder of the data using the method that best captured the potential field of RLs around each animal's position. Following the methods outlined in Schick et al. (2019), we ran propagation model radials to each of the 100 imputed tag locations for the 12 positions utilizing depth bins of 9 m. In this case, only the final range bins were retained, representing the animal's location at that imputation to create vectors of RL values from the surface to the seafloor. Schick et al. (2019) modeled RLs in depth bins of 10-m from the surface to the sea floor at each imputed location, creating vectors of RL values that varied in length depending on the depth at each location. Each propagation model run provided 2D results (full depth vs. distance), which were subsequently combined with all of the 2D results for each exposure to provide the 3D estimated RL samples for all depths.

The new method for dealing with the whale location uncertainty utilized the single *crawl* 5-min track's latitude and longitude locations as the centers of error ellipses, which were defined by scaling the standard error values provided by *crawl* for each location by a factor of 1.96, representing the 95% confidence interval (CI) for the animal location in x and y. Note that other CI's, e.g. 99%, could also be utilized if desired. Intersection of the radials from the source through the 95% CI ellipse define the x-y spatial sampling of potential animal locations for each exposure. Given the full range of geometric conditions (i.e., size of the animal location uncertainty ellipse coupled with distance from the source), equally-spaced azimuth angles were made through the ellipse, and the TL was estimated along each of these slices. Three different cross range resolutions were utilized to deal with the broad range of geometric situations (e.g., source close with large and small animal location uncertainty, distant source with both large and small animal location uncertainties). The cross-range resolutions were defined by the separation of the azimuthal slices at the center of the animal's error ellipse with three values utilized

to cover all geometric situations of 50 m, 200 m, and 500 m. These setting resulted in a minimum of 5 radials up to approximately 50 radials for each error ellipse, compared to the 100 radials required to model each imputed point. The output range binning was held constant for each ellipse by running the propagation model for each slice to the maximum range for that slice, with the model's output range bins being $1/1000^{th}$ the maximum range. In the situations where the source ship is located inside the error ellipse of the animal a slightly different approach was taken, utilizing 36 azimuthal angles with 10 degree spacing to sample the full range of possible animal locations. Since each range bin's depth vector within the error ellipse contributes to the estimated 3D RL solution there can be potentially tens of thousands of range-depth samples. Combining all of the 2D azimuthal slices through the error ellipse provides a 3-D estimated RL for each exposure over the entire water column.

Table 2.5.1 provides details for six examples of 95% CI error ellipses from three different short-finned pilot whale tags for different source-receiver geometries and whale location uncertainties. Figure 2.5.1-1 provides plan views of the relative x-y geometry for these six examples showing the 95% CI error ellipses and the azimuthal slices through the error ellipses.

Table 2.5.1. Details of six example exposures from three different pilot whales analyzed using the error ellipse method for short-finned pilot whales, including details of the exposure (Tag ID, date/time, dive depth) along with details of the major parameters in the propagation modeling: number of slices per error ellipse with slice spacing, distances from the source to the potential animal locations, and resulting estimated RLs. These ellipses are also depicted in Figure 2.5.1.

Tag ID/ Exposure number	Date	Time (GMT)	Dive Depth	# slices / angle step (deg)	Distances (km) min/center/max	Est RL (dB re 1 µPa) Median (-/+ 2*SD)	Est RL SD (dB re 1 µPa)
GmTag083 (a)	2/18/2014	23:25:00	NA [1]	23 / 0.57	44.2/49.8/55.5	143.2 (135.4-150.9) [1]	3.9 [1]
GmTag083 (b)	2/20/2014	08:50:00	NA [1]	29 / 1.9°	3.7/6/8.4	160.8 (153.7 – 167.9) [1]	3.6 [1]
GmTag082 (c)	2/20/2014	09:00:00	<54m	24 / 4.4°	0.48/2.6/4.7	170.1 (159.6 – 180.6)	5.2
GmTag081 (d)	2/20/2014	06:30:00	93.5 m	33 / 2°	4.8/12.5/20.2	150.8 (139.6 – 162.1)	5.6
GmTag081 (e)	2/20/2014	20:20:00	<54m	5 / 0.39°	28.2/29.1/30.1	142.3 (138.2 – 146.5)	2.1
GmTag083 (f)	2/20/2014	08:45:00	NA [1]	36 / 10°	0.01 / 1.7/4.44	176.6 (158 – 195.2) [1]	9.3 [1]

[1] Tag did not provide dive depth information (location-only tag), the <54 m depth assumption is presented in the table for the estimated RLs.
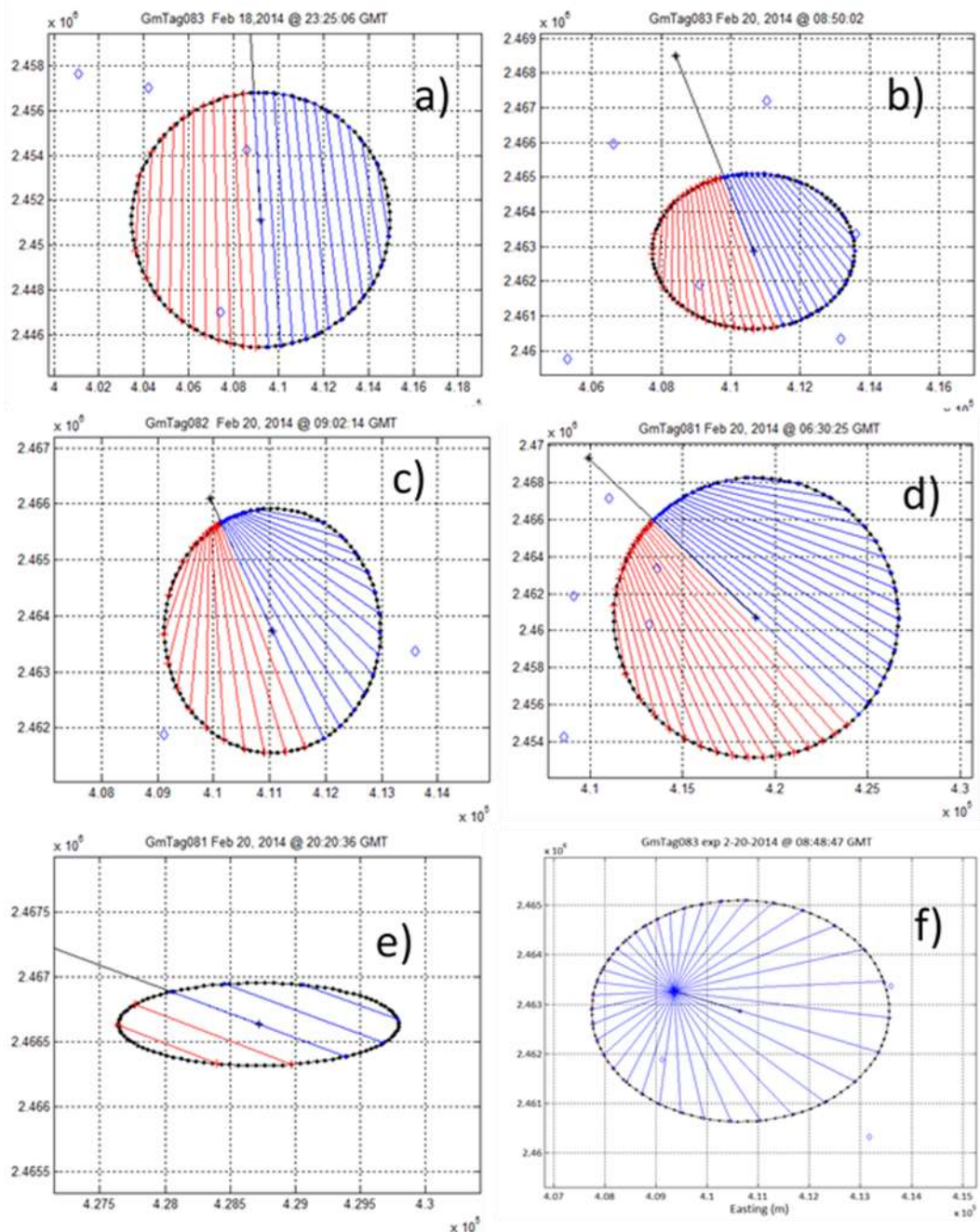
Figure 2.5.1-1. Six representative exposures with the animals' error ellipse intersections with slices from the source as plan views in the northing and easting coordinate system (scales vary with each plot). Blue diamonds indicate approximate hydrophone locations, while the animals' 95% CI error ellipses are shown in black with radial slices through each ellipse as red and blue lines. a) source 49 km from the center of the error ellipse, with 23 radial slices and an 11 km range extent; b) source 6 km from center of ellipse, with 29 slices and a 4.7 km range extent; c) source 2.6 km from center of ellipse, 24 radial slices, and a range extent of 4.2 km; d) source 12.5 km from center of ellipse, 33 radial slices, and a 15.2 km range extent; e) source 29 km from center of ellipse, with 5 slices and a range extent of 0.9 km; f) source within the animal's error ellipse and 1.35 km from the center of the ellipse, with 36 radial slices, and range extent 4.4 km.

2.5.2   Dive Behavior Model Development

In previous efforts, although dive statistics were analyzed for the Before (which included Phase A), During (Phase B only), and After periods of the SCC, all Argos or GPS locations only had RLs estimated at one or two simple depth bins, a surface bin (10 m ± 5 m) and a dive bin (rough-toothed dolphins – 50 m ± 5 m, short-finned pilot whales – 500 m ± 5 m). This created a disconnect between potential changes in dive behavior and the estimates of RL. Therefore, in this analysis we wanted to estimate RLs at the actual dive depth of the tagged animals at each 5-min location, when dive data were available. However, dive data are not recorded continuously, and only the dive shape, maximum depth, and duration are recorded. Therefore, models needed to be developed that took that information and recreated ascent and descent rates and bottom time periods, in order to capture instantaneous dive depths as accurately as possible.

For the short-finned pilot whales, there was data from 11 previously deployed CRC Time-Depth Recorder (TDR) tags that provided a continuous record of dive data (see Baird et al. 2003). These data were analyzed using the R package *diveMove* (Luque 2007), which categorizes the start of the descent, end of the descent/start of bottom time, end of bottom time/start of ascent, and total dive duration. From those data, ascent and descent rates could be calculated, and the dive shape could be generated based on the definitions from Wildlife Computers (i.e., Square-shaped dives had bottom times of greater than 50% total dive time; V-shaped dives had bottom times less than 20% of total dive time; and U-shaped dives had bottom times between 20 and 50% of total dive time). Using the dive shapes, minimum, mean, and maximum two-way travel times were calculated for each of the dives from the eight satellite-tagged short-finned pilot whales at PMRF whose tags included dive data. Then those times were compared to the ascent and descent rates calculated from the TDR tags, and the closest two-way travel times were used to estimate the dive depth at each 5-min interpolated location, based on the start and end times of each dive as well as the maximum dive depth.

There was no pre-existing TDR data for the bottlenose dolphins or rough-toothed dolphins, so although a similar process was used, there was no data on ascent and descent rates to use as reference. Rather, the minimum, mean, and maximum possible bottom times were estimated based on the dive shapes and then the two-way travel times were calculated from the remainder of dive duration after subtracting those bottom times. This often led to unrealistically fast ascent and descent rates (e.g. up to 10 m/s) if the maximum calculated bottom time left short intervals for the ascent and descent periods, so the minimum two-way travel time was always selected and used to estimate the dive depth.

There were also occasional gaps in the dive data. However, whenever satellite uplinks were attempted (even if they failed), the timestamp of the attempt was recorded, and this record was used to determine when the animals were at the surface during these gaps. These data could also be used to determine surface periods for tags without a dive record. If a 5-min interpolated position happened in the same minute as an uplink attempt, the animal was presumed to be at the surface. If an uplink happened a minute before or after the 5-min position, the animal was assumed to be within the top 54 m based upon dive rates. In all other cases of missing dive data, including the animals with tags that did not include dive data, RLs were estimated in both the surface (depths down to 54 m) and from 54 m down to the species' typical dive depths. To capture the uncertainty that still existed around the modeled dives depths, rules were established to estimate the variations of the dive depths used to calculate RLs. If the animal was assumed to be at the surface or within the top 54 m, RLs were calculated between the surface and 54 m. If dive depths were estimated to be between 54 and 100 m, the depth bin width was

calculated as the dive depth -/+ 0.2*dive depth. If the dive depth was estimated to be between 100 and 400 m, the depth bin width was calculated as the dive depth -/+ 0.1*dive depth. Finally, if the dive depth was estimated to be greater than 400 m, the depth bin width was calculated as the dive depth -/+ 0.05*dive depth. This method was chosen so that RLs at each depth were not represented by a single value but over some range, and the percentages decrease with depth to prevent that variability around the depth from getting too large as depth values increased. For cases where the species dive depth was greater than the seafloor in the azimuthal slices, those x-y estimated RLs are indeterminate and not included in the 3D estimated RL. For short-finned pilot whales, no exposures occurred where all possible 95% CI whale location depths were greater than the seafloor depths. However, this was the case for several of the nearshore bottlenose dolphin locations, where several segments of crawl tracks were re-routed around land, as well as some rough-toothed dolphin locations in depths less than 54 m.

Finally, due to some propagation modeling related issues, some TL values were not included in the analysis (i.e. only a proportion of the TL values were used to estimate the 3D RLs). A steep depression (vertical) angle issue can occur where angles are too steep (e.g., an animal 100 m from a source and at 200 m depth) and therefore TL cannot be computed. While Peregrine can be set up to utilize steeper depression angles, it comes at a large expense of the time to execute. For this study, if the propagation angle is steeper than 45 degrees, the estimates are not included in the full 3D estimate. In addition, estimated TLs associated with levels near the seafloor sometimes provide unrealistic TLs (e.g., > 300 dB) due to the model's internal and output resolutions when dealing with the seafloor. As such the bottom two depth bins above the seafloor for each range sample were dropped if dive depths included these bins. For each exposure, the ratio of 3D estimated RL samples utilized in the estimate over the total number of 3D estimated RL values (i.e., ignoring effects such as land, near seafloor effects, and near the propagation model steep angle limit) were calculated, and serve as a diagnostic metric.

2.5.3 Final Received Level Estimation

To summarize the updated methods used to estimated RLs, the closest-in-time MFAS ping from every ship present for each 5-min interpolated location were selected for analysis, and then the closest in distance/most intense ping of those was carried forward to be modeled. For each of these pings, the distance between the source and the 5-min location was calculated, and either 100 radials were modeled to each of 100 imputed points for that location (for a single tag, GmTag081), or a select number of radial slices were taken through an error ellipse that captured the 95% CI for each *crawl*-modeled location. The TL along each of these radials was calculated for the full slice distance and from the surface to the seafloor; however, the actual transmission values used for analysis were truncated to either the locations of each 100 imputed points or to the slices within each error ellipse. The TL values were further truncated to a pre-determined depth bin size around the modeled (or assumed) dive depths at each 5-min location to create a 3D volume of TL values around the best-estimated location of the tagged animal. These TL values were subtracted from the nominal source level of each MFAS source (e.g., 235 dB re 1 µPa rms for the hull-mounted 53C sonar) to derive the estimated RLs, and any indeterminate values (e.g., from the radial hitting land or the dive being deeper than the bathymetry at that location) were discarded from the 3D volume. Finally, the median RL values were extracted from the 3D volume around each location and are presented below along with 2 times the standard deviation to provide a measure of the breadth of estimated levels.

2.6 BEHAVIORAL RESPONSE ASSESSMENTS

For the response component of this study, we developed narratives for each tagged animal describing their movements in relation to MFAS use and estimated RLs. In previous assessments (i.e., Baird et al. 2014, 2017, 2019), behavioral responses to MFAS exposure were assessed by comparing movements relative to the range/source and dive statistics among periods before, during, and after MFAS use. Those efforts focused on the portion of the SCC that includes surface ship hull mounted MFAS transmissions (Phase B). The preceding portion of the SCC (Phase A) does not include surface ship hull mounted MFAS transmissions and surface ship combatants are not present. However, activity during Phase A of the SCC may elicit a response from tagged resident whales/dolphins. Therefore, in this study we compared movement patterns among all phases for each individual where data was available: 1) before (pre-Phase A), 2) Phase A, 3) between (inter-phase A-B), 4) Phase B (MFAS use), and 5) after (post-Phase B). Likewise, for individuals that were tagged with a SPLASH10 or SPLASH10-F tag, we calculated various dive and surfacing behavior statistics (e.g., median dive duration, median dive depth, dives per hour, etc.) among phases to assess potential responses to MFAS exposure in their diving behavior. Because gaps in the transmission of dive/surfacing data are common (resulting in incomplete dive/surfacing data), we calculated the percentage of coverage of dive and surfacing data during each phase to provide an indication on the robustness of comparisons among phases. In addition, we attempted to account for known dynamic drivers of dive and surfacing behavior (e.g., diel patterns, lunar light levels; Owen et al. 2019, Shaff & Baird, 2021) by separating comparisons by time of day (i.e., day or night). For all dive/surfacing behavior comparisons, only 3 days of data following the end of Phase B (i.e., post-Phase B) were used where available. Kruskal-Wallis one-way ANOVA tests were conducted to identify significant differences in dive depth and duration among phases, and by night/day period, for each tagged individual with sufficient dive/surfacing coverage (SPLASH10 tags only), and post-hoc Dunn's tests were conducted to identify phases where pairwise significant differences were detected (e.g., statistical difference between phase A and B; significance level for both tests = 0.05). These statistical procedures were not applied to summaries on dive rates (dives per hour) nor percentage of time at surface due to the nature of how these values were calculated (i.e., only single values for each SCC phase).

3 RESULTS

3.1 SATELLITE TAGGED CETACEANS

All of the tag data obtained in 2014 through 2020 were utilized in the following analyses of received level and movement and dive behavior (Table 3.1.1). At the time of this report, the propagation modeling results were not available for the SCCs from 2011 and 2013 and therefore those tags were excluded from the analyses from this point forward.

Table 3.1.1. Satellite tag data used in exposure/response analyses. Information on the percentage increase from earlier analyses using Least-squares (LS) data is included with new Kalman smoothing (KS) of tag location data.

Tag ID	Tag type	SCC	% increase in locations from LS to KS	# 5-min crawl locations during Phase B	# days location data available				
					Pre-Phase A	Phase A	Inter Phase A-B	Phase B	Post-Phase B
GmTag049*	SPOT5	Feb 2011	13.5	181	0.0	0.0	0.0	0.6	30.3
GmTag050*	SPLASH10	Feb 2011	10.7	177	0.0	0.0	0.0	0.6	36.2
GmTag070*	SPLASH10	Feb 2013	8.5	802	4.9	2.2	3.3	2.6	6.8
GmTag080	SPOT5	Feb 2014	13.7	138	10.1	2.1	3.1	0.4	0.0
GmTag081[a]	SPLASH10	Feb 2014	13.3	811	9.1	2.1	3.1	2.7	8.7
GmTag082[a]	SPLASH10	Feb 2014	40.3	805	3.3	2.1	3.1	2.7	19.1
GmTag083[a]	SPOT5	Feb 2014	18.0	814	3.3	2.1	3.1	2.7	77.8
GmTag115	SPOT5	Feb 2015	37.3	870	3.1	2.9	2.5	1.4	0.0
GmTag152[b]	SPLASH10	Feb 2016	14.1	863	0.0	0.0[b]	2.2	2.9	10.7
GmTag153[b]	SPLASH10	Feb 2016	13.8	862	0.0	0.0	2.1	2.9	10.9
GmTag214	SPLASH10-F	Aug 2018	14.2	80	0.0	0.0	2.5	0.2	20.2
GmTag231	SPLASH10-F	Feb 2020	16.6	969	3.4	2.2	4.2	3.0	2.7
SbTag002[c]*	SPOT5	Aug 2011	6.7	799	3.5	4.1	0.1	2.6	2.1
SbTag003[c]*	SPOT5	Aug 2011	3.9	799	3.6	4.1	0.1	2.6	8.1
SbTag010*	SPLASH10	Aug 2013	8.3	609	5.9	2.3	2.5	2.0	0.6
SbTag014	SPOT5	Feb 2015	9.8	1107	7.0	2.9	2.5	2.1	7.1
SbTag015	SPLASH10	Feb 2015	14.3	1108	0.2	2.9	2.5	2.1	6.6
SbTag017	SPLASH10	Feb 2016	12.5	862	0.0	0.0	1.4	2.9	5.3
SbTag018	SPLASH10	Feb 2016	13.2	877	0.0	0.0	1.4	2.9	12.7

Tag ID	Tag type	SCC	% increase in locations from LS to KS	# 5-min crawl locations during Phase B	# days location data available				
					Pre-Phase A	Phase A	Inter Phase A-B	Phase B	Post-Phase B
TtTag034[d]	SPLASH10	Feb 2020	12.9	863	0.0	0.0	3.4	3.0	7.2
TtTag035[d]	SPLASH10	Feb 2020	17.3	863	0.0	0.0	1.8	3.0	15.3

[a,b,c,d]Pseudoreplicate pairs/groups (i.e., not independent)

* Not carried forward in RL or exposure/response analyses as the propagation modeling results were not yet available

Re-processing satellite tag location data through the Kalman smoothing algorithm (Lopez et al. 2015) increased the number of Argos locations relative to previously used least-squares algorithm for all deployments (Table 3.1.1; 3.9 percent to 40.3 percent increase; median = 13.5 percent increase). Imputing positions at a 5-min interval increased the number of locations available for RL estimation by over 90 percent for all tags included in this reanalysis, compared to the number of locations available for previous RL estimates (see Baird et al. 2014, 2017, 2019b) (Table 3.1.1). This allowed us to obtain more samples for RL estimation for tags that had limited temporal overlap with periods of MFAS use (i.e., GmTag080, GmTag115) or were deployed during shortened SCC events (i.e., GmTag214).

3.2   RECEIVED LEVEL ESTIMATES

3.2.1   Propagation Modeling Methodology Comparison

A dozen locations were selected from the track of pilot whale GmTag081 to compare the two methods of estimating a field of RLs around a *crawl* interpolated position. These 12 locations were chosen as they represented different source-whale geometric situations, with differing distances and spatial extents of the error area. In addition, GmTag081 included a fairly complete dive record, allowing us to examine the RLs in 3D. Figure 3.2.1-1 illustrates one MFAS transmission time and one set of imputed location points and the associated 95% CI error ellipse. The 95% CI ellipse captured 91 of these 100 imputed points; a 99% CI error ellipse would have captured 99 of these 100 imputed points.
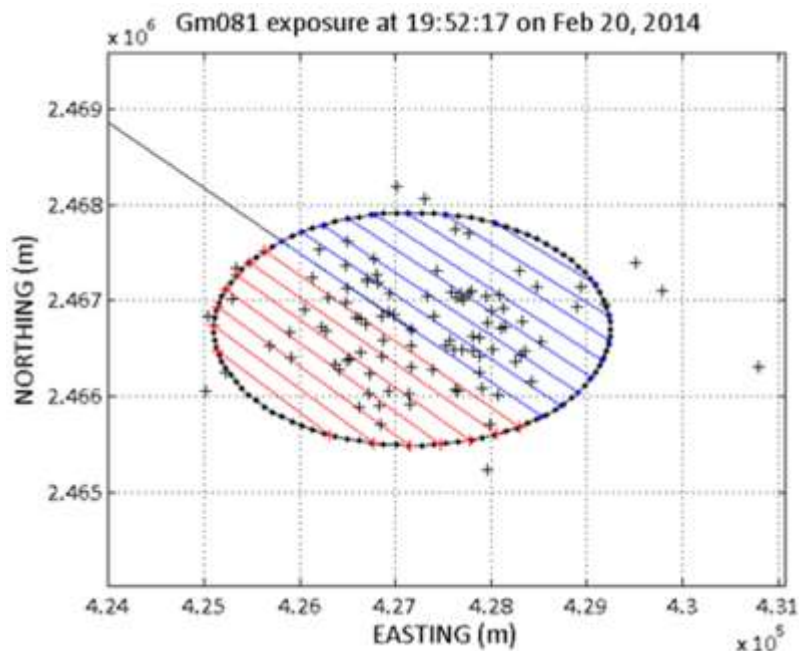
Figure 3.2.1-1. GmTag081 exposure 2/20/2014 19:52:17 GMT showing 95% confidence interval error ellipse with 15 radials from source to whale location and 100 imputed crawl locations indicated by black '+' symbols. The source is located 32.2 km to the NW of the center of the whales 95% CI error ellipse.

The exposure highlighted in Figure 3.2.1-1 included dive data that indicated the whale was in the upper 50 m of the water column. The Peregrine propagation model therefore utilized six depth bins (surface to

54 m with 9 m depth binning). The 100 imputed locations sample size for this exposure was 600 samples (100 x-y locations by six depth bins each). In comparison, the 15 radials from the source through the 95% CI error ellipse had a total sample size of 5,860 due to the much larger number of x-y locations systematically sampled. Histograms of the resulting RLs for the two methods from the exposure depicted in Figure 3.2.1-1 are given in Figure 3.2.1-2. The mean estimated RLs are within 1 dB re 1 µPa of each other, with similar standard deviations (2.0 dB re 1 µPa for the error ellipse and 2.5 dB re 1 µPa for the 100 imputed points). The imputed points do include samples outside of the 95% CI error ellipse, which accounts for the estimated RLs under 142 dB re 1 µPa (Figure 3.2.1-2).
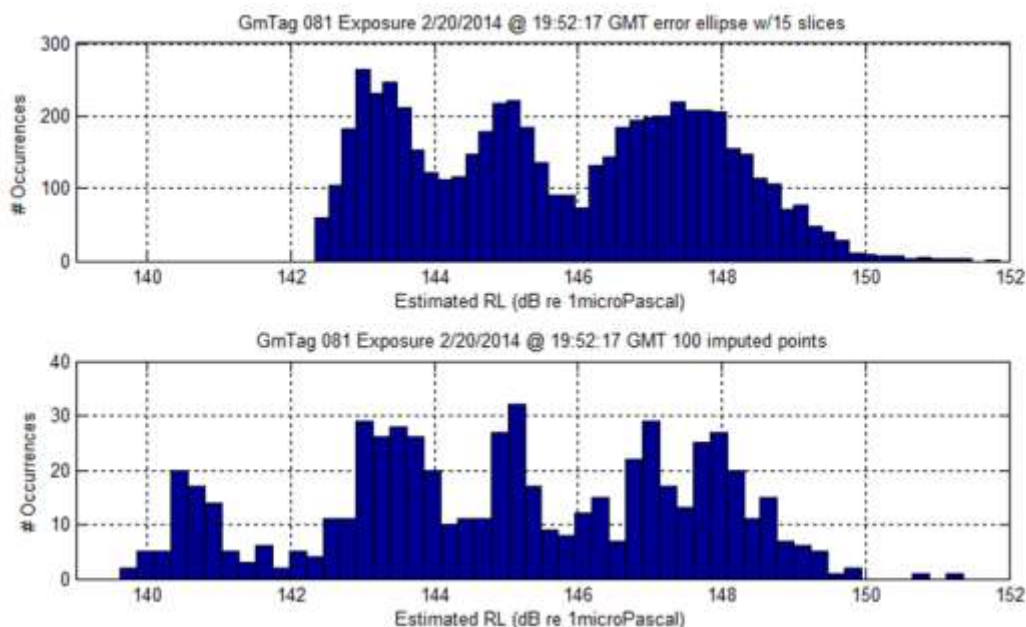
Figure 3.2.1-2. Histograms of the 3D RLs for the Gm081 exposure on 2/20/2014 @ 19:52:17 GMT depicted in Figure 3.2.1. The top plot shows the resulting values from the 15 radial slices with a mean estimated RL of 145.7 dB re 1 µPa (SD 2.07dB re 1 µPa, max/min 151.8/142.3 dB re 1 µPa). The bottom plot shows the resulting values from the 100 imputed points with a mean estimated RL of 145.0 dB re 1 µPa (SD 2.5 dB re 1 µPa, max/min 151.35 dB re 1 µPa/ 139.6 dB re 1 µPa).

To provide insight into the RL estimation process, one azimuth full depth vs. distance slice (#10 of 15) is depicted (Figure 3.2.1-3, left panel) for this exposure, illustrating the breadth of estimated RLs. The left panel shows the full depth, full range slice with the seafloor clearly visible as dark blue in the lower part of the image, with an upslope as distance increases. The dark blue on the left of the panel with an upslope towards the top left corner is an artifact of the propagation modeling, where the steep depression angle limited our ability to estimate valid TLs. Along this 'steep angle limit' the estimated RLs abruptly change from approximately 155 dB to < 125 dB re 1 µPa. The right panel of Figure 3.2.1-3 zooms into the region of the slice where the animal was most likely located, both within the animal's 95% CI error ellipse and in the upper 495 m of depth (approximating the typical dive depth for the species). The surface ducting is evident by the stronger RLs across the area for depth bins 1-5 with

19

consistently high RLs above 140 dB re 1 µPa. The complexity of the propagation at deeper depths down to the species' typical dive depth illustrates how the various multipaths can provide strongly multimodal distribution of the estimated RLs.
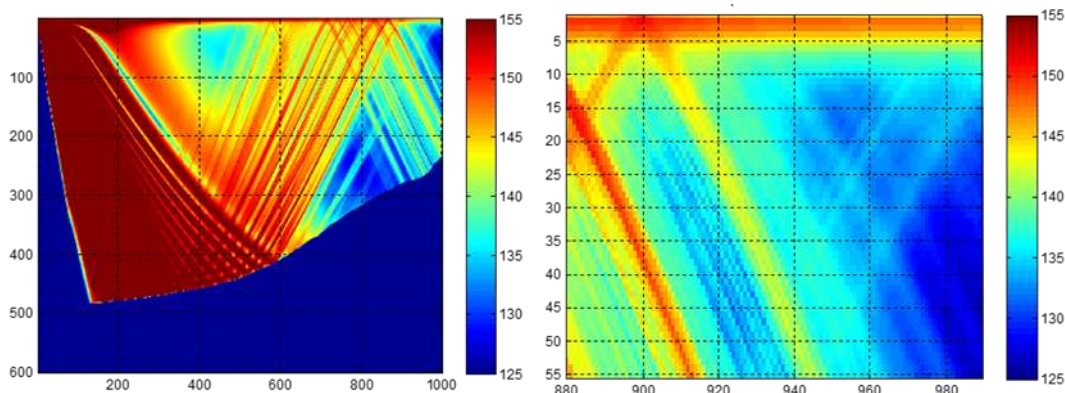
Figure 3.2.1-3. Example of estimated RLs for exposure 2-20-2014 @ 19:52:17 GMT slice 10. Both plots show the estimated RL in dB re 1 µPa SPL (value indicated by color bar) for depth vs. range – both plot axes are labeled by bin numbers (9 m per bin for depth and 32.2 m per bin for distance). The left pane is the full depth slice 10. The y-axis is depth from 0 to 5400 m with 9 m depth cell resolution, and the x-axis is the full range from 1 to 32.2 km with 32.2 m range cell resolution. The right pane zooms into a region of the left pane where the animal was most likely located. Complexity of the sound field clearly evident showing the near surface ducted layer (bins 1 to 5 in depth) and strong multipath components.

These different methodological approaches were found to be highly comparable in their RL results, with this particular exposure exhibiting a multi-modal estimate of RL, and with the 100 imputed point histogram reflecting samples at further distances than the 95% CI error ellipses. The error ellipse method was computationally less expensive (this sample exposure required 15 propagation model runs compared to 100 for all imputed points), provided a much larger sample size of estimated RLs, and covered nearly the same area as the 100 imputed locations. In addition, each new imputed set of points could potentially change the maximum/minimum estimated RLs depending upon exactly where the samples were located. Therefore, the error ellipse method was chosen to use for all remaining 21 tracks.

3.2.2 Individual Tag Results

Due to unforeseen delays from the COVID-19 pandemic in running the Peregrine propagation model for all tags, only a subset of the tags had a complete RL analysis included in this report (tags from 2014-2020). The summary statistics for these tags are highlighted in .

Table 3.2.1, including the number of 5-min locations that overlapped with down-sampled sonar ("exposures"), the number of those bins with dive depth information, the estimated RL grand mean, and the ranges of the median estimated RLs and the range of the median estimated RLs +/- 2*SDs. The latter was selected as the nominal presentation metric to convey the breadth and variability of the estimated.

Plots are provided for each tagged animal to consistently represent the median estimated RL +/- 2*SDs. Additional plots may be included to highlight issues associated with some of the resulting RL data (e.g., cases with potentially extremely high estimated RLs, cases where the median RL +/- 2*SDs are significantly different from the actual minimum and maximum estimated RLs, histograms of the 3D estimated RLs, etc.). The estimated median RL +/- 2*SD plots are presented in a timeline format to convey the temporal pattern of the exposures. Ancillary information is also available for each tag's dive data, including periods the animal was at the surface acquiring satellites or sending data to the Motes, as well as which estimated RL samples were not included (due to issues such as part of the error ellipse being located on land, under the seafloor, or at too steep of elevation angle from the source as discussed in the methods). These ancillary data are included in a table for each tagged animal.

Table 3.2.1. Overall estimated RL results by individual tagged animal.

Tag ID	# 5 min bins w/estimated RLs	# bins w/dive depth	Estimated RL grand mean (dB re 1µPa)	Range of estimated median RLs (dB re 1µPa)	Range of estimated median RLs +/- 2*SD (dB re 1µPa)
GmTag080	49	NA	146.9	141.5-152.3	135.1 - 161.5
GmTag081	250	248	145.3	126.4-162.8	113.8 - 184.2
GmTag082	250	250	149.9	137.6-175.4	133.1 - 194.8
GmTag083	250	NA	148.4	137.7-176.6	133.1 - 195.3
GmTag115	148	NA	137.7	109.8-157.5	90.8 - 171.1
GmTag152	302	302	125.0	101.2-146.2	93.8 - 155.8
GmTag153	277	277	128.5	102.3-146.8	98.7 - 156.0
GmTag214[1]	15	15	128.1	119.3-133.8	112.9 - 144.6
GmTag231[1]	45	45	143.0	130.2-155.2	126.9 - 160.0
SbTag014	189	NA	142.6	114.1 – 159.8	95.3 – 170.6
SbTag015	182	160	140.1[2]	110.7 – 155.1	96.5 - 167.7
SbTag017[2]	295	295	137.3	103.1 – 146.7	73.0 – 155.9
SbTag018[2]	290	290	140.9	117.2 – 157.1	114.9 – 163.6
TtTag034[3]	39	39	133.4	122.5 – 145.7	114.3 – 154.0
TtTag035[3]	41	41	129.1	118.6 – 146.0	110.1 – 151.9

[1] Utilizing both GPS and ARGOS positions

[2] Exposures removed due to extremely low estimated RLs (see text)

[3] The fixed path (corrected for no land median locations) results for TtTag034 & TtTag035. For TtTag034 2 of the 41 exposures did not have paths to estimate RLs, likely due to water depths where relocated did not support dive depths. TtTag035 had 2 exposures removed for clusters of estimated RLs that were unrealistically low (< 0dB). See text for details.

3.2.2.1   GmTag080

The tag deployed on GmTag080 was a SPOT5 (i.e., location-only) tag, so both shallow (surface to 54 m depth) and deep (63 m to 500 m depth) exposures were estimated. The grand mean RL was 146.9 dB re 1 µPa, with a range of median estimated RLs from 141.2 to 152.3 dB re 1 µPa, and a range of median RLs +/- 2*SD from 135.1 – 161.5 dB re 1 µPa. This tag stopped transmitting during Phase B and only had 49 5-min locations that overlapped with MFAS, which is a lower number of exposures compared to the

other tagged short-finned pilot whales in Feb 2014 (i.e., GmTag081, 082 & 083) that each had 250 locations that overlapped with sonar. Figure 3.2.2-1 provides two plots comparing 3D RL estimates generated at shallow depths (left panel) with those generated at deep/typical dive depths (right panel) with the same axes scales for comparison. The shallow estimated RLs at PMRF are typically higher than estimates at depth given the typical presence of a near-surface sound duct which results in less TL (higher RLs). Overall this animal's exposures were at relatively low levels, with a maximum median estimated RL for shallow data of 152.3 dB re 1 μPa just prior to noon on 18 February. The two standard deviations also show that the deep estimated RLs were typically much lower (on the order of 10 dB re 1 μPa), with larger standard deviations due to the focusing effects of the sound propagation.

Due to the typical near surface ducting present at PMRF, for the remainder of results when two estimates (shallow and deep) are performed (i.e. there is no dive data for that tag or time period), only the shallow estimated RLs will be plotted. In some cases (such as GmTag080), some of the highest and lowest estimates using 2*SDs are greater than the minimum/maximum values due to the non-Gaussian, multimodal distributions of estimated propagation modeled RLs.
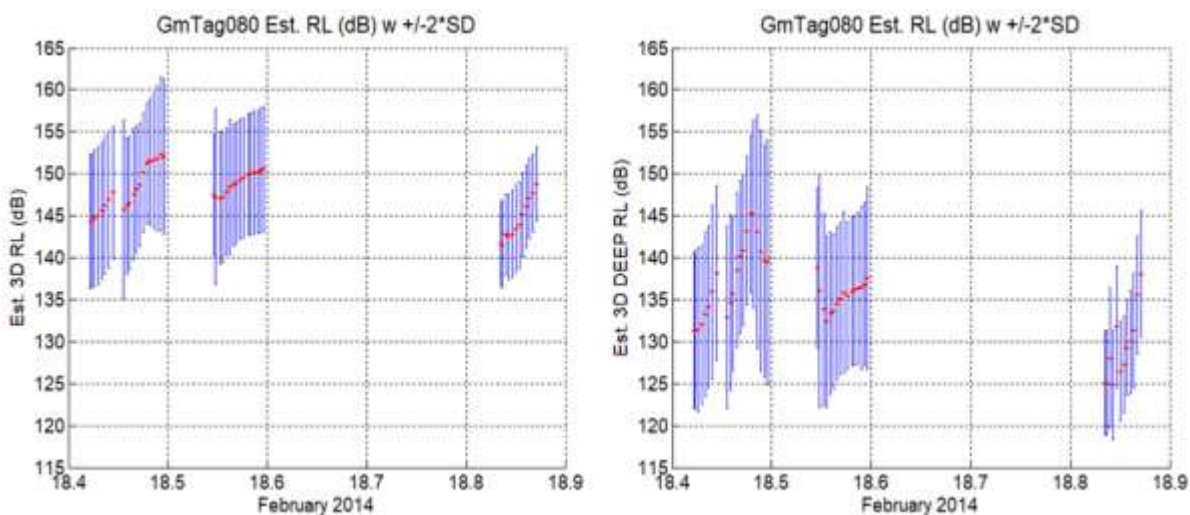
Figure 3.2.2-1. Estimated 3D RLs for GmTag080 for both shallow depths (left, surface to 54 m depth) and deep depths (right, 63 m to 500 m depth) over time (GMT). RL estimates are shown as red points on the same scales along with whiskers for ± two standard deviations.

Table 3.2.2 provides several exposure details for this animal. In situations where portions of the radial slices through the animal's error ellipse were either on land, below the seafloor, or too close with too steep of a propagation vertical angle, the proportion of TL samples used in the 3D RL estimation decreases from 1.0; this value (proportion of samples utilized) was used as a diagnostic tool in interpretation of the propagation model results.

Table 3.2.2. Details for several exposures of the 49 locations from GmTag080 that overlapped with MFAS.

Date/Time (GMT)	Estimated median RL (dB re 1 µPa) shallow	Range of estimated RLs ± 2*SD shallow	Animal depth range (m)	Min / Max distance from source (km)	# slices / range step (m)	# samples / proportion of samples utilized
2/18.2014 @ 10:09:00	144.3 [1]	136.4-152.2	0-54	35.7 – 47.3	26 / 47.3	29,706 / 1.0
2/18/2014 @ 11:49:00	152.3 [2]	143.1 – 161.5	0-54	12.8 - 26.6	29 / 26.6	70,632 / 0.985
2/18/2014 @ 13:59:00	149.9	142.7 – 157.1	0-54	21.8 – 29.2	15 / 29.2	17,226 / 1.0
2/18/2014 @ 20:04:00	141.5 [3]	136.4 – 146.6	0-54	38.6 – 39.0 [3]	19 / 39	978[3] / 1.0
2/18/2014 @ 20:54:0	148.8 [4]	144.4 – 153.2	0-54	22.4 – 26.0	12 / 26	3,786 / 1.0

[1] First exposure

[2] Highest estimated median RL for this animal

[3] Lowest estimated median RL for this animal, with small error ellipse (350m x 950m) and sample size

[4] Last exposure

3.2.2.2   GmTag081

This animal was tagged with a SPLASH10 tag which included dive depth information for the 250 5-min locations that overlapped with MFAS. This animal was tagged in the same group as GmTag082 and GmTag083 and they remained in association throughout the SCC. The grand mean RL was 145.3 dB re 1 µPa for the 250 exposures. The median RLs ranged from 126.4 dB to 162.8 dB re 1 µPa, while the range of median RLs ± 2*SDs was 113.8 – 184.2 dB re 1 µPa. Figure 3.2.2-2 provides the time aligned history of the 250 estimated RLs along with the ± 2*SDs, illustrating that most of the time, the exposure whiskers rarely exceeded 165 dB re 1 µPa, with the exception of the whiskers exceeding 180 dB re 1 µPa around 08:30 on the 20th of February.
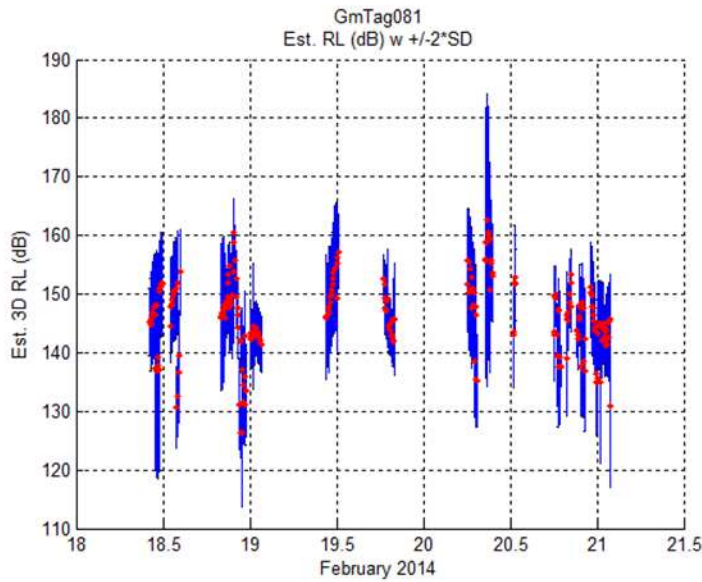
Figure 3.2.2-2. Estimated 3D RLs (red points) with whiskers representing ± 2*SDs for GmTag081 3.5-day period (X-axis scale in days GMT). Note the highest estimated median RL of 162.8 dB re 1 µPa around 08:30 on February 20th also has the two standard deviation values exceeding 180 dB re 1 µPa.
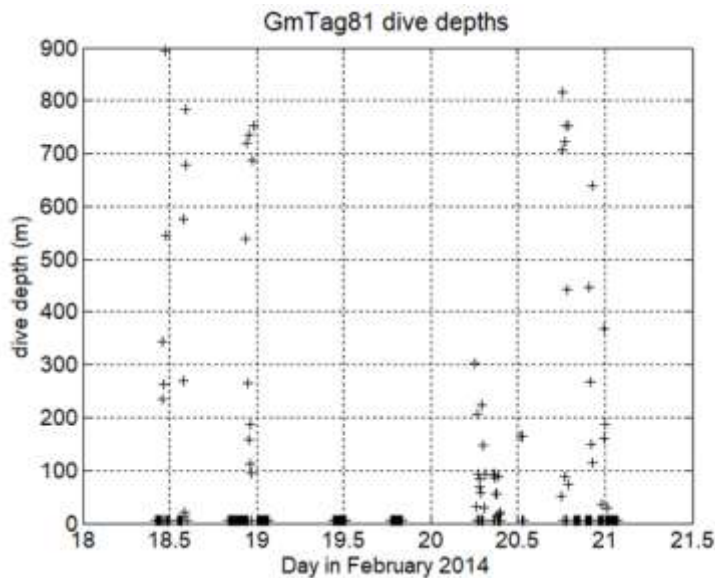
Figure 3.2.2-3. GmTag081 dive depths utilized in the RL analysis for 250 exposures plotted over a 3.5-day period (X-axis scale in days GMT).

Figure 3.2.2-3 provides the dive depths for the 250 dives also plotted against time similar to Figure 3.2.2-2. Of the 250 dive depths, in 195 locations the animal was in water less than 54 m deep, with the deepest dive recorded down to a depth of 894 m.

Table 3.2.3 provides several details for some exposures (e.g. first, last, highest, lowest). The highest estimated exposure for the tagged animal was a shallow dive depth (<54 m) where the ship was inside the animal's 95% CI error ellipse (Figure 3.2.2-4) with a median RL of 162.8 dB re 1 µPa (±10.7 dB re 1 µPa). A second entry in Table 3.2.3 is provided for a matching lowest median estimated RL on 2-18-2014 22:55 GMT, however, this dive depth is over twice the dive depth in the entry 5 min earlier, and half of the estimated RLs were discarded due to the water depth not supporting such a deep dive as evidence by the proportion of samples utilized being down at 50%. The closest distances to the source started at 10 m, with range steps of 18.2 m (Table 3.2.3). The median estimated RL plus 2*SD is 184.2 dB re 1 µPa, although there were estimated RLs even closer to the ship. However, the four deepest of the six depth bins (i.e. 27, 36, 45, and 54 m) were all at too steep of propagation angles (i.e. > 45 degrees down) for each radial closest to the ship to provide estimated RLs, which accounts for the 144 estimated 3D RLs being removed. This exposure's maximum estimated RL was 216.1 dB re 1 µPa, which is extraordinarily high, and exists only for the two closest range bins at 10 and 28.2 m from the source.

Table 3.2.3. Details for select exposures of the 250 locations from GmTag081 analyzed that overlapped with MFAS.

Date / Time (hh:mm) GMT	Estimated median RL (dB)	Range of estimated RLs +/- 2*SD	Animal depth range (estimate) (m)	Min / Max distance from source (km)	# slices / range step (m)	# samples / proportion of samples utilized
2/18/2014 @ 10:05	145.3 [1]	139.6-151.1	0-54	42.7 – 51.2	13 / 51.2	10,020 / 1.0
2/18/2014 @ 11:20	139.2 [2]	126.0- 152.4	855-936 (894)	24.6 – 35.9	19 / 35.9	40,643 / 0.846
2/18/2014 @ 13:50	130.7	123.8 – 137.6	243-288 (269)	19.7 – 23.5	18 / 23.5	5,274 / 1.0
2/18/2014 @ 14:00	151.8	143.1 – 160.5	0-54	18.6 – 22.1	18 / 22.1	9,120 / 1.0
2/18/2014 @ 21:50	160.5	154.9 – 166.1	0-54	4.8 – 9.5	22 / 9.5	51,102 / 1.0
2/18/2014 @ 22:50	126.4 [4]	122.1 – 130.6	243-288 (266)	36.2 – 43.8 [4]	15 / 43.8	12,666 / 1.0
2/18/2014 @ 22:55	126.4 [4]	113.8 – 139.1	702-765	39.9 – 47.5	15 / 47.5	7,984 / 0.502
2/20/2014 @ 08:45	162.8 [3]	141.3 – 184.2	0 -54	0.01 – 18.2 [3]	36 / 18.2	81,522 / 0.998
2/21/2014 @ 01:50	131.0 [5]	117.1 – 144.9	0-54	25.6 – 38.5	22 / 38.5	33,226 / 0.999

[1] First exposure
[2] Deepest dive of 894 m
[3] Highest estimated median RL for this animal when source was within the animal's 95% CI error ellipse
[4] Lowest estimated median RL for this animal
[5] Last exposure

Figure 3.2.2-4 shows the plan view of the highest estimated RL exposure geometry on 2/20/2014 at 08:45. This is a large error ellipse and with the source just inside the ellipse one can see how the 36

radials sample the area. The highest estimated RLs only exist extremely close to the source (within approximately 25m); however, it is obvious that the area within about 100 m from the source is a very small proportion of the total area of the entire 95% CI ellipse. Given we are sampling this area with 36 radials with 10 degree spacing, the probability of exposure at higher levels is overestimated with this geometry. A histogram of estimated 3D RLs (Figure 3.2.2-5) shows that the high estimated RLs have a low probability of occurring as they exist in the heavy positive tail of the histogram. For the 36 radial slices utilized in this analysis (with 9 m depth binning and 18.2 m range bins starting at 10 m), the probability of being exposed to over 200 dB re 1 µPa can be estimated as the total number of 3D estimated RL samples >200 dB re 1 µPa (648) relative to the total number of 3D estimated RL samples (81,522) for a resulting probability of less than 0.8%. Similarly, the probability of being exposed to levels over the median plus two SD (184.2 dB re 1 µPa) is approximately 7% (5,760) due to the heavy tail on the right side of the histogram. Furthermore, these estimated probabilities are overestimates due to the spatial sampling of the 36 radials. To simply state the highest maximum estimated RL values can be extremely misleading as seen in this case, where being exposed to levels over 200 dB re 1 µPa has a probability of less than 0.8% or even lower considering proportions of the entire areas (close to source and for the full ellipse). Therefore, if one utilized a 100 m starting distance from the source for the radials, the highest estimated RLs would reduce by at least 10 dB due to propagation effects.
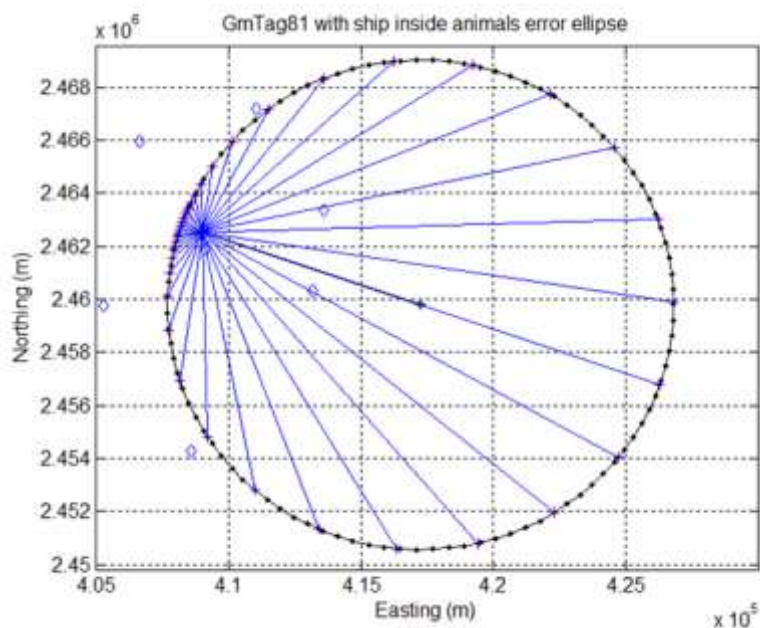
Figure 3.2.2-4. Plan view of ship location and GmTag081's 95% CI error ellipse for the highest estimated median RL on 2/20/2014 at 08:45 GMT; the minor grids in Northing are 2km and the minor grids in Easting are 5km. Blue diamond symbols indicate approximate location of the hydrophones utilized in the analysis. The central animal location is indicated by the black asterisk near the center of the plot, with the ship located at the origin of the blue lines indicating the 36 radial slices inside the animal's error ellipse.
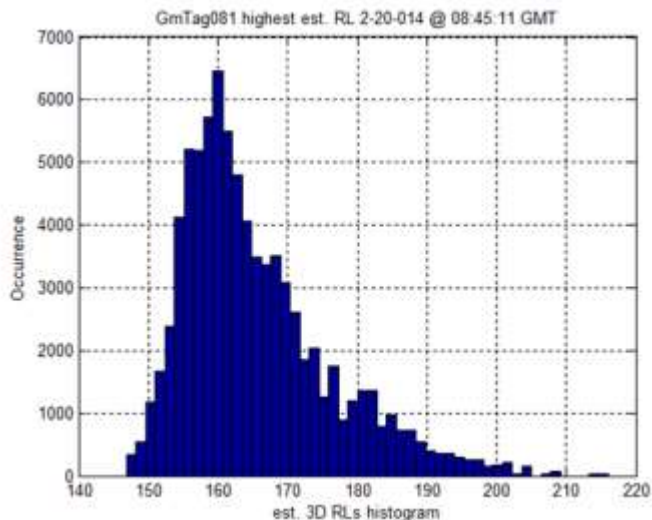
Figure 3.2.2-5. Histogram of the shallow estimated RL for GmTag081 on 2-20-2014 at 08:45:11 GMT, highlighting the heavy right tail in the distribution, with real, albeit low probability, potential exposures over 200dB re 1 µPa for this animal at this time depending upon its true location in space.

3.2.2.3   GmTag082

GmTag082 (tagged with a SPLASH10 tag) was the second of three animals in a group of short-finned pilot whales that were all associated during the February 2014 SCC and as such had similar results to GmTag081, with the source ship inside the animal's 95% CI error ellipse mid-morning on the 20th (GMT). While the grand mean of exposures was only 149.9 dB re 1 µPa re 1 µPa, the range of estimated median values was 137.6 – 175.4 dB re 1 µPa, the median ± 2*SD extends from 133.1 to 194.8 dB re 1 µPa, similar to high estimated median RLs around this time for GmTag081. Three periods show nearly monotonically increasing estimated median RLs, which could be useful for potential behavioral responses; however, the estimated median RLs were under 160 dB re 1 µPa for those periods. Figure 3.2.2-6 provides the plot of median estimated RL with ± 2*SD whiskers as a function of time. Dive data were obtained for 45 of the 250 locations that overlapped with MFAS, and the animal was in shallow depths (54 m or less) for all those locations. The proportion of 3D samples utilized were 1.0 for 230 of the 250 exposures, with the lowest value of 0.925 and only 4 other values less than 0.98.
Table **3.2.4** provides details for select exposures for GmTag082.
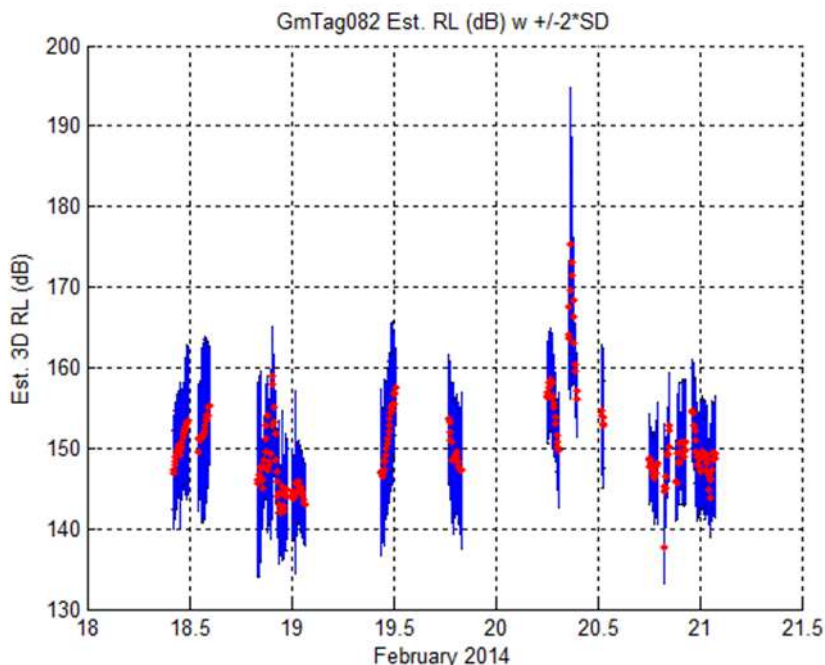
Figure 3.2.2-6. Estimated 3D median RLs (red markers) with ± 2*SD whiskers shown over a 3.5-day period (X-axis scale in days GMT) for the 250 exposures on GmTag082. Note the whiskers extend above 190 dB re 1 µPa with max at 194.8 dB re 1 µPa around 08:45 on February 20, 2014.

Table 3.2.4. Details for select exposures of the 250 total locations from GmTag082 that overlapped with MFAS.

Date / Time (hh:mm GMT)	Estimated median RL (dB re 1 µPa) shallow	Range of estimated RLs ± 2*SD shallow	Animal depth range (estimate) (m)	Min / Max distance from source (km)	# slices / range step (m)	# samples / proportion of samples utilized
2/18/2014 @ 10:05	147.4 [1]	142.4-152.3	0-54	40.6 – 46.2	29 / 46.2	16,290 / 1.0
2/18/2014 @ 21:50	159.0	152.8 – 165.1	0-54	4.6 – 12.8	30 / 12.8	83,766 / 1.0
2/20/2014 @ 06:30	158.6	152.3 – 164.9	0-54	5.5 – 9.6	17 / 9.6	32,280 / 1.0
2/20/2014 @ 08:49	175.2 [2]	156.0 – 194.8	0 -54	0.01 – 3.35	36 / 3.35	77,109 / 0.987
2/20/2014 @ 19:45	137.6 [3]	133.1 – 142.1	(266)	38.8 – 40.9	9 / 40.9	1,884 / 1.0
2/21/2014 @ 01:50	148.8 [4]	141.4 – 156.2	0-54	20.9 – 30.4	29 / 30.4	42,876 / 1.0

[1] First exposure

[2] Highest estimated median RL for this animal when source was within the animal's 95% CI error ellipse

[3] Lowest estimated median RL for this animal

[4] Last exposure

3.2.2.4 GmTag083

GmTag083 results were also similar to GmTag081 and GmTag082 results given the animals were associated throughout their deployments. However, GmTag083 was tagged with a SPOT5 tag with no dive depth information, resulting in RLs estimated at two depths (shallow and deep) for each exposure (Table 3.2.5). The grand mean RL was 148.4 dB re 1 µPa, while the range of estimated median RLs was 137.7 – 176.6 dB re 1 µPa, and the range of median RLs ± 2*SD was 133.1 – 195.3 dB re 1 µPa. The shallow estimated 3D median RLs ± 2*SDs (Figure 3.2.2-7) were higher and had less variance than the estimates at depth. This is similar as to what was depicted for GmTag080 earlier and as one would expect given both the surface ducted channel typically present and the additional depth values over which the 3D estimated RL was evaluated. The proportion of 3D estimated RLs utilized for the shallow estimates were 1.0 or very close to 1.0 for all of the 250 estimated 3D RLs, with the lowest proportions occurring for the maximum estimated 3D RLs; this was due only to the propagation angle being too steep (> 45 degrees) for the estimates, which began at 10 m from the source for depths > 18 m and up to 64 m. For the cases where the source is inside of the animal's 95% CI error ellipses, the proportion of 3D estimated RLs that were used may decrease significantly due primarily to the larger number of depth/range/azimuth bins where the propagation vertical angle was > 45 degrees.
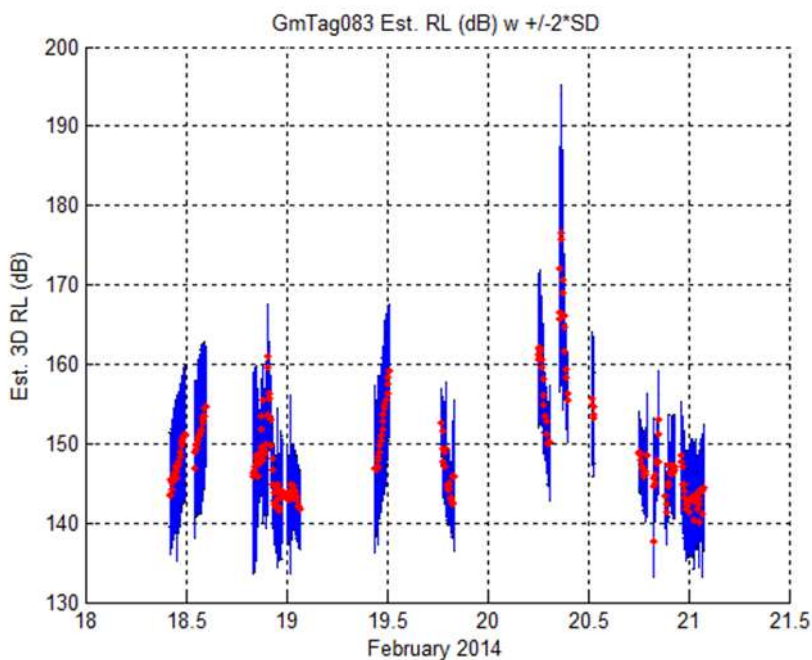
Figure 3.2.2-7. Results of estimated 3D RLs (red points) with ± two standard deviation whiskers for shallow (surface to 54m) depths for GmTag083 over 3.5- day period (X-axis scale in days GMT). Similar geometric situations occurred as for GmTags 081 & 082, however this tag did not have dive depth related information.

Table 3.2.5. Details for select exposures of the 250 total locations from GmTag083 that overlapped with MFAS.

Date / Time (hh:mm GMT)	Estimated median RL (dB re 1 µPa) shallow	Range of estimated RLs ± 2*SD shallow	Animal depth range (m)	Min / Max distance from source (km)	# slices / range step (m)	# samples / proportion of samples utilized
2/18/2014 @ 10:05	145.4 [1]	139.5 - 151.3	0 - 54	42.6 – 52.4	25 / 52.4	21,846 / 1.0
2/19/2014 @ 12:05	157.6 [2]	147.9 – 167.3	0 - 54	5.5 – 18	29 / 18	96,342 / 1.0
2/19/2014 @ 12:05	147.8 [2]	137.6 – 158.0	63 - 495	5.5 – 18	29 / 18	781,172 / 0.993
2/20/2014 @ 08:45	176.6 [3]	158.0 – 195.2	0 - 54	0.01 – 4.4	36 / 4.4	101,670 / 0.993
2/20/2014 @ 08:50	175.7[3]	157.3 – 194.0	0 - 54	0.01 – 4.1	36 / 4.1	122,382 / 0.994
2/20/2014 @ 19:45	137.7 [4]	133.1 – 142.2	0 - 54	38.6 – 40.5	9 / 40.5	2,040 / 1.0
2/21/2014 @ 1:50	144.3 [5]	136.6 – 152.2	0 - 54	25.9 – 41.9	25 / 41.9	41,160 / 1.0

[1] First exposure

[2] Example of estimated 3D RL for depths of 63 -495 m

[3] Highest estimated median RL for this animal when source was within the animals 95% CI error ellipse

[4] Lowest estimated median RL for this animal

[5] Last exposure

3.2.2.5   GmTag115

GmTag115 was also tagged with a SPOT5 tag without dive depth information. Figure 3.2.2-8 provides the 148 shallow dive depth estimated 3D median RLs with ± 2*SD whiskers over time. This animal was estimated to have not experienced relatively high exposure levels, but did experience increasing levels over the first 2 days followed by lower estimate RLs. The grand mean was 115 dB re 1 µPa, while the range of median values was 109.8 – 157.5 dB re 1 µPa, and the range of median values ± 2*SD was 90.8 – 171.1 dB re 1 µPa. Some distances from the source were up to 159 km, with the animal west of Ni'ihau at the time (Figure 3.3.1-4). Due to the long propagation distances, many of the estimated 3D RLs had multimodal distributions as evidenced by the first exposure with a standard deviation of 9.3 dB re 1 µPa (Figure 3.2.2-9). Even with the non-Gaussian distribution, the animal was exposed to relatively low levels of MFAS for the first group of exposures 15-16 February 2015. The initial MFAS exposures late on the 15th of February into the 16th were from a single ship MFAS training activity against a Mk30 submarine simulator target during a ULT, which was not officially part of the SCC but occurred between the two phases of the training; this accounts for the 1.5-day delay from that sonar block to the first sonar block of the SCC.

Table 3.2.6 provides details from five locations that overlapped with sonar. The median RLs + 2*SDs maximum was 171.1 dB re 1 µPa. Overall relatively low exposure levels occurred for this animal.
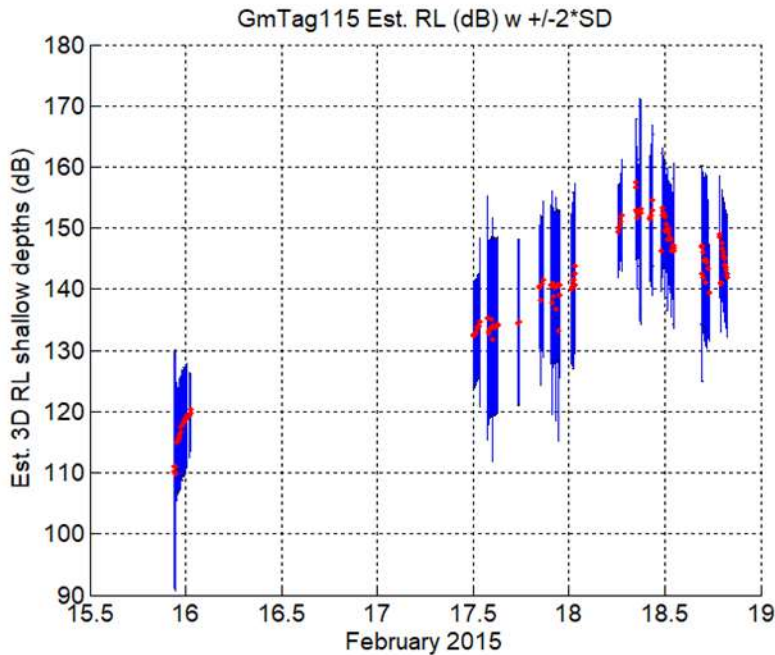
Figure 3.2.2-8. Estimated 3D median RLs (red points) with ± 2*SD whiskers for GmTag115 for shallow depths (surface to 54 m) shown over a 3.5-day period (X-axis scale in days GMT).
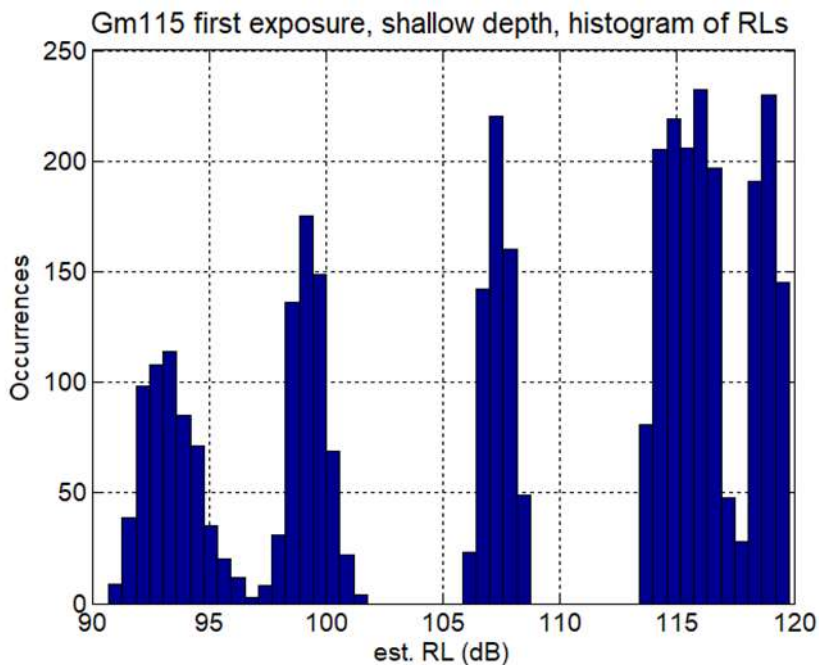
Figure 3.2.2-9. First exposure to GmTag115 for distances from the source between 147.7 and 154.8 km. The median for this exposure was 111.1 dB re 1 µPa with a standard deviation of 9.3 dB re 1 µPa. However, the multimodal distribution is obvious from the histogram of estimated 3D RLs.

Table 3.2.6. Details for select exposures of the 148 total locations from GmTag115 that overlapped with MFAS.

Date / Time (hh:mm GMT)	Estimated median RL (dB re 1 µPa) shallow	Range of estimated RLs ± 2*SD shallow	Animal depth range (m)	Min / Max distance from source (km)	# slices / range step (m)	# samples / proportion of samples utilized
2/15/2015 @ 22:35	111.1 [1]	92.5-129.7	0 - 54	147.7– 154.8	17 / 154.8	3,564 / 1.0
2/15/2015 @ 22:45	109.8 [3]	90.8 – 128.8	0 - 54	149.3 – 156.8	19 / 156.8	4,338 / 1.0
2/18/2015 @ 08:25	157.5 [2]	147.1 – 167.9	0 - 54	79 – 128.1	8 / 128.1	9,234 / 1.0
2/18/2015 @ 11:35	152.2	142 – 162.4	0 - 54	13.9 – 28.4	21 / 28.4	50,010 / 1.0
2/18/015 @ 19:50	142.0 [4]	132.2 – 151.8	0 - 54	37.4 – 54.6	30 / 54.6	32,982 / 1.0

[1] First exposure

[2] Highest estimated median RL for this animal

[3] Lowest estimated median RL for this animal

[4] Last exposure

3.2.2.6   GmTag152

GmTag152 was a SPLASH10 tag and was associated with another individual tagged in the same group (GmTag153). GmTag152 had 302 locations that overlapped with MFAS as illustrated (Figure 3.2.2-10, Table 3.2.7). The grand mean RL was 125.0 dB re 1 µPa, with a range of median RLs from 101.2 – 146.2 dB re 1 µPa, and median ± 2*SD RLs ranging from 93.8 to 155. 8 dB re 1 µPa. Estimated 3D median RLs for this tag were between 119 and 146 dB re 1 µPa over Phase B of the SCC.
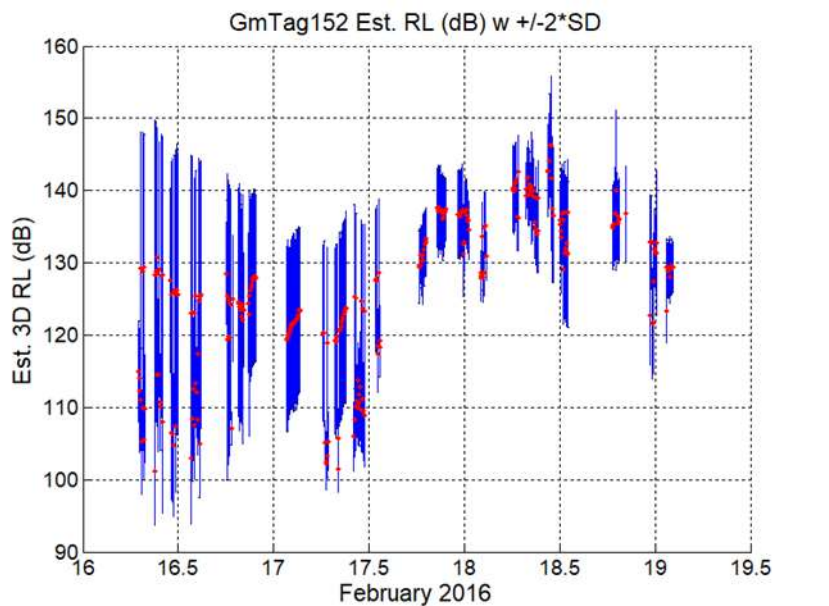
Figure 3.2.2-10. Estimated 3D RLs (red points) with ± 2*SD whiskers for GmTag152 over a 3.5-half day period (X-axis scale in days GMT).

Table 3.2.7. Details for selected exposures of the 302 total locations from GmTag152 that overlapped with MFAS.

Date / Time (hh:mm GMT)	Estimated median RL (dB)	Range of estimated RLs +/- 2*SD	Animal depth range (m)	Min / Max distance from source (km)	# slices / range step (m)	# samples / proportion of samples utilized
2/16/2016 @ 07:03	114.9 [1]	107.9-121.9	135-153	80.3– 85.3	33 / 85.3	4,611 / 1.0
2/16/2016 @ 09:03	101.2 [3]	93.8 – 108.7	162-180	79.4 – 92.1	24 / 92.1	4,086 / 1.0
2/18/2016 @ 10:58	146.2 [2]	133.6 – 155.8	0 - 54	31.3 – 48.3	28 / 48.3	46,542 / 1.0
2/19/2016 @ 02:13	129.4 [4]	125.9 – 132.9	0 - 54	80.2 – 85.9	34 / 85.9	9,666 / 1.0

[1] First exposure

[2] Highest estimated median RL for this animal

[3] Lowest estimated median RL for this animal

[4] Last exposure

3.2.2.7 GmTag153

GmTag153 (tagged a SPLASH10 tag) had dive data for 179 out of the 277 locations that overlapped with MFAS (Figure 3.2.2-11, Table 3.2.8). This whale had a similar exposure profile as GmTag152, which is expected given they were in the same group, with a grand mean RL of 128.5 dB re 1 µPa, median RLs ranging from 102.3 to 146.8 dB re 1 µPa, and median ± 2*SD RLs of 98.7 – 156.0 dB re 1 µPa.
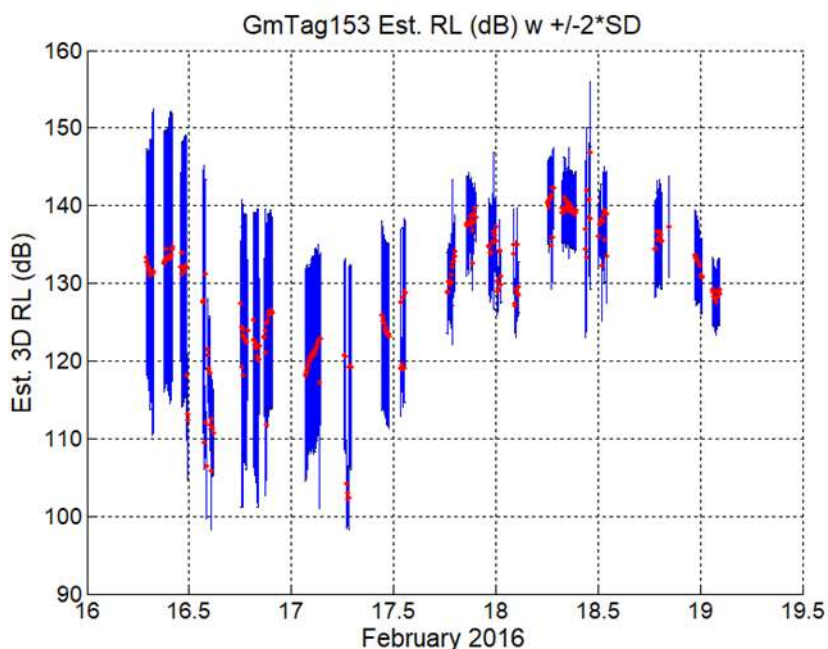
Figure 3.2.2-11. Estimated median 3D RLs (red points) with ± 2*SD whiskers for 277 locations from GmTag153 that overlapped with MFAS over a 3.5-day period (X-axis scale in days GMT).

Table 3.2.8. Details for selected exposures of the 277 total locations from GmTag153 that overlapped with MFAS.

Date / Time (hh:mm GMT)	Estimated median RL (dB)	Range of estimated RLs +/- 2*SD	Animal depth (m)	Min / Max distance from source (km)	# slices / range step (m)	# samples / proportion of samples utilized
2/16/2016 @ 07:02	133.3 [1]	122.5 - 144.2	0 - 54	85.4– 87.5	7 / 87.5	846 / 1.0
2/17/2016 @ 06:37	102.3 [3]	98.7 – 105.8	108 - 117	131.2 – 137.4	29 / 137.4	2,064 / 1.0
2/18/2016 @ 11:02	146.8 [2]	137.7 – 156	0 - 54	29.8 – 43.5	26 / 43.5	38,718 / 1.0
2/19/2016 @ 02:17	129.0 [4]	125.1 – 133.2	0 - 54	79.7 – 84.2	21 / 84.2	5,550 / 1.0

[1] First exposure

[2] Highest estimated median RL for this animal

[3] Lowest estimated median RL for this animal

[4] Last exposure

3.2.2.8   GmTag214

For GmTag214 (tagged with a SPLASH10-F tag) the results presented utilized both the Argos and the GPS positions in the *crawl* track. The Aug 2018 SCC training was abbreviated due to the approach of Hurricane Lane, with only 15 locations that overlapped with sonar from surface ship MFAS. Figure 3.2.2-12 presents the time aligned 3D median estimated RL ± 2*SDs for the 15 exposures. The grand mean RL was 128.1 dB

re 1 µPa, while the median RLs ranged from 119.3 to 133.8 dB re 1 µPa, and the median ± 2*SD RLs ranged from 112.9 – 144.6 dB re 1 µPa.

This animal's exposures were estimated to be relatively low

Table 3.2.9). The closest distance over the 15 exposures was 25 km, with a maximum distance 50.6 km. The diagnostic proportion of samples utilized was 1.0. Some exposures had a small number of azimuthal slices given the small animal error ellipse coupled with the longer distances (e.g. the last exposure had 9 slices with distances between 49 and 50.6 km).
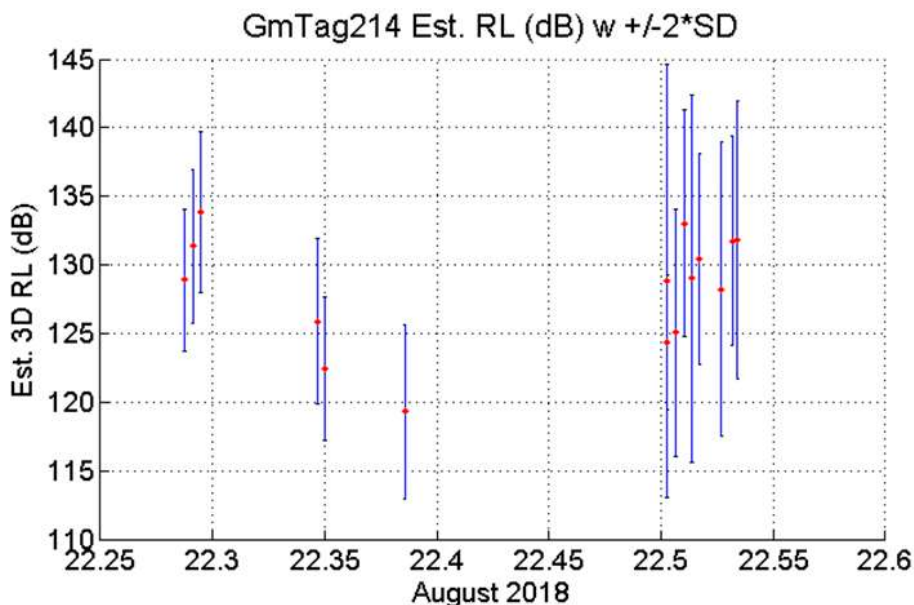
Figure 3.2.2-12. Estimated 3D RLs (red points) with ± 2*SD whiskers for 15 locations from GmTag214 that overlapped with MFAS on 22 August 2018 (X-axis scale in days GMT).

Table 3.2.9. Details for selected exposures of the 15 total locations from GmTag214 that overlapped with MFAS.

Date / Time (hh:mm GMT)	Estimated median RL (dB re 1 µPa) shallow	Range of estimated RLs ± 2*SD shallow	Animal depth range (estimate) (m)	Min / Max distance from source (km)	# slices / range step (m)	# samples / proportion of samples utilized
8/22/2018 @ 06:54	128.9 [1]	123.8-134.0	0 - 54	32.2– 33.7	7 / 33.7	1,554 / 1.0
8/22/2018 @ 09:14	119.3 [3]	112.9 – 125.6	0 - 54	33.7 – 36.9	15 / 36.9	6,428 / 1.0
8/22/2018 @ 12:14	133.0 [2]	124.8 – 141.3	(479)	38.1 – 39.8	27 / 47.1	1,445 / 1.0
8/22/2018 @ 12:49	131.8 [4]	121.7 – 142	(131)	49 – 50.6	9 / 50.6	627 / 1.0

[1] First exposure

[2] Highest estimated median RL for this animal

[3] Lowest estimated median RL for this animal

[4] Last exposure

3.2.2.9   GmTag231

GmTag231 (tagged with a SPLASH10-F tag) had 52 locations that overlapped with MFAS during the Feb 2020 SCC. Figure 3.2.2-13 presents the median estimated RL vs time with ± 2*SD. The grand mean RL was 143.0 dB re 1 µPa, the range of median RLs was 130.2 – 155.2 dB re 1 µPa, and the range of median ± 2*SD RLs was 126.9 – 160.0 dB re 1 µPa (Table 3.2.10). The bulk of the exposures (41 of 52) occurred on the second half of 19 Feb and at distances between 40 km and 80 km. Additional closer exposures occurred late 21 Feb and on 22 Feb of under 20 km (closest 7.5km), leading to higher estimated RLs. All exposures utilized all of the potential depth/range bins from the 95% CI error ellipse.
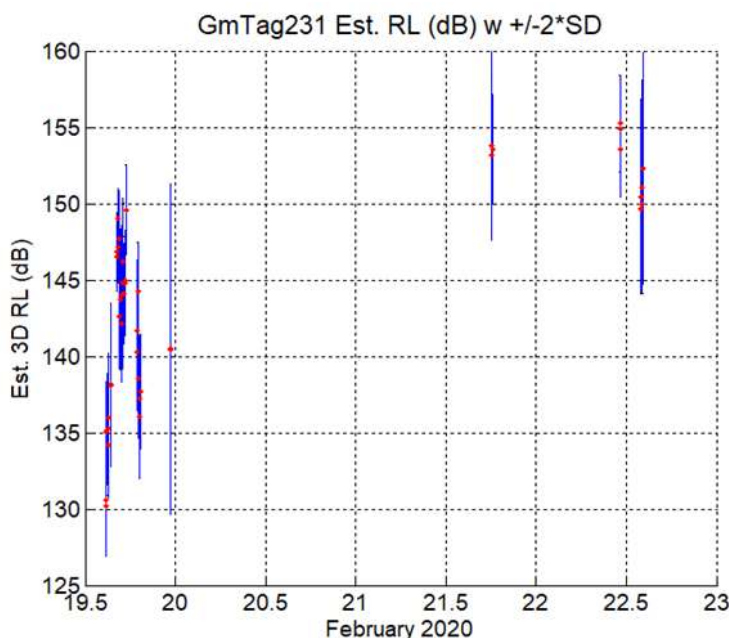
Figure 3.2.2-13. Estimated median RLs (red points) with ± 2*SD whiskers for GmTag231 over a 3.5-day period (X-axis scale in days GMT).

Table 3.2.10. Details of select exposures of the 52 locations from GmTag231 that overlapped with MFAS.

Date / Time (hh:mm GMT)	Estimated median RL (dB re 1 µPa)	Range of estimated RLs ± 2*SD shallow	Animal depth range (m)	Min / Max distance from source (km)	# slices / range step (m)	# samples / proportion of samples utilized
2/19/2020 @ 14:43	130.2 [1,3]	126.9 - 133.5	0 - 54	75– 76.3	7 / 76.3	564 / 1.0
2/22/2020 @ 11:09	155.2 [2]	152 – 158.4	0 - 54	104.8 – 122	9 / 122	5,874 / 1.0
2/22/2020 @ 14:14	152.3 [4]	144.8 – 159.9	0 - 54	7.5 – 15.7	18 / 15.7	43,608 / 1.0

[1] First exposure

[2] Highest estimated median RL for this animal

[3] Lowest estimated median RL for this animal, also the first exposure

[4] Last exposure

3.2.2.10 SbTag014

SbTag014 (tagged with a SPOT5 tag), similar to GmTag115, had location data during the ULT viable for RL estimation, although the animal was south of the Kaulakahi Channel. Fourteen of the 189 exposures were for the ULT period, with 2 of those exposures having around half of the radials from the source to the animal as they were blocked by Kaua'i. Each of these two exposures had a single slice between the shadowing and unobstructed paths, with situations such as the bottom of the slice having minimum depths over the channel of only one depth bin, or 9 m. The sound propagated south of the channel of these slices was finite (e.g., a real number), but had TL values from 200 dB to more than 300 dB re 1 μPa. In comparison, the slices with unobstructed propagation paths over the channel for these two exposures had TLs in the range of 90 to 120 dB re 1 μPa. This caused extremely high standard deviations when results with those slices were included. Therefore, slices with these unrealistically high levels of TL were removed from estimated 3D RL exposures for both the deep and shallow estimates. The 3D estimated RL values with those two slices of two exposures removed were recombined to arrive at the results in Figure 3.2.2-14.

The grand mean of the 189 exposures for the shallow depth estimates was 142.6 dB re 1 μPa, with median RLs ranging from 114.1 to 159.8 dB re 1 μPa, and the median RL +/- 2*SD ranging from 95.3 dB to 170.6 dB re 1 μPa. Figure 3.2.2-15 provides the fraction of TLs utilized for the 3D estimated RLs for all 189 exposures; there were low fractional values for the first 43 exposures but these increased to 1.0 for both deep and shallow estimates for the remaining 146 exposures estimated (

Table **3.2.11**).
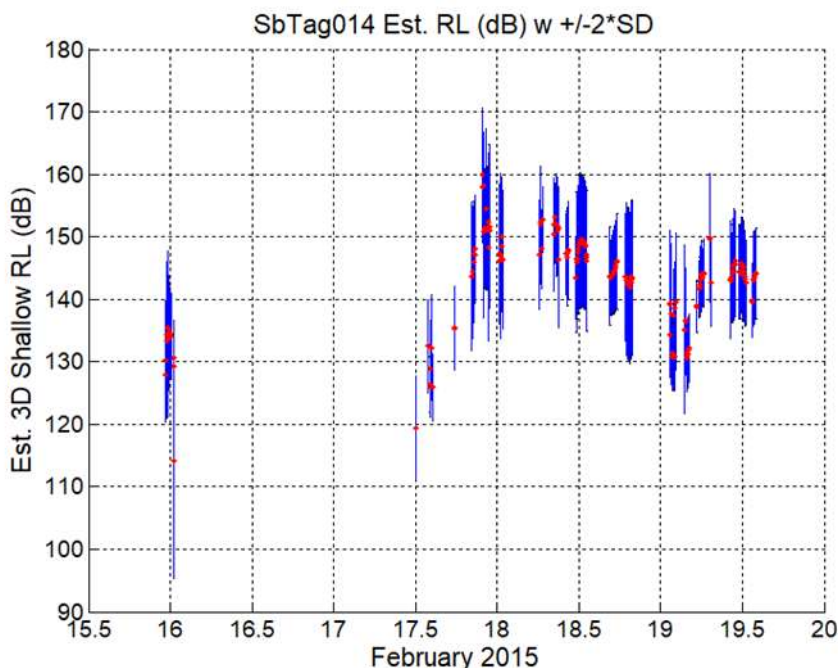
Figure 3.2.2-14. Estimated 3D median RLs (red markers) with whiskers for +/- 2*SD for SbTag014 over a 4.5-day period (with X-axis labels in decimal days GMT).
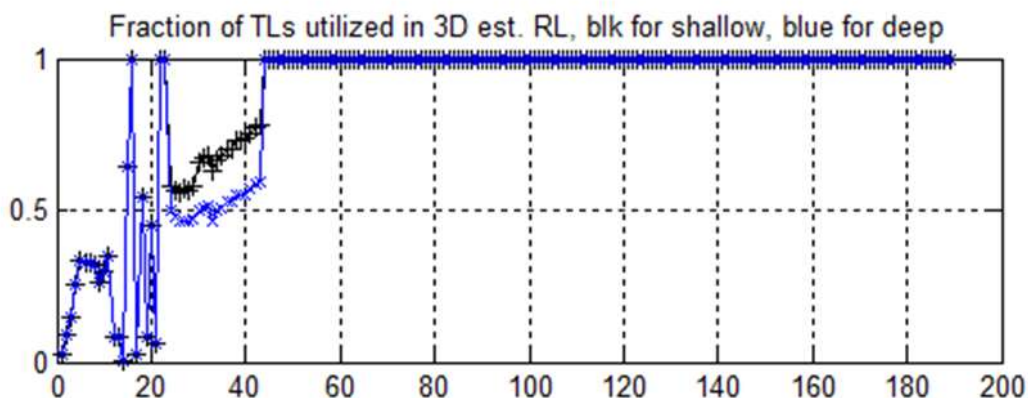
Figure 3.2.2-15. Fraction of TLs utilized vs. exposure number for the shallow (blk) and deep (blue) estimated RLs for SbTag014.

Table 3.2.11. Details of select exposures of the 189 locations from SbTag014 that overlapped with MFAS. Note that both shallow and deep RL estimates were included for the location with the highest median estimated RL, and deep estimate was included for the location with the lowest estimated median RL.

Date / Time (hh:mm GMT)	Estimated median RL (dB re 1 µPa)	Range of estimated RLs +/- 2*SD	Animal depth range (m)	Min / Max distance from source (km)	# slices / range step (m)	# samples / proportion of samples utilized
2/15/2015 @ 23:15	128.0 [1]	121.4-133.3	0-54	42.6– 57.9	31 / 57.9	822 / 0.022
2/16/2015 @ 00:30	105.7 [3]	89 – 122.4	63 - 99	59.2 - 67	15 / 67	600 / 0.085
2/17/2015 @ 21:55 (shallow)	159.8 [2]	149 – 170.6	0-54	5.3 – 22.7	37 / 22.7	89,043 / 0.67
2/17/2015 @ 21:55 (deep)	155.4 [2]	142.3 – 168.6	63 - 99	5.3 – 22.7	37 / 22.7	56,119 / 0.58
2/19/2015 @ 14:05	144.1 [4]	136.9– 151.4	0-54	34.8 – 42.7	15 / 42.7	13,632 / 1.0

[1] First exposure

[2] Highest estimated median RL for this animal for both shallow and deep estimates

[3] Lowest estimated median RL for this animal

[4] Last exposure

3.2.2.11 SbTag015

SbTag015 (tagged with a SPLASH10 tag) was south of Kaua'i for the ULT (i.e., MFAS activities 2/15/2015 ~22:00 to 2/16/2015 01:30) and thus no path to the source was available to estimate exposure levels (Figure 3.2.2-16; Table 3.2.12). The animal began experiencing exposures 2/17/2015 at 12:01 GMT (Phase B) and had 160 exposures with usable dive depth data and 22 exposures without dive data for a

total of 182 exposures. One exposure had artificially low estimated RLs, which was removed from the original 183 exposures. The grand mean RL was 140.1 dB re 1 µPa, while median RLs ranged from 110.7 – 155.1 dB re 1 µPa, and median RL ± 2*SD were 96.5 – 167.7 dB re 1 µPa.
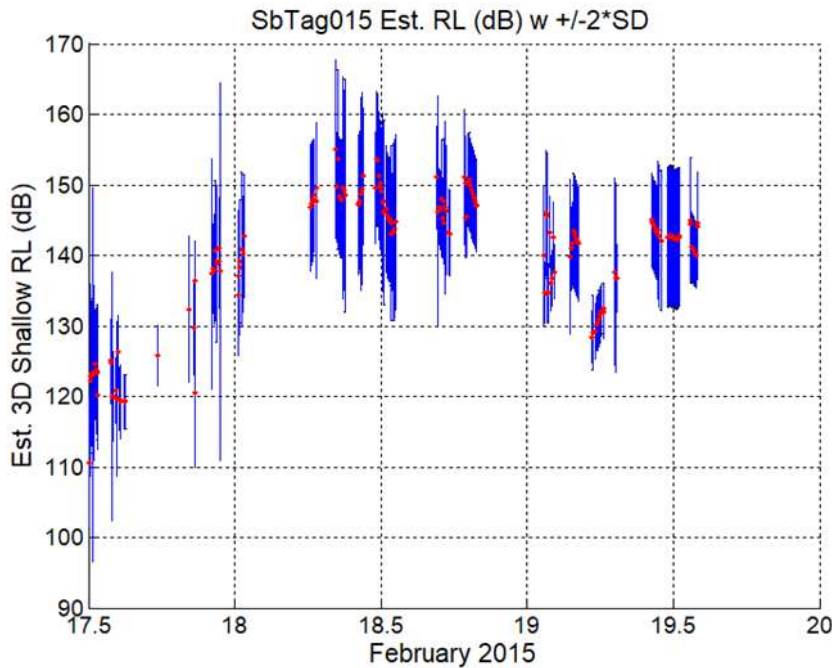
Figure 3.2.2-16. Estimated 3D median RLs (red markers) with ± 2*SD whiskers for SbTag015 over a 2.5-day period (X axis units in days GMT).

Table 3.2.12. Details for selected exposures of the 182 total locations from SbTag015 that overlapped with MFAS.

Date / Time (hh:mm GMT)	Estimated median RL (dB re 1 µPa)	Range of estimated RLs +/- 2*SD shallow	Animal depth range (m)	Min / Max distance from source (km)	# slices / range step (m)	# samples / proportion of samples utilized
2/17/2015 @ 12:01	110.7 [1]	101.6 - 119.8	0 - 54	83.1– 105.7	49 / 105.7	49,416 / 0.996
2/17/2015 @ 12:01	109.4 [3]	96.5 – 167.7	63 - 99	83.1 – 105.7	49 / 105.7	41,180 / 0.996
2/18/2015 @ 08:16	155.1 [2]	142.5 – 167.7	0 - 54	6.6 – 26.7	46 / 26.7	158,616 / 1.0
2/19/2015 @ 14:01	144.6 [4]	137.3 – 151.8	0- 54	31.4 – 39.4	17 / 39.4	16,494 / 1.0

[1] First exposure

[2] Highest estimated median RL for this animal

[3] Lowest estimated median RL for this animal

[4] Last exposure

3.2.2.12 SbTag017

SbTag017 (tagged with a SPLASH10 tag) had 302 locations that overlapped in time with MFAS, of which 295 exposures had estimated RLs with associated dive depths. The seven exposures without RL estimates (e.g. 0 of the TL values were viable to estimate an RL) were a result of those locations not having acoustic paths supported from the source to the animal using the 95% CI error ellipses. In addition, eight further exposures had estimated RLs that exhibited extremely high variations; these were captured in the exposures SDs and are also readily observed in the whiskers plots of all propagation model results. The largest SD of these eight exposures was 34.5 dB, which occurred on 2/17/2016 @ 23:12 GMT, and this extremely high SD causes the median estimated RL +/- 2*SD metric to exceed 200 dB re 1 μPa, even though that exposure's median RL was 132 dB re 1 μPa and its highest propagation modeled estimated RL was only 143.5 dB re 1 μPa. Therefore, the results presented here are for 287 exposures (Figure 3.2.2-17; Table 3.2.13), given further investigation is warranted for these eight exposures before results are presented for them.

Results for 287 exposures show a grand mean of 137.3 dB re 1 μPa, median RLs 103.1 – 146.7 dB re 1 μPa, and estimated median RLs -/+ 2*SD of 73.0 – 155.9 dB re 1 μPa (Figure 3.2.2-17). Figure 3.2.2-17 shows fairly well behaved estimated RLs, with the maximum estimated RLs slightly over 155 dB re 1 μPa for the estimated medians + 2*SD. The majority of estimated 3D RLs were over 115 dB re 1 μPa, however the median estimated RL – 2*SD minimum was 73 dB re 1 μPa appears to be an outlier, which also warrants additional investigation.

The majority of the dive depths (267 of the 287) were within 0-54 m, with the deepest dive of 127.5 m. The fraction of TLs utilized in the 3D estimated RL was over 0.98 for 204 of the exposures, with the lowest value of 0.065 and only a total of 8 samples under 0.5.
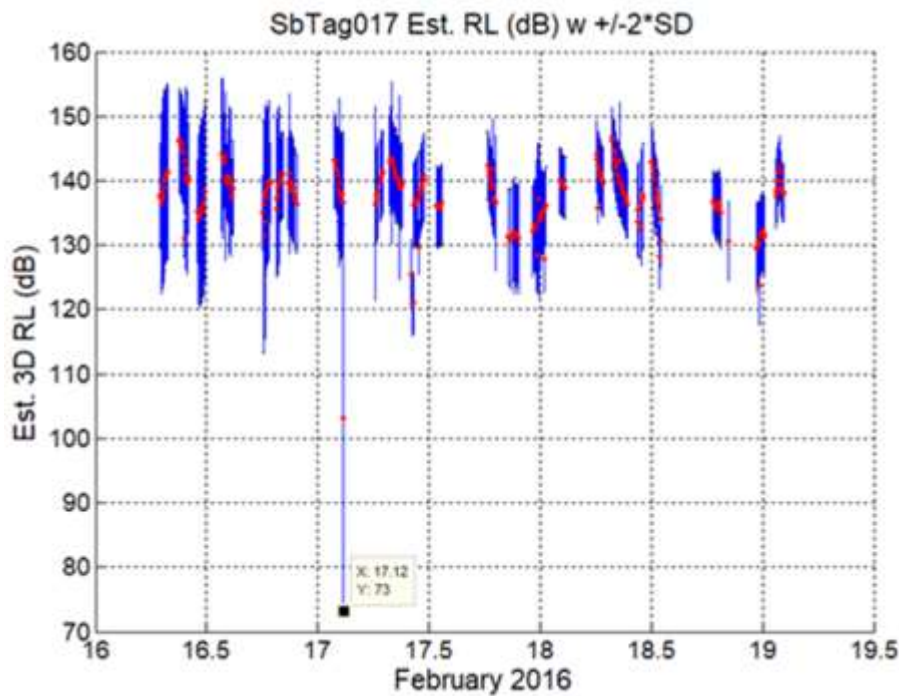
Figure 3.2.2-17. Estimated 3D median RLs (red markers) with ± 2*SD whiskers for SbTag017 over a 3.5-day period (X axis units in days GMT).

Table 3.2.13. Details for selected exposures of the 287 total locations from SbTag017 that overlapped with MFAS.

Date / Time (hh:mm GMT)	Estimated median RL (dB re 1 µPa)	Range of estimated RLs +/- 2*SD shallow	Animal depth range (m)	Min / Max distance from source (km)	# slices / range step (m)	# samples / proportion of samples utilized
2/16/2016 @ 07:02	137.4 [1]	129.5 - 145.4	0 - 54	64.4 – 68.1	23 / 68.1	6.012 / 1.0
2/17/2016 @ 02:47	103.1 [3]	73 – 133.2	0 - 54	49.9 – 53.7	19 / 53.7	432 / 0.065 [5]
2/18/2016 @ 07:47	146.7 [2]	142.1 – 151.3	0 - 54	30 – 32.9	21 / 32.9	8,790 / 1.0
2/19/2016 @ 02:17	138.2 [4]	133.9 – 142.6	0 - 54	40.6 – 45.7	25 / 45.7	12,834 / 1.0

[1] First exposure

[2] Highest estimated median RL for this animal

[3] Lowest estimated median RL for this animal

[4] Last exposure

[5] exposure with minimum diagnostic (fraction of TLs used in 3D estimated)

3.2.2.13   SbTag018

SbTag018 (tagged with a SPLASH10 tag) had 300 locations that overlapped with MFAS in this analysis; all 300 had valid dive depths. The tag's data were similar to SbTag017 in that multiple exposures had clusters of estimated RLs well under their median values (Figure 3.2.2-18, Table 3.2.14). For example, four exposures had a cluster of estimated RLs under - 93 dB re 1 µPa, with 3 exposures having a cluster between 0 and -80 dB re 1 µPa. The other exposures had isolated clusters of estimated RLs between 70 and 0 dB re 1 µPa. For expediency, these 10 exposures were removed from this analysis resulting in estimated 3D RLs being presented for 290 exposures. More analysis is warranted to understand the reasons for these 10 exposures having clusters of estimated RLs isolated to the majority of the estimated 3D RLs.

The grand mean of the estimated mean RLs for the 290 exposures analyzed was 140.9 dB re 1 µPa. The range of estimated median RLs varied from 117.2 to 157.1 dB re 1 µPa while the range of the median estimated RLs -/+ 2*SD was 114.9 to 163.6 dB re 1 µPa. Dives occurred in 3 periods separated by over half a day of no dives deeper than 54 m. The diagnostic fraction of TLs utilized in the 3D estimated RLs had 220 of the 290 estimates with fractions of 1.0 with the lowest fraction at 0.69.
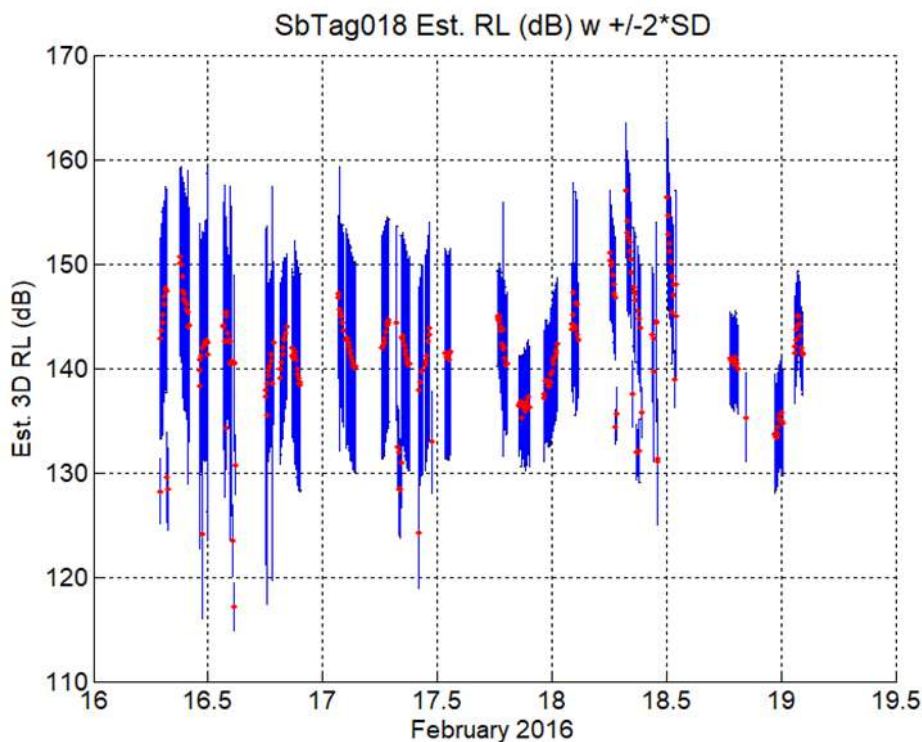
Figure 3.2.2-18. Estimated 3D RLs with median values (red markers) and whiskers depicting +/- 2*SD for SbTag018 over a 3.5-day period (GMT).

Table 3.2.14. Details for selected exposures of the 290 total locations from SbTag018 that overlapped with MFAS.

Date / Time (hh:mm GMT)	Estimated median RL (dB)	Range of estimated RLs +/- 2*SD shallow	Animal depth range (m)	Min / Max distance from source (km)	# slices / range step (m)	# samples / proportion of samples utilized
2/16/2016 @ 07:01	142.8[1]	133.2 - 152.4	0 - 54	48.8 – 51.1	21 / 51.1	4,470 / 1.0
2/16/2016 @ 14:46	117.2 [3]	114.9 – 119.4	63 - 81	51.5 – 54.4	15 / 54.4	1,896 / 1.0
2/18/2016 @ 07:46	157.1 [2]	150.6 – 163.5	0 - 54	11.2 – 13.1	22 / 13.1	14,862 / 1.0
2/19/2016 @ 02:16	141.3 [4]	137.3 – 145.2	0 - 54	35.3 – 39.8	21 / 39.8	11,628 / 1.0

[1] First exposure

[2] Highest estimated median RL for this animal

[3] Lowest estimated median RL for this animal

[4] Last exposure

3.2.2.14 TtTag034

The results for TtTag034 (tagged with a SPLASH10 tag) using the crawl track fixed (i.e., re-routed off land) had 39 locations that overlapped with MFAS, and all 39 locations had valid dive data for the animal. The grand mean of the 39 exposures was 133.4 dB re 1 µPa, with median RLs ranging from 122.5 to 145.7 dB re 1 µPa, and median estimated RLs +/- 2*SD of 113.9 – 154.0 dB re 1 µPa (Table 3.2.15). Figure 3.2.2-19 provides the estimated median RLs with whiskers representing +/- 2*SD over time.
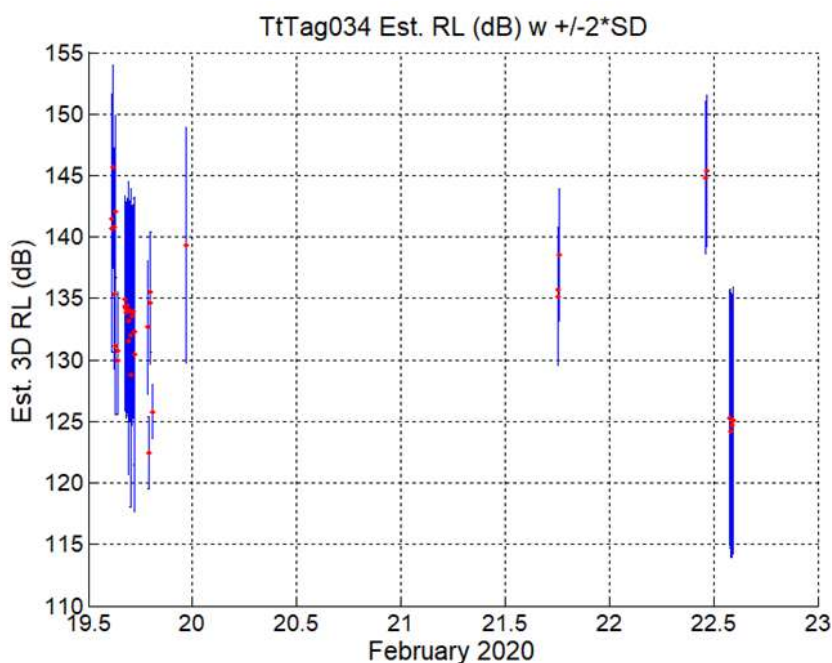
Figure 3.2.2-19. TtTag034 estimated RLs (red points) with +/- 2*SD whiskers over a 3.5-day period (GMT). Crawl data used for these RL estimates was re-routed around land.

Table 3.2.15. Details for 4 exposures, the first, last, highest and lowest estimated RL for TtTag034.

Date/Time (hh:mm GMT)	Estimated median RL (dB re 1 µPa)	Range of estimated RLs +/- 2*SD	Animal depth range (m)	Min / Max distance from source (km)	# slices / range step (m)	# samples / proportion of samples utilized
2/19/2020 @ 14:45	141.5 [1]	131.3 - 151.7	162 - 189	17.8 – 42.1	51 / 42.1	52,018 / 0.57
2/19/2020 @ 14:50	145.7 [2]	137.5 – 153.9	0 - 54	19.9 – 44.2	49 / 44.2	90,500 / 0.71
2/19/2020 @ 18:55	122.5 [3]	119.6 – 125.4	333 - 396	51.3 – 57.7	13 / 57.7	1,757 / 0.19
2/22/2020 @ 14:15	125.1 [4]	114.3 – 135.9	0 - 54	36 – 59.1	49 / 59.1	59,017 / 0.65

[1] First exposure

[2] Highest estimated median RL for this animal

[3] Lowest estimated median RL for this animal

[4] Last exposure

3.2.2.15 TtTag035

The overall results for TtTag035 (tagged with a SPLASH10 tag) using the crawl track re-routed around land had two exposures removed from the analysis due to having a cluster of estimated RLs < 0 dB, resulting in 41 of the 43 exposures in the down-sampled set being analyzed. The clusters of extremely low estimated RL are due to effects as described earlier and require more manual investigation to fully understand which slices had issues or whether seafloor boundary effects are causing the unrealistic TLs leading to RLs below 0 dB. Inclusion of these data makes the SD extremely large (e.g. 22 and 18.4 dB re 1 µPa in these cases), which resulted in the median estimated RL +/- 2*SD going far beyond the actual measured values of min/max RLs. For this reason, they have been removed, and a detailed investigation can confirm the cause(s) and identify the relevant depth/range/azimuth data for removal to potentially retain the exposures in this analysis. Figure 3.2.2-20 illustrates the median estimated RL +/- 2*SD for the 41 exposures. All 41 exposures had depth data available.

The grand mean for TtTag035 was 129.1 dB re 1 µPa, with median estimated RLs ranging from 118.6 to 146 dB re 1 µPa, and estimated median RLs +/- 2*SD ranging from 110.1 to 151.9 dB re 1 µPa (Table 3.2.16).
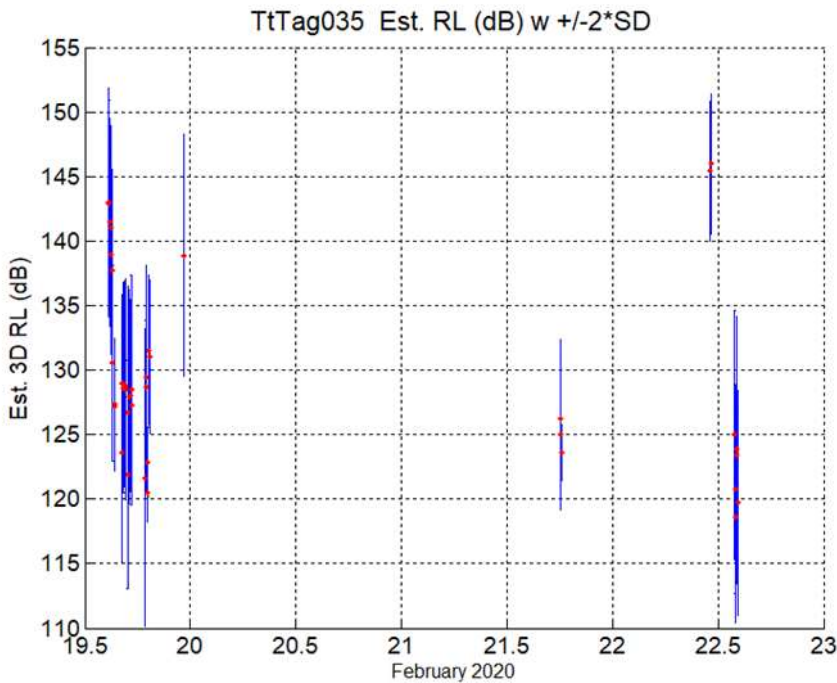
Figure 3.2.2-20. Estimated 3D median RLs (red markers) with ± 2*SDs whiskers for TtTag035 over a three and a half-day period (X-axis label in days GMT). This is for the 41 exposures (2 removed for reasons noted in text) and RL estimates shown here were derived from crawl mean positions re-routed to be off land.

Table 3.2.16. Details for selected exposures of the 41 total locations from TtTag035 that overlapped with MFAS.

Date/Time (GMT)	Estimated median RL (dB)	Range of estimated RLs +/- 2*SD	Animal depth range (m)	Min / Max distance from source (km)	# slices / range step (m)	# samples / proportion of samples utilized
2/19/2020 @ 14:45	143 [1]	134.2 - 151.9	0 - 54	22.4 – 43.6	43 / 43.6	79,402 / 0.81
2/22/2020 @ 11:10	146.0 [2]	140.6 – 151.4	0 - 54	18.6 – 36.7	37 / 36.8	38,591 / 0.45
2/22/2020 @ 14:00	118.6 [3]	110.4 – 126.8	234 - 279	40.5 – 61.5	43 / 61.9	32,517 / 0.48
2/22/2020 @ 14:15	119.7 [4]	111.0 – 128.4	216 - 261	38.3 – 58.9	41 / 58.3	33,531 / 0.489

[1] First exposure

[2] Highest estimated median RL for this animal

[3] Lowest estimated median RL for this animal

[4] Last exposure

3.3 EXPOSURE AND RESPONSE ANALYSIS

The following sections document the movements and estimated RLs for short-finned pilot whales, rough-toothed dolphins, and bottlenose dolphins across phases from five separate SCC training events. In addition, dive and surface statistics were examined across phases and during day and night times for changes in dive behavior. Kruskal-Wallis one-way ANOVA tests were used to identify the presence of significant differences in dive depth and duration among SCC phases, and post-hoc Dunn's tests were conducted to identify which phases were significantly different. When reviewing the following results it is important to remember the phases of the SCC training event include: Pre-Phase A (before the SCC training event), Phase A (does not include surface ship hull mounted MFAS and surface ship combatants are not present), Inter Phase A-B (typically a weekend period between Phase A and B, Phase B (includes surface ship hull mounted MFAS and surface ship combatants are present), and Post-Phase B (after the SCC training event). For comparisons of dive statistics among exposure periods, only 3 days of data post-phase B were used for tags with >3 days of dive/surfacing data.

3.3.1 Pilot Whale Tag Analysis

Table 3.3.1. Percentage of dive/surfacing data by phase for short-finned pilot whales.

	Percentage of dive/surfacing data				
Individual	Pre-Phase A	Phase A	Inter Phase A-B	Phase B	Post-Phase B
GmTag081					
Duration overall (days)	9.2	2.1	3.1	2.7	5.2
Days surfacing/dive data	9.1	2.1	3.1	2.7	5.2
Percentage coverage	98.9	99.2	99.0	100.0	99.4
GmTag082					
Duration overall (days)	0.1	2.1	3.1	2.7	2.9
Days surfacing/dive data	0.1	0.0	0.2	0.1	0.2
Percentage coverage	100.0	0.0	6.0	5.3	5.8
GmTag152					
Duration overall (days)	0.0	2.2	2.8	2.9	4.1
Days surfacing/dive data	0.0	0.0	2.0	2.8	4.1
Percentage coverage	0.0	0.0	70.7	97.4	100.0
GmTag153					
Duration overall (days)	0.0	2.2	2.8	2.9	4.1
Days surfacing/dive data	0.0	0.0	1.1	1.9	3.8
Percentage coverage	0.0	0.0	39.0	67.1	93.8
GmTag214					
Duration overall (days)	0.0	2.0	4.0	0.3	5.6
Days surfacing/dive data	0.0	0.0	2.5	0.3	5.5
Percentage coverage	0.0	0.0	63.0	100.0	98.9
GmTag231					
Duration overall (days)	0.4	2.2	4.2	3.0	0.0

Individual	Percentage of dive/surfacing data				
	Pre-Phase A	Phase A	Inter Phase A-B	Phase B	Post-Phase B
Days surfacing/dive data	0.4	2.1	3.2	2.8	0.0
Percentage coverage	100.0	98.7	75.4	92.3	100.0

Table 3.3.2. A comparison of night-time diving parameters from short-finned pilot whales exposed to MFAS. Note, tags in decreasing order of estimated maximum median MFAS RLs. Kruskal-Wallis one-way ANOVA significant results (i.e., significant differences among phases were detected) are shown in bold. Pairs of phases where significant differences were detected are listed in the associated post-hoc Dunn's test column (level of significance 0.05).

Dive parameter per individual	Pre-Phase A	Phase A	Inter-Phase A-B	Phase B	Post-Phase B	Kruskal-Wallis Test p-value*	Post-hoc Dunn's test significant pairs
Night-time dive rate (dives/hour)							
GmTag081	3.2	3.4	3.4	2.2	3.8	-	
GmTag231	3.7	3.0	3.3	3.2	4.9	-	
GmTag153	NA	NA	4.0	4.4	3.3	-	
GmTag152	NA	NA	3.9	3.2	2.9	-	
GmTag214	NA	NA	3.4	2.8	2.9	-	
% time in surface periods at night							
GmTag081	52.6	39.0	50.8	70.0	49.6	-	
GmTag231	47.8	52.1	46.9	51.9	39.7	-	
GmTag153	NA	NA	29.0	32.2	43.2	-	
GmTag152	NA	NA	32.5	36.0	40.3	-	
GmTag214	NA	NA	37.0	52.1	48.9	-	
Median dive depth night (m)							
GmTag081	**106.5**	**207.5**	**143.5**	**123.5**	**115.5**	**<0.001**	**A–Inter; A–B; A–Post-B; Inter–Post-B; A–Pre-A; B–Pre-A**
GmTag231	**305.5**	**311.5**	**211.5**	**167.5**	**119.5**	**0.001**	**A–B**
GmTag153	NA	NA	233.5	235.5	359.5	0.105	NA
GmTag152	**NA**	**NA**	**231.5**	**287.5**	**319.5**	**<0.001**	**Inter–B; Inter–Post-B; B–Post-B**
GmTag214	NA	NA	335.5	487.5	279.5	0.597	NA

Dive parameter per individual	Pre-Phase A	Phase A	Inter-Phase A-B	Phase B	Post-Phase B	Kruskal-Wallis Test p-value*	Post-hoc Dunn's test significant pairs
Median dive duration night (min)							
GmTag081	**9.00**	**10.10**	**8.30**	**7.90**	**8.33**	**<0.001**	**A–Inter; A–B; A–Post-B; A–Pre-A; Post-B–Pre-A**
GmTag231	8.62	10.03	9.73	8.83	7.77	0.113	NA
GmTag153	NA	NA	11.18	9.50	11.17	**0.016**	**Inter–B; B–Post-B**
GmTag152	**NA**	**NA**	**11.00**	**12.57**	**12.53**	**<0.001**	**Inter–B; Inter–Post-B**
GmTag214	NA	NA	12.08	12.02	11.07	0.217	NA

*Values for dive rates and percentage time in surface periods represent single values for each individual for each period, thus no statistical testing was undertaken.

Table 3.3.3. A comparison of day-time diving parameters from short-finned pilot whales exposed to MFAS. Note, tags are presented in decreasing order of estimated maximum median MFAS RLs. Kruskal-Wallis one-way ANOVA significant results (i.e., significant differences among phases were detected) are shown in bold. Pairs of phases where significant differences were detected are listed in the associated post-hoc Dunn's test column (level of significance 0.05).

Dive parameter per individual	Pre-Phase A	Phase A	Inter-Phase A-B	Phase B	Post-Phase B	Kruskal-Wallis Test p-value*	Post-hoc Dunn's test significant pairs
Day-time dive rate (dives/hour)							
GmTag081	1.7	2.1	2.3	1.1	1.3		
GmTag231	1.3	1.2	1.2	0.9	NA		
GmTag153	NA	NA	5.9	7.4	1.7		
GmTag152	NA	NA	1.5	0.7	0.9		
GmTag214	NA	NA	0.77	NA	0.97		
% time in surface periods during day							
GmTag081	66.9	78.0	67.9	78.4	74.9		
GmTag231	82.8	78.1	77.0	80.8	NA		
GmTag153	NA	NA	29.6	40.4	77.3		
GmTag152	NA	NA	69.9	82.8	74.9		
GmTag214	NA	NA	84.44	NA	80.76		
Median dive depth day (m)							

Dive parameter per individual	Pre-Phase A	Phase A	Inter-Phase A-B	Phase B	Post-Phase B	Kruskal-Wallis Test p-value*	Post-hoc Dunn's test significant pairs
GmTag081	387.5	34.5	35	719.5	471.5	<0.001	A–B; Inter–B; A–Post-B; A–Post-B; Inter–Post-B; B–Post-B; A–Pre-A; Inter–Pre-A; B–Pre-A
GmTag231	75.5	527.5	291.5	497.5	NA	0.048	B–Pre-A
GmTag153	NA	NA	48	40	42	0.012	Inter–B
GmTag152	NA	NA	575.5	583.5	599.5	0.267	NA
GmTag214	NA	NA	327.5	NA	247.5	0.735	NA
Median dive duration day (min)							
GmTag081	11.73	3.97	5.70	13.50	12.50	<0.001	A–Inter; A–B; Inter–B; A–Post-B; Inter–Post-B; A–Pre-A; Inter–Pre-A
GmTag231	7.43	12.50	11.63	12.73	NA	0.032	Inter–Pre-A; B–Pre-A
GmTag153	NA	NA	6.18	3.95	6.03	<0.001	Inter–B; B–Post-B
GmTag152	NA	NA	13.63	15.40	16.57	<0.001	Inter–Post-B
GmTag214	NA	NA	12.43	NA	13.07	0.832	NA

*Values for dive rates and percentage time in surface periods represent single values for each individual for each period, thus no statistical testing was undertaken.
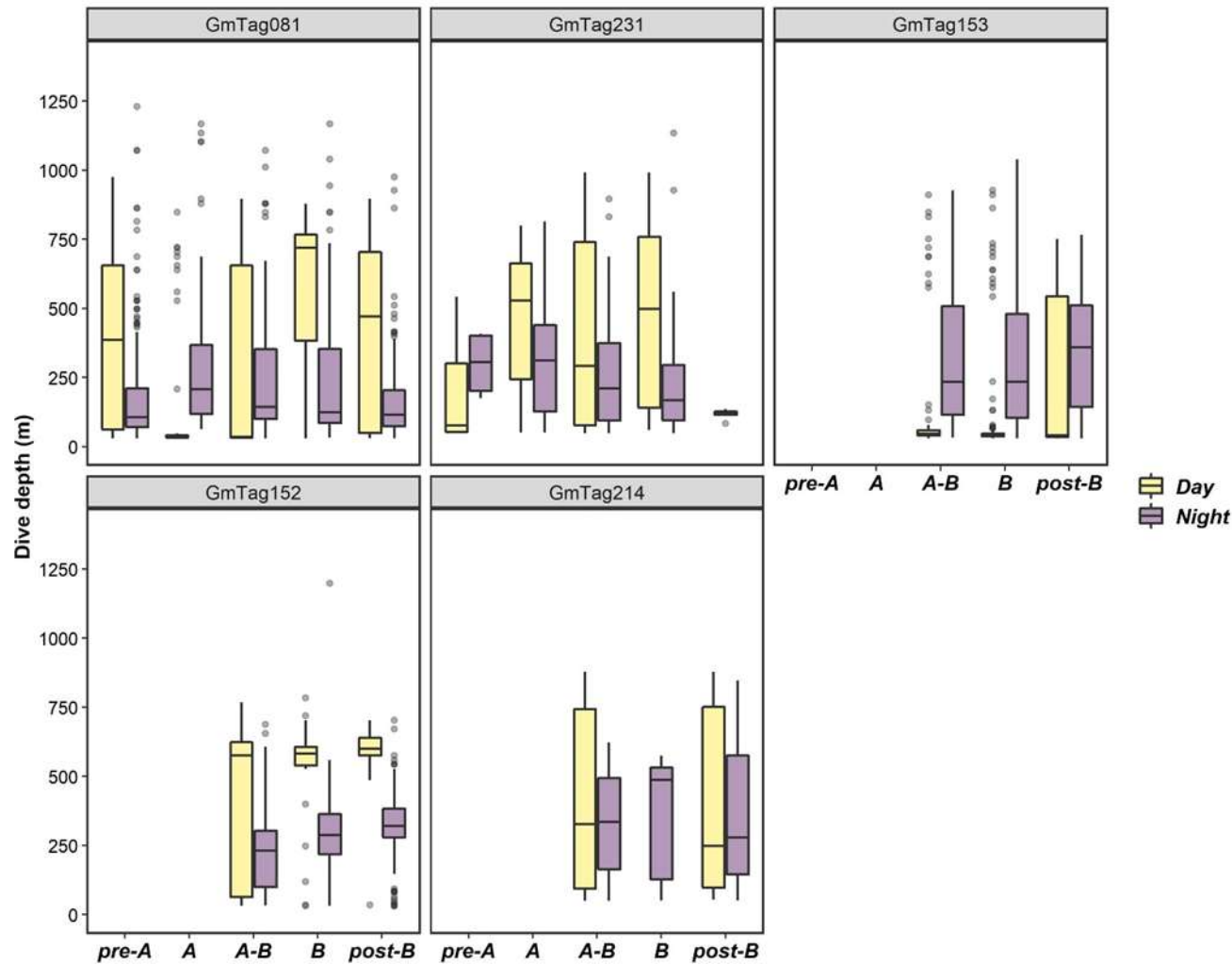
Figure 3.3.1-1. Distribution of dive depths by exposure/SCC phase, colored by day/night, for each short-finned pilot whale with a SPLASH tag deployment. Tags are ordered left to right with decreasing maximum median estimated RL (RL). Lower and upper hinges correspond to the first and third quartiles (25th and 75th percentiles) and the upper and lower whiskers extend from the hinges to +/- 1.5*IQR (interquartile range), respectively. The horizontal line within each box represents the median value, and outliers are shown as gray points. Note GmTag082 is excluded due to inadequate coverage over Phase B and post-Phase B.

3.3.1.1 GmTag081, GmTag082, GmTag083

These three individuals were tagged within the same group and generally remained associated over the period of tag attachment. Information was available on movement patterns for pre-Phase A (3+ days), as well as all of Phase A (2.1 days), the inter-phase period (3.1 days), all of Phase B, and a period post-Phase B (8+ days; Table 3.3.1). Although all three remained generally associated (distance apart means ranging from 2.21-3.87 km; medians ranging from 1.64-2.8 km), individuals did move maximum distances apart ranging from 10.7 to 25.7 km, and these differences in locations influenced RLs (see below).

Prior to Phase A, the three individuals were primarily on the southern half of the range (i.e., south BSURE and all of BARSTUR), but moved 25-35 km south of the range starting two days prior to Phase A. During Phase A the whales remained 20-40 km south of the range. The whales remained south of the range during the two days post-Phase A, but then moved north onto the eastern part of the range in the 15 hours prior to the start of Phase B. All three whales were on the range at the start of MFAS use and moved off the range about two hours later (approximately 5 km east of range); they stayed off-range for about 4.5 hours and then returned onto the range approximately 6.5 hours after the start of Phase B, and remained on the range for almost two days. No large-scale movements of the individuals away from areas of relatively high RLs, for example to areas in the lee of Kaua'i or Ni'ihau, were observed, and all three moved into areas with higher RLs during the period of overlap. The highest median RLs varied among the three individuals. GmTag081 was exposed at estimated RLs exceeding 160 dB re 1 µPa on two different days for three different exposures (two at the surface and one at an estimated 55 m depth), with the highest estimated median level of 162.8 dB re 1 µPa (SD=10.7 dB). GmTag082 had estimated RLs exceeding 160 dB re 1 µPa for nine exposures (over a 45-min span), all at the surface, with the highest estimated median RL of 175.4 dB re 1 µPa (SD=9.7 dB). GmTag083 had estimated RLs exceeding 160 dB re 1 µPa on two different days during Phase B, all at the surface. These included a single exposure with a median RL of 161.0 dB re 1 µPa (SD=3.25 dB), six exposures (over a 23-minute span) with the highest median RL of 162.1 dB re 1 µPa (SD=4.9 dB), and another eight exposures (over a 40-minute span) with the highest median RL of 176.6 dB re 1 µPa (SD=9.3 dB). Differences among the three individuals reflect location distances relative to the MFAS source (Figure 3.3.1-2, Figure 3.3.1-3).

Both GmTag081 and GmTag082 transmitted dive and surfacing data during all exposure phases (pre-Phase A, Phase A, inter-phase, Phase B, and post-Phase B); GmTag083 was a location-only tag, and thus no dive behavior data was transmitted. Although information on dive/surfacing behavior was available for both GmTag081 and GmTag082, coverage for GmTag082 was very limited over the exposure phases (Table 3.3.1), and thus, we only discuss dive behavior in relation to exposure periods for GmTag081, which had much higher percentage data coverage (Table 3.3.1). This individual's night-time dive rate remained relatively consistent among exposure phases, although slightly lower during Phase B (2.2 dives/hour; Table 3.3.2), and the proportion of its time at the surface during the night varied, ranging from 39% during Phase A to 70% during Phase B and around 50% during other phases (Table 3.3.2). Night-time dive depth and duration varied significantly among exposure phases (Kruskal-Wallis One-Way ANOVA, $p < 0.001$ for both), where dives were the shallowest and shortest during pre-Phase A with an increase (i.e., deeper and longer) during Phase A followed by a gradual decrease (i.e., shallower, shorter) throughout the rest of the SCC (Table 3.3.2, Figure 3.3.1-1). Day-time dive and surfacing behavior was relatively consistent, with the lowest dive rate (1.1 dives/hour) and greatest percentage at surface (78.4

percent) occurring during Phase B (Table 3.3.3). However, day-time dive depths and durations varied significantly among exposure phases (Kruskal-Wallis One-Way ANOVA, p < 0.001 for both) (Table 3.3.3). For example, median day-time dive depths during Phase A and the inter-phase period were as low as 34.5 m and during Phase B was 719.5 m (Table 3.3.3). Similarly, day-time dive durations were much shorter during Phase A and the inter-phase period (3.97 min and 5.70 min, respectively) compared to the rest of the phases which were more similar (11.73-13.50 min, Table 3.3.3). Given the high median estimated RLs this individual was exposed to we might expect to see differences in dive and surfacing behavior between Phase B and post-Phase B; however, the most drastic differences in dive statistics occurred during Phase A and the inter-phase period (Table 3.3.2, Table 3.3.3).
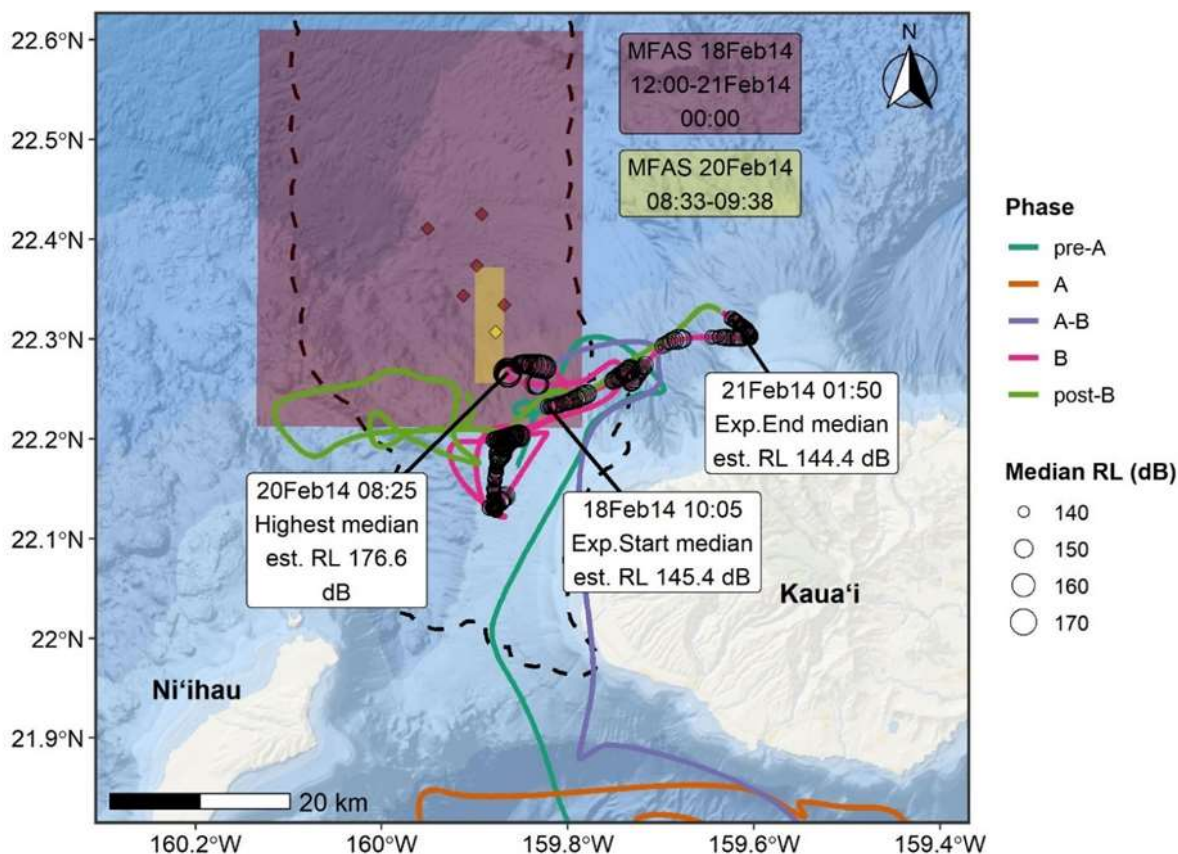
Figure 3.3.1-2. Movements of GmTag083 during the Feb 2014 SCC event. Crawl tracks are colored by phase; see text for description of phases. Median estimated RLs (RL) are plotted as open circles, with the size of the circle scaled to RL level. Shaded boxes represent area of ship activity during blocks of MFAS use (for time periods as specified), and corresponding colored diamond points represent the mean ship location for that time period. For the red-shaded box, the five mean ship position points correspond to mean positions at 12-hour intervals over that time period. The dashed black line represents the PMRF boundary.
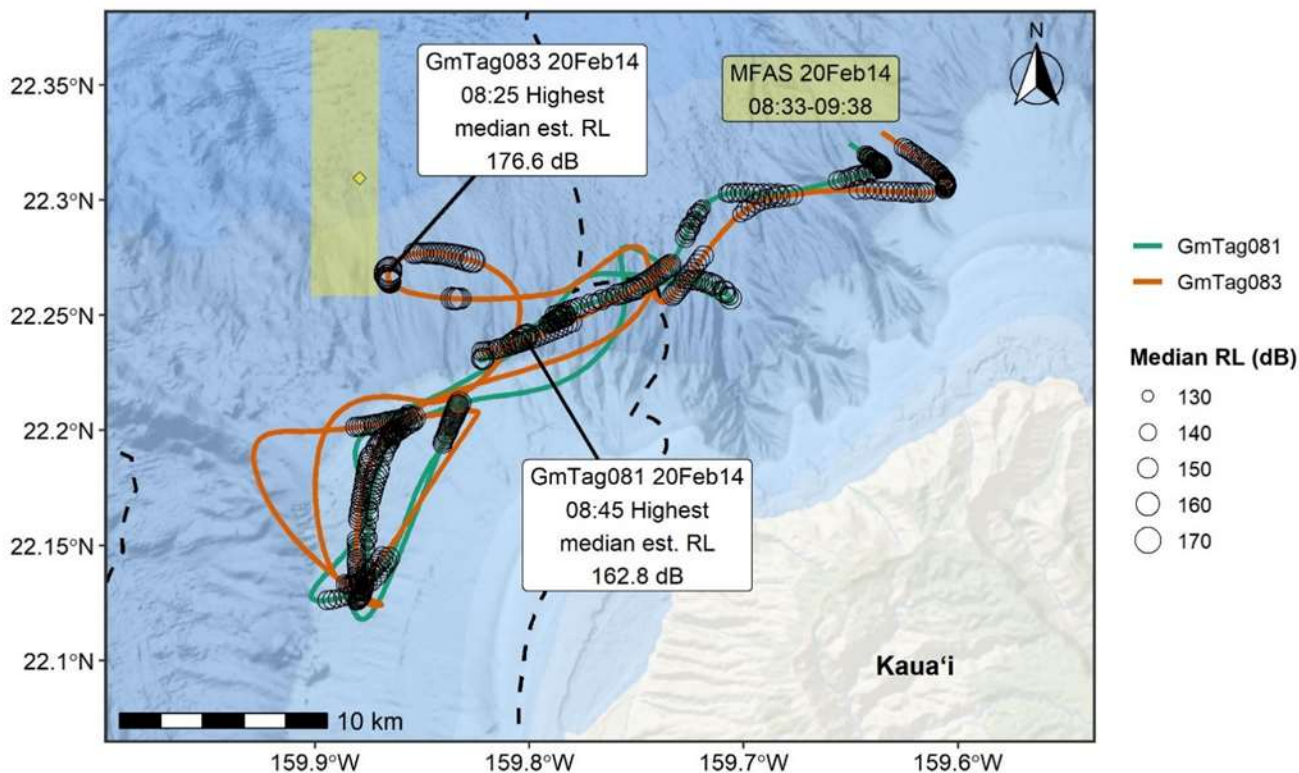
Figure 3.3.1-3. Movements of GmTag081 and GmTag083 during Phase B (MFAS use) of the Feb 2014 SCC event, highlighting the relationship between whale proximity to source and RLs (RL). Crawl tracks are colored by tag ID (only Phase B shown); see text for description of phases. Median estimated RLs are plotted as open circles, with the size of the circle scaled to RL level. Shaded box represents area of ship activity during blocks of MFAS use (for time periods as specified), and corresponding colored diamond point represents the mean ship location for that time period. The dashed black line represents the PMRF boundary.

3.3.1.2   GmTag115

Movement data for this individual was available for periods prior to Phase A (3.1 days), all of Phase A (2.9 days), the inter-phase period (2.5 days) and part of Phase B (1.4 days or 67% of Phase B) when this tag stopped transmitting, and thus, no information was available for the period following Phase B (Table 3.3.1). In addition to MFAS use during Phase B, during this SCC event (February 2015), a ULT was conducted prior to the start of Phase B such that RLs could be estimated for this individual during both the ULT and Phase B.

GmTag115 was tagged on the south end of BSURE and moved approximately 55 km north, within the range boundary, over the next 30 hours before moving southwest and off of the range (approximately 125 km SW of Ni'ihau) over the 3 days prior to the start of Phase A (Figure 3.3.1-4). During Phase A, this individual remained south of Ni'ihau for 1 day and then moved far offshore northwest of Kaua'i/Ni'ihau (127 km from western edge of PMRF, 126 km from westernmost coast of Ni'ihau). At the start of the

inter-phase period, this individual moved south and west (~50 km) before turning east, moving towards Niʻihau. The ULT occurred shortly after this directional change and median RL estimates gradually increased as the whale moved east, reaching a maximum of 120.3 dB re 1 µPa (SD=2.66 dB) over a total span of 125 minutes (out of 22 exposures) (Figure 3.3.1-4). Following the ULT, this individual continued to move east and was approximately 27 km west of Niʻihau at the beginning of Phase B. At the start of Phase B, this individual moved northeast and briefly entered the southwest edge of BSURE, where it was exposed to its highest median estimated RL of 157.5 dB re 1 µPa (SD=5.19 dB) of 10 exposures over a 45-min span. After this exposure, this animal reversed its direction and moved approximately 32 km southwest for 10 hours until the tag stopped transmitting (**Error! Reference source not found.**). RL estimates increased from 132.4 dB re 1 µPa (SD=4.39, over 45-min span) up to the highest estimated exposure inside the range and generally decreased as the individual reversed and moved away from the range (minimum post-highest exposure level: 139.4 dB re 1 µPa (SD=3.92 dB) over 1-hour span), thus reflecting the whale's proximity to the source. Because this individual was tagged with a location-only tag, RLs were estimated near the surface (< 54 m depth) and the region past 54 m to the species' typical dive depths (short-finned pilot whale typical dive depth = 500 m).
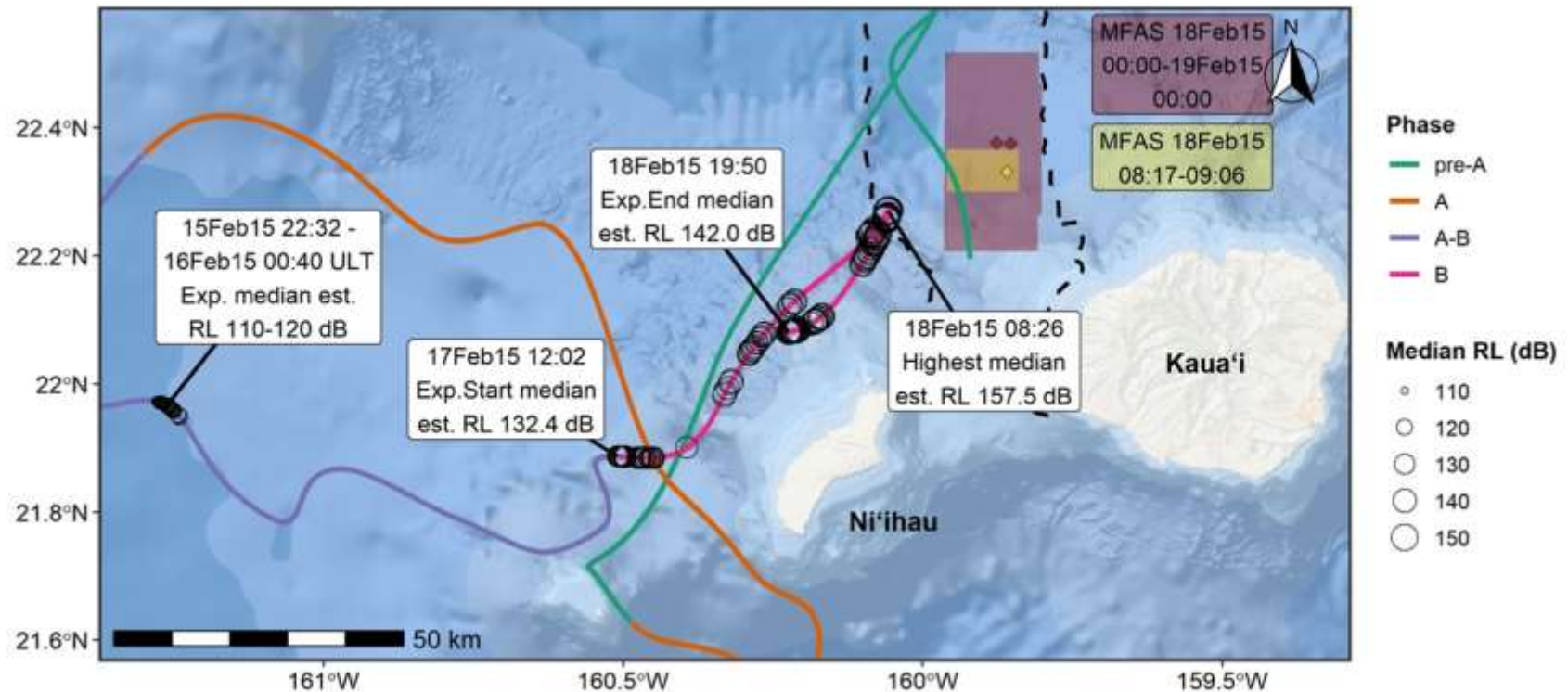
Figure 3.3.1-4. Movements of GmTag115 during the Feb 2015 SCC event. Crawl tracks are colored by phase; while MFAS is normally only used during Phase B, an additional unit-level test (ULT) was conducted during the interval between Phase A and B (beginning 15 February 2015) from which RLs (RL) could be estimated. Median estimated RLs are plotted as open circles, with the size of the circle scaled to RL level. Shaded boxes represent area of ship activity during blocks of MFAS use (for time periods as specified), and corresponding colored diamond points represent the mean ship location for that time period. For the red-shaded box, the two mean ship position points correspond to mean positions at 12-hour intervals over that time period. The dashed black line represents the PMRF boundary.
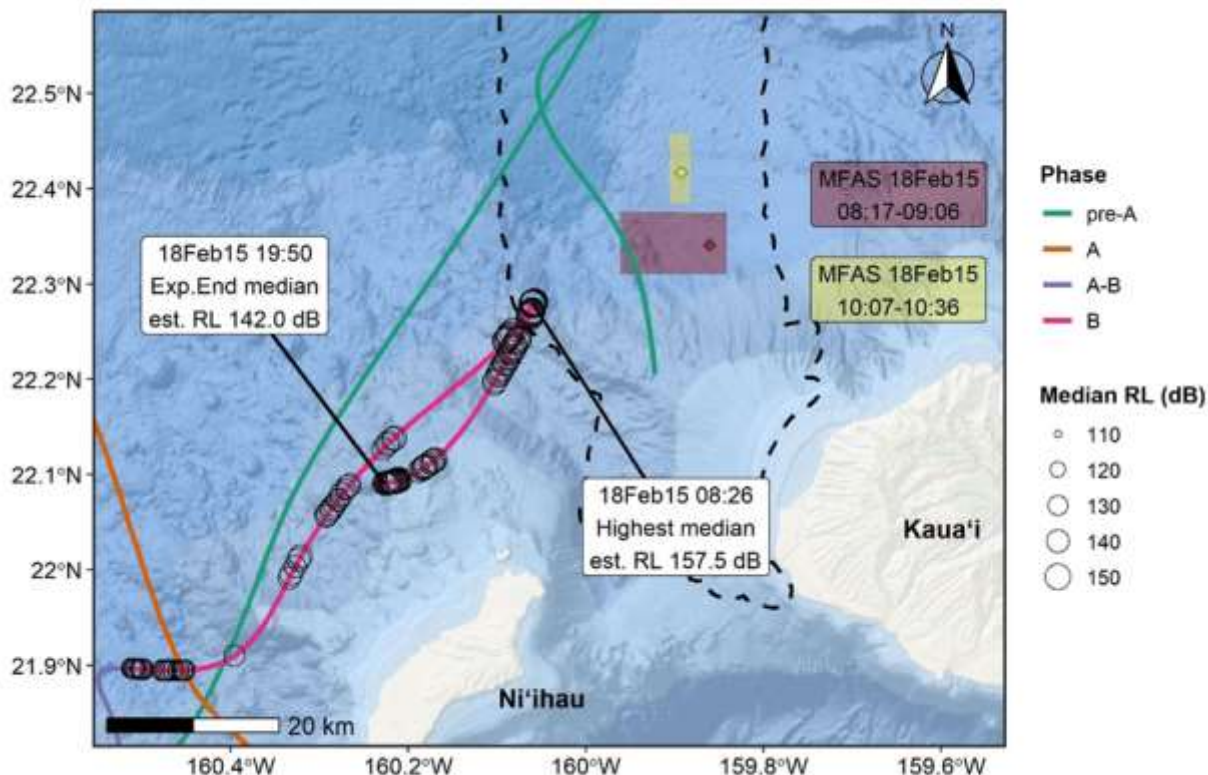
Figure 3.3.1-5. Movements of GmTag115 during the Feb 2015 SCC event, zoomed-in to the period of directional change after entry onto PMRF/highest exposure. Crawl tracks are colored by phase. Median estimated RLs (RL) are plotted as open circles, with the size of the circle scaled to RL level. Shaded boxes represent area of ship activity during blocks of MFAS use (for time periods as specified), and corresponding colored diamond points represent the mean ship location for that time period. The dashed black line represents the PMRF boundary.

3.3.1.3 GmTag231

Satellite tag data from this deployment was available for pre-Phase A (3.4 days), Phase A (2.2 days), the inter-phase period (4.2 days), Phase B (3 days), and post-Phase B (2.7 days) (Table 3.3.1). Although more than 2 days of movement data were available following Phase B, behavior data (dive/surfacing) only transmitted within a few hours after the end of Phase B. This individual was tagged south of Kaua'i and in the days preceding Phase A travelled along the west coast of Kaua'i, passing through BARSTUR/south BSURE, to offshore waters north of Kaua'i (Figure 3.3.1-6). This whale then moved west onto the south end of BSURE and occupied this region for all of Phase A (2+ days) and about half of the inter-phase period. In the ~2 remaining days of the inter-phase period, this individual exited the southeast side of BSURE and moved north (parallel to the range) approximately 55 km, maintaining a 10-30 km distance from the eastern boundary of the range throughout this time. For the first day of Phase B this individual had median exposure levels ranging from 130.2 dB re 1 µPa (SD=1.65 dB) to 149.6 dB re 1 µPa (SD=1.45 dB) (exposure periods ranging from 25-90 minutes, total of 30 exposures), all of which were either at the surface or shallow dive depths (25-60 m), and moved 15-20 km northeast (away from the range). In the following day, this whale moved 15-20 km back to its original position at the start of Phase B (where exposures occurred), and then south and gradually west (~55 km total) back onto the range in the same

general area it occupied during Phase A and the inter-phase period (south BSURE/north BARSTUR). This whale stayed in this region, which overlapped with MFAS activity, through the end of Phase B and no large or frequent movements were made in relation to areas with high median estimated RLs. The highest estimated median exposure level was 155.2 dB re 1 µPa (SD=1.60 dB) (over 10-minute time span, 2 exposures) where the animal was at the surface (preceding a 655 m dive depth) and occurred near the end of Phase B where the whale was approximately 10-15 km from the mean ship position for the 12-hour period that this exposure took place. After Phase B, this individual stayed on the range slightly west of the region of high MFAS exposure for 2 days, and then moved west and outside of the range over the next 3 days.

GmTag231 was within range of both Kaua'i and Ni'ihau Motes for part of its deployment period, thus increasing throughput of dive and surfacing data. Dive and surfacing data transmitted during all phases before, during, and after MFAS use (i.e., pre-Phase A, Phase A, inter-phase A-B, Phase B, and post-Phase B), although limited data is available during the pre-phase A period (deployed shortly before Phase A) and post-Phase B period (just an hour following the end of phase B, night-time only) when behavior data stopped transmitting (Table 3.3.1). A Kruskal-Wallis One-way ANOVA indicated a significant difference in night-time dive depths among exposure periods (p=0.001), and a post-hoc Dunn's Test revealed a significant difference (p=0.001) between Phase A and Phase B periods (Table 3.3.2), where shallower night-time dives occurred during Phase B (i.e., MFAS exposure). The Kruskal-Wallis test indicated no significant difference in night-time dive duration among exposure periods (p=0.113, Table 3.3.2). There was a significant difference in day-time dive depth among exposure periods (p=0.048, Table 3.3.3), where dives were shallower during pre-Phase A relative to phase B (p=0.032) and duration (p=0.032) where dive durations were shorter during pre-Phase A compared to inter-phase A-B (p=0.024) and Phase B (p = 0.029). Although it should be noted that less than half a day (0.39 days) of behavior data transmitted during the pre-Phase A period, and thus, statistical inference is limited. Diel variation in diving and surfacing behavior seen in GmTag231 was generally similar among exposure periods (Figure 3.3.1-1).
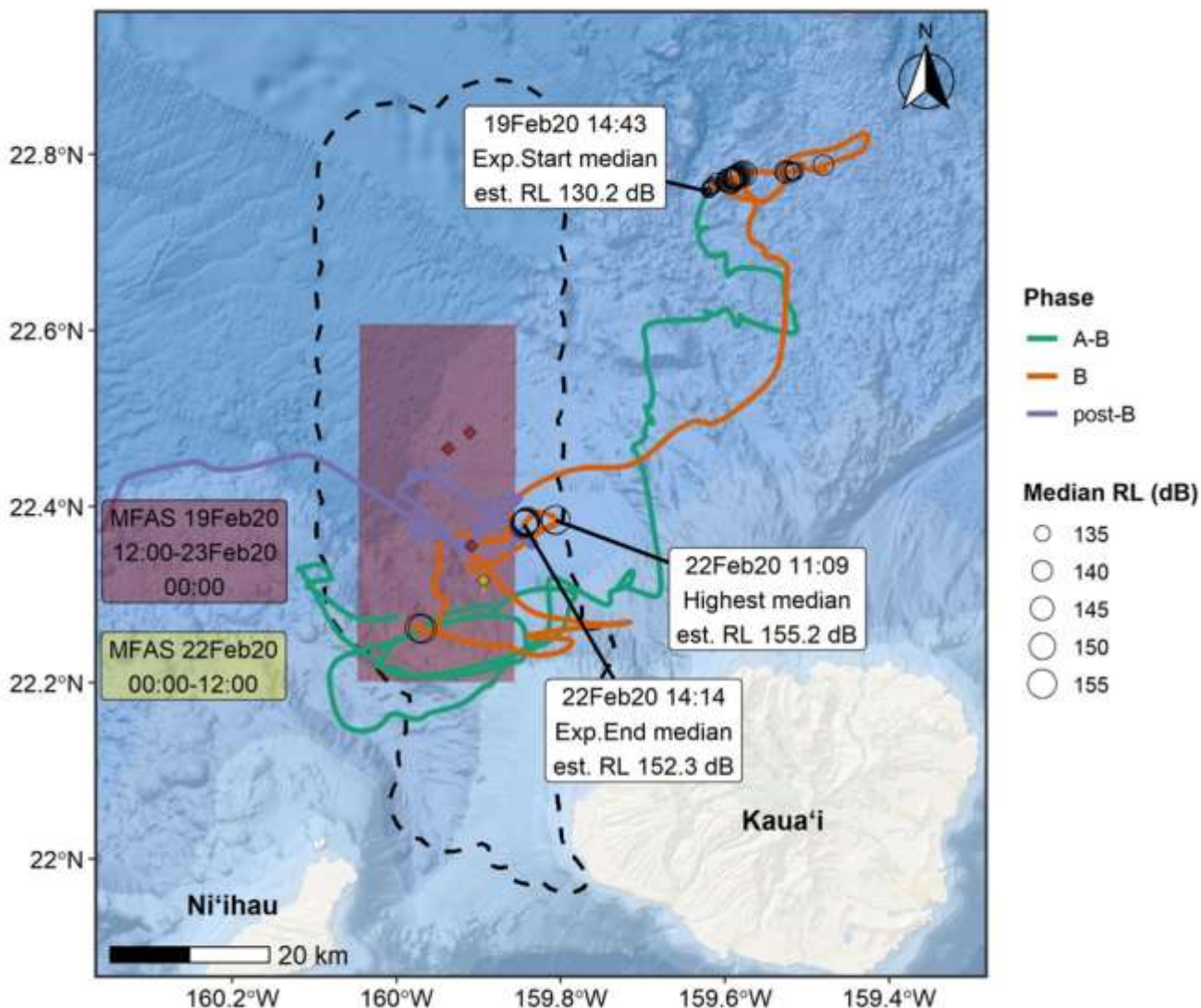
Figure 3.3.1-6. Movements of GmTag231 during the Feb 2020 SCC event. Crawl tracks are colored by phase (tracks before and during Phase A not shown). Median estimated RLs (RL) are plotted as open circles, with the size of the circle scaled to RL level. Shaded boxes represent area of ship activity during blocks of MFAS use (for time periods as specified), and corresponding colored diamond points represent the mean ship location for that time period. For the red-shaded box, the five mean ship position points correspond to mean positions at 12-hour intervals over that time period. The dashed black line represents the PMRF boundary.

3.3.1.4   GmTag080

This individual was tagged (with a SPOT5 tag) in a separate group from the other short-finned pilot whales tagged during the February 2014 SCC, and generally did not associate with these other whales during its deployment period (distance apart means ranging from 41.3-46.6 km; medians ranging from 38.77-59.95 km). Satellite tag data was available for 10.1 days pre-Phase A, all of Phase A (2.1 days), the

inter-phase period (3.1 days), and only part of Phase B (0.4 days or 15% of Phase B) when this tag stopped transmitting, and thus, no data is available for days following Phase B (Table 3.3.1).

This individual was tagged on BARSTUR prior to Phase A and moved south and out of the range within approximately 8 hours of deployment. This whale continued to move south and then east, gradually circumnavigating Kaua'i over the 10.1 days preceding Phase A. During this time, this individual spent approximately 60 hours within the PMRF range (south BSURE/north BARSTUR) before moving to SE Kaua'i at the start of Phase A. During Phase A, this individual began circumnavigating Kaua'i again, heading north and gradually west towards the eastern part of the range. This individual was approximately 5.5 km east of the southern part of BSURE at the end of Phase A, and continued moving west onto the range in the days following Phase A and prior to the start of Phase B. This individual moved northwest inside the southern portion of BSURE, crossing the range completely within 19 hours. After exiting the range for 5 hours and moving 13 km south, this individual re-entered and crossed back over to the southeast area of BSURE. Over the next day, this whale moved 19-20 km north, briefly moving west within the far east boundary of BSURE, and subsequently back 19-20 km south near the southeastern edge of BSURE. During the day prior to Phase B, this individual moved northeast of the range and was approximately 13.5 km east of the range at the start of Phase B. During Phase B, this individual moved west towards the range for 6 hours and then ~4 km south for the remaining 10 hours of this tag's deployment. The maximum RL estimated during the westward movement towards the range was 152.3 dB re 1 µPa (SD=4.60 dB) (over 45-min span of nine exposures), and while no MFAS was in use during the point of directional change, the maximum median estimated RL during the southward movement was 147.7 dB re 1 µPa (SD=2.33 dB) out of 10 exposures over a 50-minute time span.
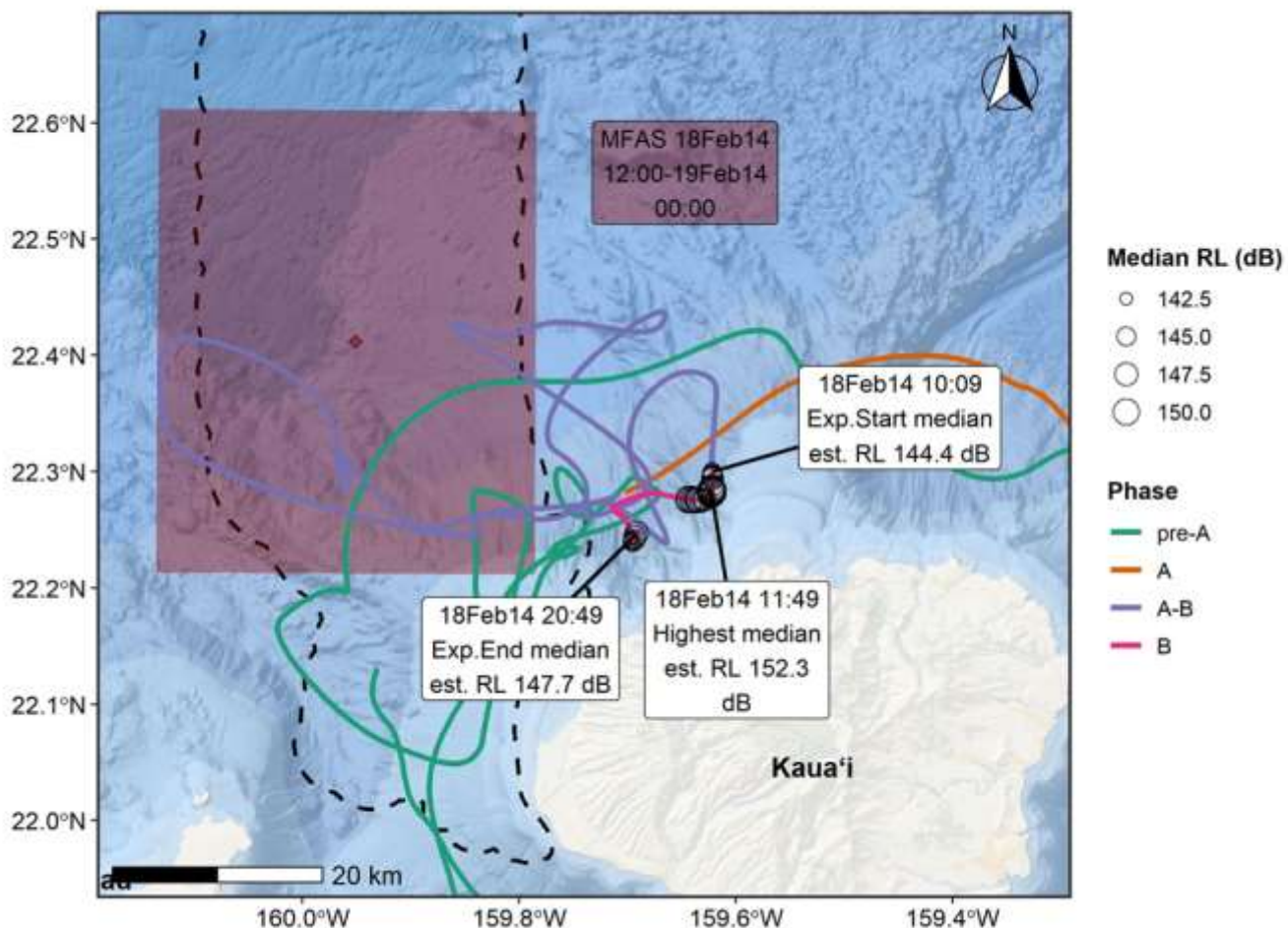
Figure 3.3.1-7. Movements of GmTag080 during the Feb 2014 SCC event. Crawl tracks are colored by phase. Median estimated RLs (RL) are plotted as open circles, with the size of the circle scaled to RL level. The red-shaded box represents the area of ship activity during blocks of MFAS use (for time periods as specified), and the corresponding colored diamond point represents the mean ship location for that time period. The dashed black line represents the PMRF boundary.

3.3.1.5 GmTag152, GmTag153

These are the only two short-finned pilot whales for which we have exposure data that are not considered to be part of the island-associated western community of short-finned pilot whales. Thus their prior exposure history to Navy activities on PMRF may be limited in comparison to the other tagged short-finned pilot whales. These two individuals were tagged in the same group during the February 2016 SCC and remained closely associated throughout their deployments (mean distance apart = 3.29 km; median distance apart = 2.48 km; maximum distance apart = 18.75 km). These tags were deployed after Phase A (no pre-Phase A data), such that information on movements were available for the inter-phase period (2+ days), the entire Phase B period (2.9 days), and days following Phase B (10+ days) (Table 3.3.1). These individuals were generally associated during Phase B (MFAS exposure), with similar exposure levels, thus only a single individual is illustrated in Figure 3.3.7.

Prior to Phase B both individuals were on the southern end of BSURE but moved approximately 25-30 km northeast before exiting the range (over a period of 20 hours). These individuals briefly continued north, maintaining a distance of 15-20 km east of the north end of the range for 15 hours, and subsequently moved 65 km east leading up to the start of Phase B (Figure 3.3.1-8). During Phase B, both individuals moved farther northeast (115 km from the range) before turning back and moving southwest towards the range for the remainder of this phase (30-50 km from the range). RL estimates were similar between the two individuals as would be expected given their close spatial association throughout tag attachment. Exposure levels at the start of Phase B (first ~3 hours) were between 101.2 dB re 1 µPa (SD=3.72 dB) and 129.3 dB re 1 µPa (SD=9.24 dB) for GmTag152 (majority at dive depth, ranging from 92-479 m) and between 113.2 dB re 1 µPa (SD=3.85 dB) and 134.7 dB re 1 µPa (SD=8.61 dB) for GmTag153 (majority at surface, few shallow dives 56-68 m depth). Median RL estimates generally decreased as both individuals moved away from the range over the next ~25 hours, to minimum median RLs of 102.3 dB re 1 µPa (SD=1.85 dB, at 498 dive depth) for GmTag152 and 102.3 dB re 1 µPa (SD=1.76, at 113 m dive depth) for GmTag153, although these varied with estimated position in the water column (surface/dive; generally lower with deeper depth and higher at surface). When both individuals were closest to the range and sound source (~30-35 km), median RLs were the highest (GmTag152: 146.2 dB re 1 µPa, SD=3.55 dB, estimated at surface over 15-minute span of three exposures; GmTag153: 146.8 dB re 1 µPa, SD=4.57 dB, estimated at surface following a 512 m dive, over 105-minute span of 21 exposures). After these exposures, both individuals moved 15 km southeast away from the range and then north through the end of Phase B and first few days post-Phase B.
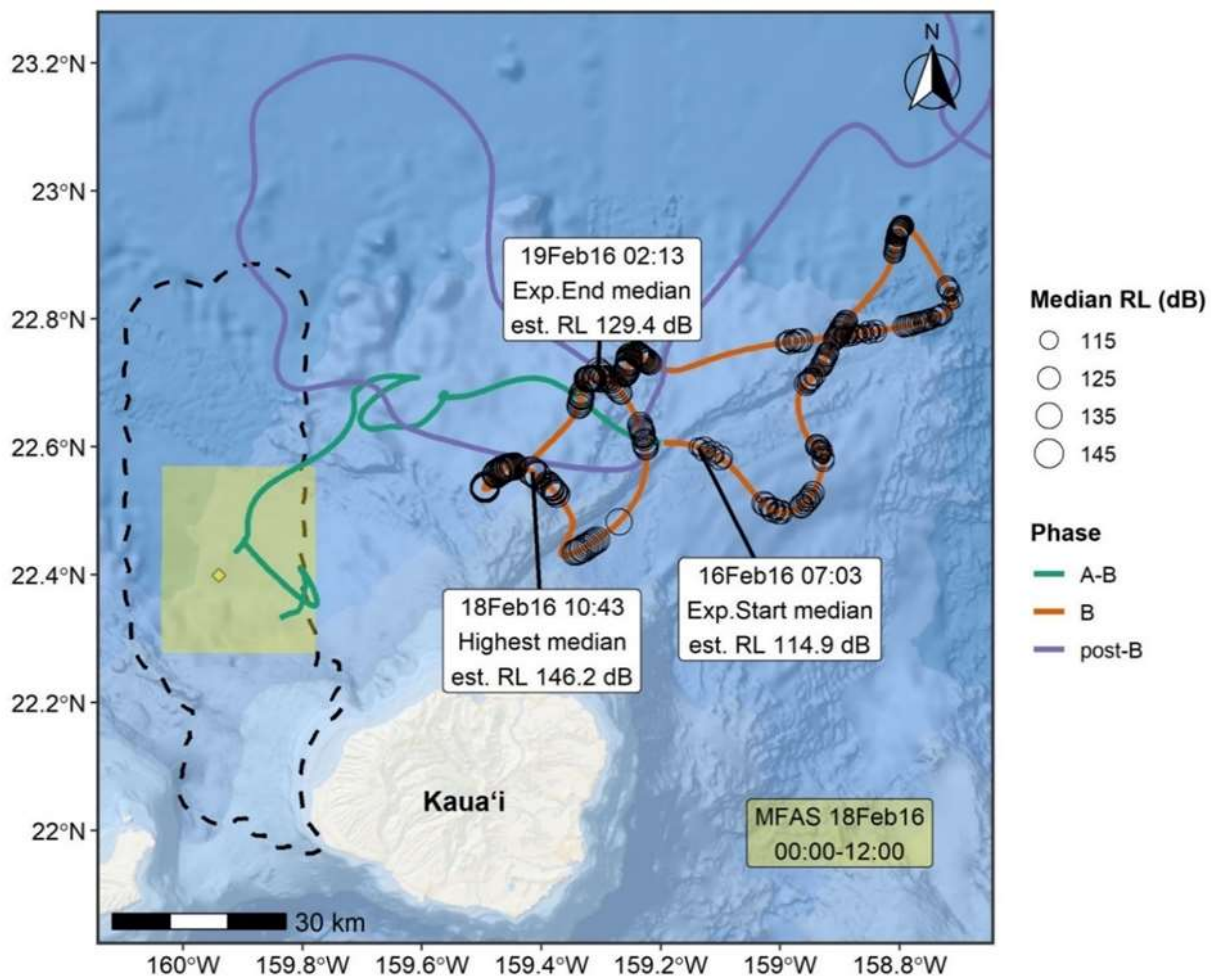
Figure 3.3.1-8. Movements of GmTag152 during the Feb 2016 SCC event. Crawl tracks are colored by phase. Median estimated RLs (RL) are plotted as open circles, with the size of the circle scaled to RL level. Shaded boxes represent area of ship activity during blocks of MFAS use (for time periods as specified), and corresponding colored diamond point represents the mean ship location for that time period. The dashed black line represents the PMRF boundary.

Dive and surfacing data for both individuals were available for all three phases where satellite tag data transmitted (inter-phase, Phase B, post-Phase B), albeit with limited coverage during some phases (Table 3.3.1). As both individuals primarily occupied offshore waters throughout their deployment periods, neither were within range of a land-based Mote on Kaua'i to adequately supplement transmission of dive and surfacing behavior. These two individuals exhibited similar night-time diving behavior over the three exposure phases, with respect to dive rates (dives per hour), percentage time at surface, and dive depth and duration (Table 3.3.2, Figure 3.3.1-1). However, their day-time dive and surfacing behavior varied considerably yet consistently over exposure phases (inter-phase, Phase B, post-Phase B), and thus, unlikely related to MFAS exposure (Table 3.3.3, Figure 3.3.1-1). GmTag152 dived less frequently (0.7-1.5 dives/hour) and spent more time at the surface (70-83 percent) compared

to GmTag153 who dived more frequently (1.7-7.4 dives/hour) and spent less time at the surface (30-77 percent) (Table 3.3.3). GmTag152's day-time dives were generally both deeper and longer, while GmTag153's day-time dives were shallower and shorter (Table 3.3.3). There were significant differences in both night-time and day-time dive statistics among exposure phases for both individuals, however these did not change consistently (Table 3.3.2, Table 3.3.3).

3.3.1.6   GmTag214

Information on movements of GmTag214 were available for 2.5 days during the inter-phase period, all of Phase B (0.2 days; terminated early due to Hurricane Lane), and 20+ days post-Phase B period (Table 3.3.1). Because Phase B only lasted approximately 6 hours, movements of this individual were minor and thus inference on any movement response is limited.

Prior to Phase B, this individual moved from the south end of BSURE (NW of Kauaʻi) towards the north side of Kauaʻi and remained there for a day and a half. This individual then moved west and onto the range (BARSTUR) for the start of the Phase B. This whale stayed on the range, moving northwest within BARSTUR, for the first 3 hours of Phase B. During this time, the highest estimated median RL was 133.8 dB re 1 µPa (SD=2.93 dB) (estimated at surface) over a 10-minute period. GmTag214 continued moving northwest and eventually outside of the range boundary for the following 1-2 hours, where exposure levels generally decreased (minimum of three exposures over a 55-minute span: 119.3 dB re 1 µPa, SD = 3.17 dB at surface, following a 464 m dive). This individual then turned and moved south, maintaining a distance of 3-6 km from the west edge of BARSTUR for the remainder of Phase B. Median estimated RLs from this time period ranged from 125.1 dB re 1 µPa (SD=4.51 dB) at an estimated 200 m dive depth to 133.03 dB re 1 µPa (SD=4.12 dB) at an estimated dive depth of 479 m (over 45-minute time span, out of 8 exposures). In the days following the end of Phase B, this individual continued moving south, while briefly turning north to the southern end of BARSTUR, and eventually moved to waters off the south coast of Kauaʻi.

Dive and surfacing behavior data transmitted during the inter-phase period, all of Phase B, and for 5.5 days after Phase B (Table 3.3.1). Only night-time dive and surfacing data were available during Phase B due to the early termination of this SCC, and thus, we only focused on comparisons of night-time dive behavior among exposure phases. Kruskal-Wallis One-Way ANOVA tests indicated no significant differences in night-time dive depths nor durations among the three exposure phases (p=0.597 and p=0.217, respectively, Table 3.3.2), although the median night-time dive depth during Phase B (487.5 m) was elevated compared to the inter-phase period (335.5 m) and post-Phase B period (279.5 m) (Table 3.3.2, Figure 3.3.1-1).
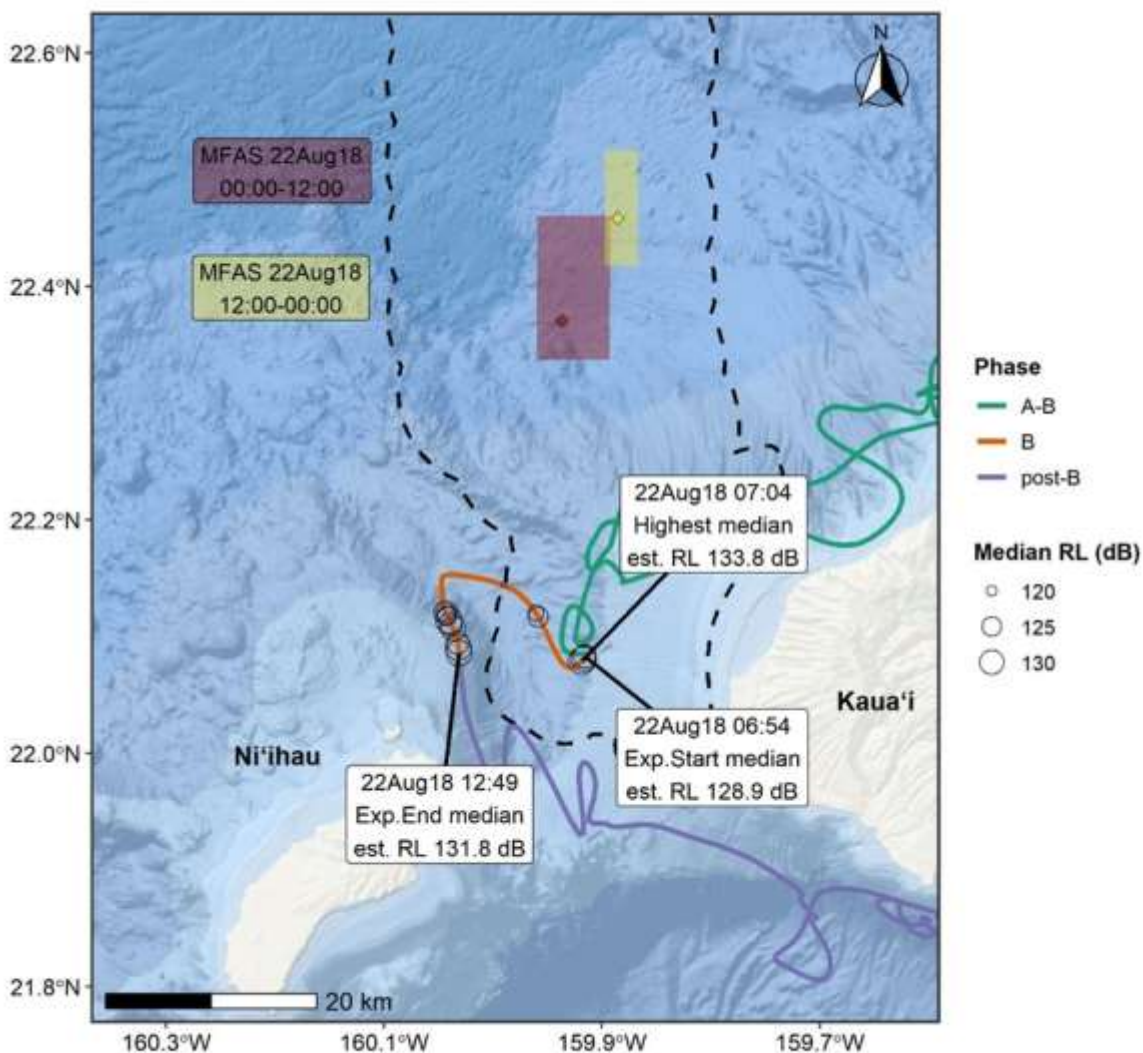
Figure 3.3.1-9. Movements of GmTag214 during the Aug 2018 SCC event. Crawl tracks are colored by phase. Median estimated RLs (RL) are plotted as open circles, with the size of the circle scaled to RL level. Shaded boxes represent the areas of ship activity during blocks of MFAS use (for time periods as specified), and the corresponding colored diamond points represent the mean ship location for that time period. The dashed black line represents the PMRF boundary.

3.3.2   Rough-Toothed and Bottlenose Dolphins

Seven rough-toothed dolphins were considered for this analysis, three with location only SPOT5 tags (SbTag002, SbTag003, and SbTag014), and the remaining four equipped with SPLASH10 tags also providing dive behavior information (SbTag010, SbTag015, SbTag017, and SbTag018). Two bottlenose dolphins, both tagged with SPLASH10 tags, were included in the analyses as they were tagged in 2020

and had not been previously assessed for exposure and response (TtTag034, TtTag035). At the time of this report, estimated RLs have not been completed for SbTag002, SbTag003, and SbTag010). Movement responses can consist of a combination of horizontal movement responses and dive depth responses. Table 3.3.4 provides dive data for the four rough-toothed dolphins and the two bottlenose dolphins. Notice the percentage of dive coverage has cases with no Pre-Phase A and post-Phase B data. In addition, SbTag010 and SbTag015 both had limited percentage of dive coverage in the Phase B periods compared to SbTag017 and SbTag018. The two bottlenose dolphins were tagged during the inter-phase period so no data are available for pre-Phase A or Phase A (Table 3.3.4). As with the pilot whale analyses, only the first three days of the post-Phase B period were included when longer periods were available post-Phase B.

Table 3.3.4. Percentage of dive and surfacing data for rough-toothed dolphins and common bottlenose dolphins by phase.

Individual	Percentage of dive/surfacing data				
	Pre-Phase A	Phase A	Inter Phase A-B	Phase B	Post-Phase B
SbTag010					
Duration overall (days)	6.0	2.3	2.5	2.0	0.0
Days surfacing/dive data	5.7	1.6	0.2	0.9	0.0
Percentage coverage	94.9	71.6	7.8	43.3	0.0
SbTag015					
Duration overall (days)	0.0	2.9	2.5	2.1	5.8
Days surfacing/dive data	0.0	1.0	0.7	0.2	2.4
Percentage coverage	0.0	34.2	28.9	11.5	41.0
SbTag017					
Duration overall (days)	0.0	2.2	2.8	2.9	4.4
Days surfacing/dive data	0.0	0.0	1.3	2.6	3.0
Percentage coverage	0.0	0.0	47.7	90.6	66.6
SbTag018					
Duration overall (days)	0.0	2.2	2.8	2.9	11.6
Days surfacing/dive data	0.0	0.0	1.2	2.2	7.9
Percentage coverage	0.0	0.0	44.1	78.2	68.0
TtTag034					
Duration overall (days)	0.0	2.2	4.2	3.0	3.2
Days surfacing/dive data	0.0	0.0	3.7	3.0	3.2
Percentage coverage	0.0	0.0	88.1	100.0	100.0
TtTag035					
Duration overall (days)	0.0	2.2	4.2	2.98	3.6
Days surfacing/dive data	0.0	0.0	1.8	2.98	3.6
Percentage coverage	0.0	0.0	42.3	100.0	100.0

Table 3.3.5. Comparison of rough-toothed dolphin dive data among SCC phases. Only the two rough-toothed dolphin with SPLASH10 tags and dive data from all three periods are included in this table. Kruskal-Wallis one-way ANOVA significant results (i.e., significant differences among phases were detected) are shown in bold. Pairs of phases where significant differences were detected are listed in the associated post-hoc Dunn's test column (level of significance 0.05).

Dive parameter per individual	Inter-Phase A-B	Phase B	Post-Phase B	Kruskal-Wallis Test p-value*	Post-hoc Dunn's test significant pairs
Night-time dive rate (dives/hour)					
SbTag017	10.5	3.5	5.4		
SbTag018	7.9	9.3	5.9		
% time in surface periods at night					
SbTag017	49.4	83.1	71.2		
SbTag018	49.2	44.2	64.5		
Median dive depth night (m)					
SbTag017	**79.5**	**92.5**	**97.5**	**<0.001**	**Inter–B; Inter–Post-B**
SbTag018	**85.5**	**77.5**	**119.5**	**<0.001**	**Inter–B; Inter–Post-B; B–Post-B**
Median dive duration night (min)					
SbTag017	**2.9**	**3.0**	**3.3**	**<0.001**	**Inter–Post-B; B–Post-B**
SbTag018	**3.9**	**3.7**	**3.7**	**0.037**	**Inter–B**

*Values for dive rates and percentage time in surface periods represent single values for each individual for each period, thus no statistical testing was undertaken.
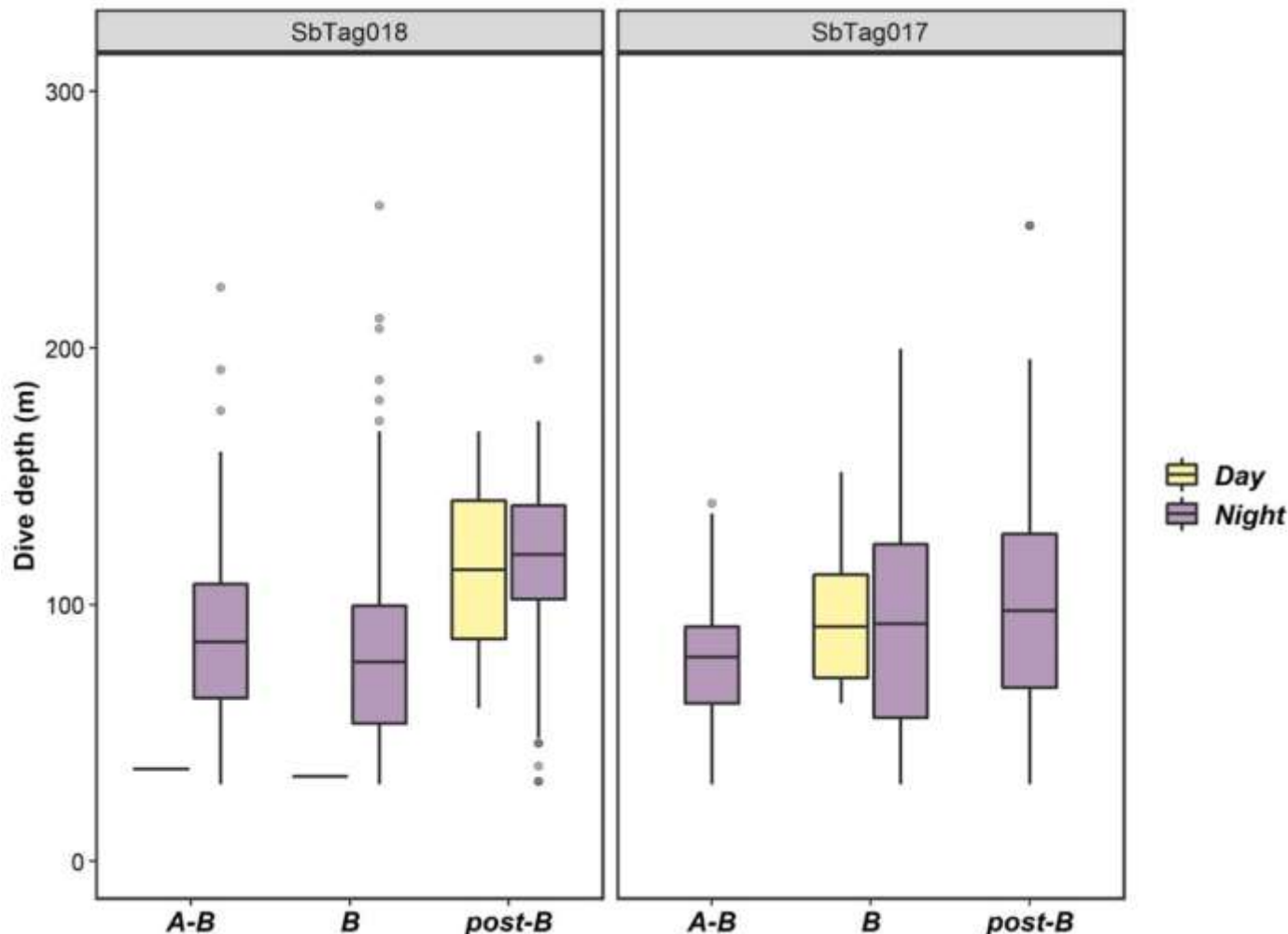
Figure 3.3.2-1. Distribution of dive depths by exposure/SCC phase by day/night, for each rough-toothed dolphin with sufficient dive and surfacing data coverage. Note the relatively lack of day-time dives reflects lower day-time dive rates for rough-toothed dolphins (Shaff and Baird, 2021). Lower and upper hinges correspond to the first and third quartiles (25th and 75th percentiles) and the upper and lower whiskers extend from the hinges to +/- 1.5*IQR (interquartile range), respectively. The horizontal line within each box represents the median value, and outliers are shown as gray points.

3.3.2.1 SbTag014

Information on this individual's movements were available for 7 days before Phase A, all phases (2.9 days Phase A, 2.5 days inter-phase, 2.1 days Phase B) and 7.1 days after Phase B (Table 3.3.4). Similar to GmTag115, satellite tag data from this individual was available during the February 2015 ULT that was conducted prior to Phase B from which we could estimate RLs for, in addition to those estimated during Phase B of the SCC.

Before Phase A this individual moved south along the east coast of Kauaʻi for 14 hours and then returned towards northeastern Kauaʻi over the next 24 hours (Figure 3.3.2-2). During the next day this dolphin continued travelling north and then west along the north coast of Kauaʻi, moving onto the

southern end of BSURE. This individual moved west across the range and then 40 km south (to BARSTUR) over a period of 23 hours. This individual remained on the southern portion of BARSTUR for 15 hours and then moved northeast off the range, following a similar route along the northern coast of Kauaʻi and eventually towards the northeastern coast immediately prior to the start of Phase A. During Phase A this individual briefly moved south (12 km, east Kauaʻi) before moving to waters off the northeastern coast of Kauaʻi. This individual remained in this general region (northeast/east Kauaʻi) throughout Phase A. During the inter-phase period this individual moved along the south coast of Kauaʻi and eventually northwest and within 5-10 km of the south end of BARSTUR. The ULT during this time occurred during this northwestern movement and median estimated RLs started at 128.0 dB re 1 µPa (SD=3.81 dB), increased to a maximum of 135.4 dB re 1 µPa (SD=3.59 dB) as it moved closer to the range, and ended at 129.2 dB re 1 µPa (SD=2.94 dB) (~1 hour span of 13 exposures) when this individual was 20-25 km southeast of BARSTUR. However, it should be noted that limited proportions of TLs were available for RL estimation during the ULT (<40% for all exposures) as there were no direct paths for portions of the error ellipses from the tagged animal locations. After moving 10-15 km closer to BARSTUR, this individual moved southeast to offshore of south Kauaʻi (40 km southeast from the range) through the end of the inter-phase period (15 hours). During Phase B this individual moved north along west Kauaʻi adjacent to the eastern boundary of BARSTUR, and exposure levels increased reaching a maximum median estimated RL of 159.8 dB re 1 µPa (SD=5.40 dB) over a 60-minute span of nine exposures. Exposure levels decreased slightly as this individual continued moving north and then northeast along the northern coast of Kauaʻi, but generally ranged between 140-150 dB re 1 µPa. This individual remained off the north coast of Kauaʻi through the end of Phase B (distance from BSURE ranging from 20-50 km) where RL estimates were between 130-145 dB re 1 µPa (decreasing with distance from the range). After Phase B this individual spent the rest of its deployment moving along the northeast/east coast of Kauaʻi.
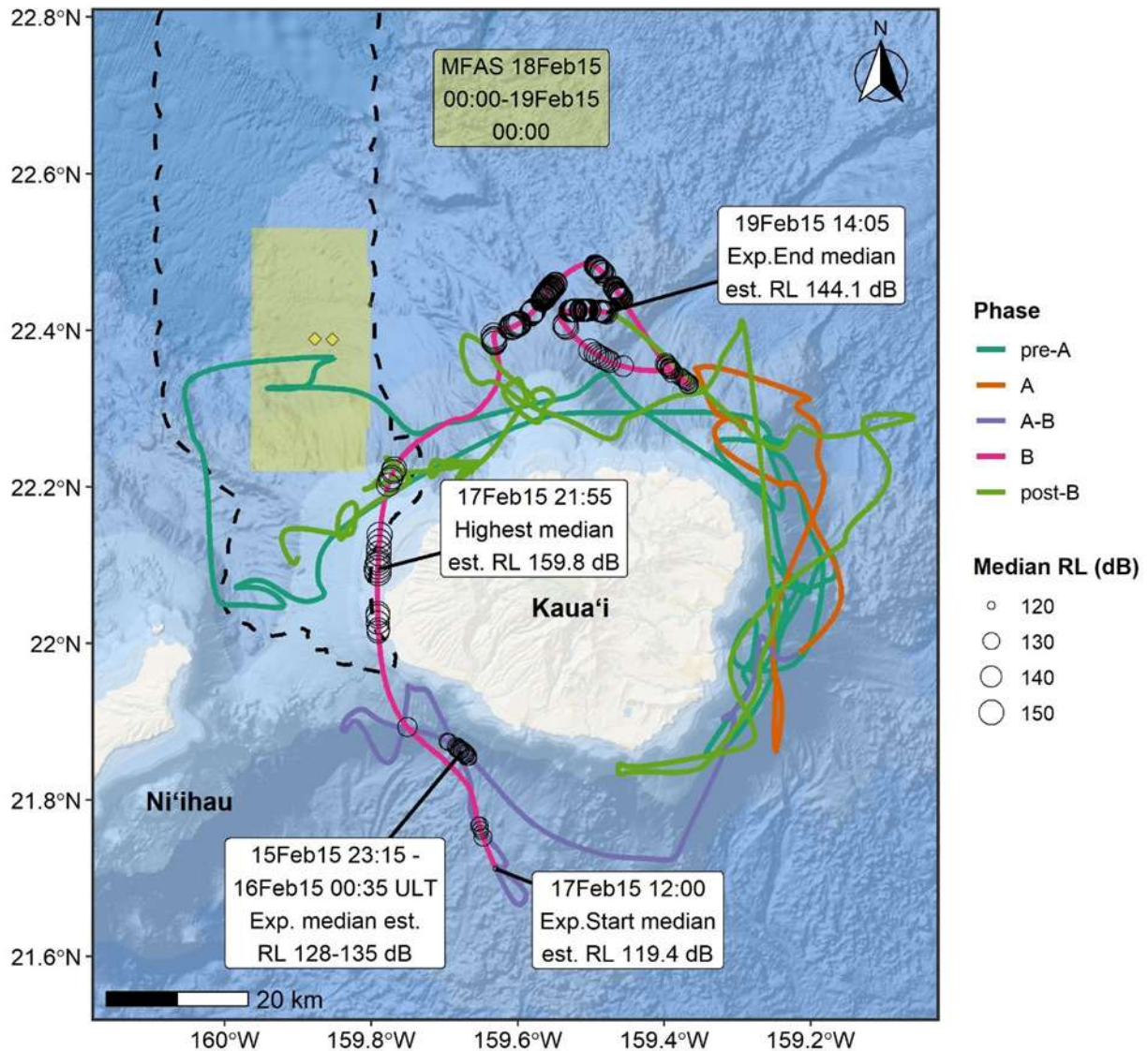
Figure 3.3.2-2. Movements of SbTag014 during the February 2015 SCC event. Crawl tracks are colored by phase; while MFAS is normally only used during Phase B, an additional unit-level test (ULT) was conducted during the interval between Phase A and Phase B (on 15 February 2015) from which RLs (RL) could be estimated. Median estimated RLs are plotted as open circles, with the size of the circle scaled to the RL. Shaded boxes represent area of ship activity (for time periods as specified), and corresponding colored diamond points represent the mean ship location for that time period (for this figure, the yellow diamonds correspond to mean ship position at a 12-hour interval). The dashed black line represents the PMRF boundary.

3.3.2.2   SbTag017, SbTag018

These two individuals were tagged (with SPLASH10 tags) in the same group during the February 2016 SCC, and although were generally associated during the initial period after deployment, they did not appear to be associated throughout the rest of their deployments (distance apart mean = 13.3 km; median = 8.34 km; maximum = 51.6 km). This is reflected in differences between their exposure levels. Satellite tag data for both individuals transmitted 1.4 days before Phase B (inter-phase period), through the entire period of Phase B (2.9 days), and several days after Phase B (5+ days) (Table 3.3.4), and there was reasonable coverage of dive and surface data during Phase B (90.6% and 78.2% for SbTag017 and SbTag018, respectively; Table 3.3.5).

Both individuals were tagged on BARSTUR during the inter-phase period. Both individuals moved south off of the range, although SbTag017 remained off and south of BARSTUR (within 5-10 km of range) prior to Phase B, whereas SbTag018 moved back onto BARSTUR (near the southern boundary) for five hours before the start of Phase B. During Phase B SbTag017 continued to occupy an area 5-15 km south of the range between Kauaʻi and Niʻihau, except for a brief period (3.5 hours) where this individual moved along the southern boundary of BARSTUR. Median estimated RLs for this individual reached a maximum of 146.7 dB re 1 µPa (SD=2.31 dB, at surface) during a 95-min time span (20 exposures) where this dolphin was at the surface inside the south BARSTUR boundary. After the highest exposure level, this individual moved south near the area it previously occupied, and RL estimates decreased (minimum during the same 95-min time span: 136.4 dB re 1 µPa, SD=2.66 dB, at surface).

Exposure levels for SbTag017 had little variability throughout Phase B, generally ranging between 130-145 dB re 1 µPa, which would be expected given its minimal displacement relative to the source throughout this phase. In contrast, within the first 2 hours of Phase B, SbTag018 moved northwest off the range and then southwest along the northwestern coast of Niʻihau. As this individual was moving out of BARSTUR, exposure levels reached a maximum of 147.6 dB re 1 µPa (SD=4.87 dB, at surface) over a 45-min span of 10 exposures preceding a 106 m dive where RLs were estimated at a median of 128.4 dB re 1 µPa (SD=1.98 dB). This individual remained in this region (northwest coast of Niʻihau) for approximately 35 hours, where exposure levels generally decreased with increased distance from the range, although remained between 135-145 dB re 1 µPa with some variation at estimated dive depths. SbTag018 then moved east back onto BARSTUR, and once inside the boundary, moved 15 km northeast for 5 hours and then reversed direction travelling south for the remainder of Phase B. The highest median estimated RL for this individual occurred when it reached its northernmost point within BARSTUR immediately after turning south (157.1 dB re 1 µPa, SD=3.22 dB, at surface, over 100-minute span of 20 exposures), and RL estimates gradually decreased through the end of Phase B as it moved south. SbTag018 was just outside of the southern end of BARSTUR (2.5 km away) at the end of Phase B. After Phase B, both individuals remained south of the range for 14-16 hours and subsequently moved 30-35 km south (SE Niʻihau) over the next day, although not in concert. During the rest of their deployments, these individuals moved north to the north end of Niʻihau, briefly passing through the southwestern corner of BARSTUR.

Both SbTag017 and SbTag018 transmitted dive and surfacing behavior data during all exposure phases, albeit with variable coverage during those periods (Table 3.3.5). Dive and surfacing data were

particularly limited during the day (Figure 3.3.2-1), and thus, we only focus on night-time dive and surfacing behavior statistics among exposure phases. Night-time dive rates varied among the three exposure phases (inter-phase, Phase B, post-Phase B) for both individuals (Table 3.3.5). Similarly, percentage time in surface periods at night varied within individuals and among individuals (Table 3.3.5). SbTag017's time in surface bouts at night generally increased compared to the inter-phase period whereas SbTag018's time in surface bouts remained generally the same until post-Phase B (Table 3.3.5). Night-time dive depth and duration varied significantly among exposure phases for both individuals although not in a consistent way (Kruskal-Wallis One-Way ANOVA, p < 0.001 for all except SbTag018 duration, p=0.04; Table 3.3.5). For SbTag017, night-time dive depths and durations increased with each exposure phase although the amount of increase between Phase B and post-Phase B was minimal (Table 3.3.5, Figure 3.3.2-1). SbTag018's dive depths and durations were the shallowest/shortest during Phase B and the deepest during post-Phase B but longest during the inter-phase period/pre-Phase B (Table 3.3.5, Figure 3.3.2-1).

3.3.2.3   SbTag015
This individual was tagged on a separate day from SbTag014 and was generally not associated with that individual throughout its deployment (distance apart mean = 25 km; median = 23.2 km; maximum = 65.8 km). Information on movements for this individual were available prior to Phase A (0.2 days), Phase A (2.9 days), the inter-phase period (2.5 days), Phase B (2.1 days), and post-Phase B (6.6 days) (Table 3.3.4).

During the ~6 hours of movement data available prior to Phase A, this individual was off the southeast coast of Kauaʻi and moved southwest along the coast (13 km) leading up to the start of Phase A (Figure 3.3.2-3). During Phase A, this individual briefly moved north, then directly south (20 km) over 4 hours and then north near its initial position southeast of Kauaʻi. Over the next day, this individual moved ~20 km northeast (away from Kauaʻi) and then 35-40 km northwest along the eastern/northeastern coast of Kauaʻi. During the remaining 30 hours of Phase A, this individual moved back south along the eastern coast of Kauaʻi, approximately 5 km west of its deployment location by the end of Phase A. This individual continued to move south and west along the southern coast of Kauaʻi towards the southwestern coast through the first 30 hours of the inter-phase period. This individual then moved 35 km south of Kauaʻi and remained there leading up to the start of Phase B. Within the first eight hours of Phase B, this individual moved northwest onto the range (BARSTUR). This individual continued moving northwest over the next five hours and briefly exited the western boundary of BARSTUR (6.5 hours) before re-entering the range and moving east towards Kauaʻi. The highest median estimated RL was 155.1 dB re 1 µPa (SD=6.31 dB; over an 8-minute span of three exposures) and occurred during this period of directional change and initial movement back onto the range. RLs following this exposure were similar (ranging from 140-150 dB re 1 µPa). This individual then moved south of BARSTUR for 5 hours (maximum 8 km south of range), where RL estimates were slightly lower (ranging from 129.1 dB re 1 µPa [SD=2.66 dB] to 145.2 dB re 1 µPa [SD=3.20 dB]), before turning back north and inside the southern part of BARSTUR for the remainder of Phase B. Variance in exposure levels appear to reflect the distance between the individual and the general area of ship activity during Phase B (Figure 3.3.2-3). During the first three days after Phase B ended, this individual moved east along the northern coast of Kauaʻi to south Kauaʻi, almost completely circumnavigating the island, and then turned and moved up the eastern coast to north Kauaʻi.

Although this individual was tagged with a SPLASH10 tag, limited dive and surfacing data transmitted during the deployment period (ranging from 11.5 to 41 percent data coverage, Table 3.3.5). Therefore, we did not analyze this individual's dive and surfacing behavior in relation to exposure phases.
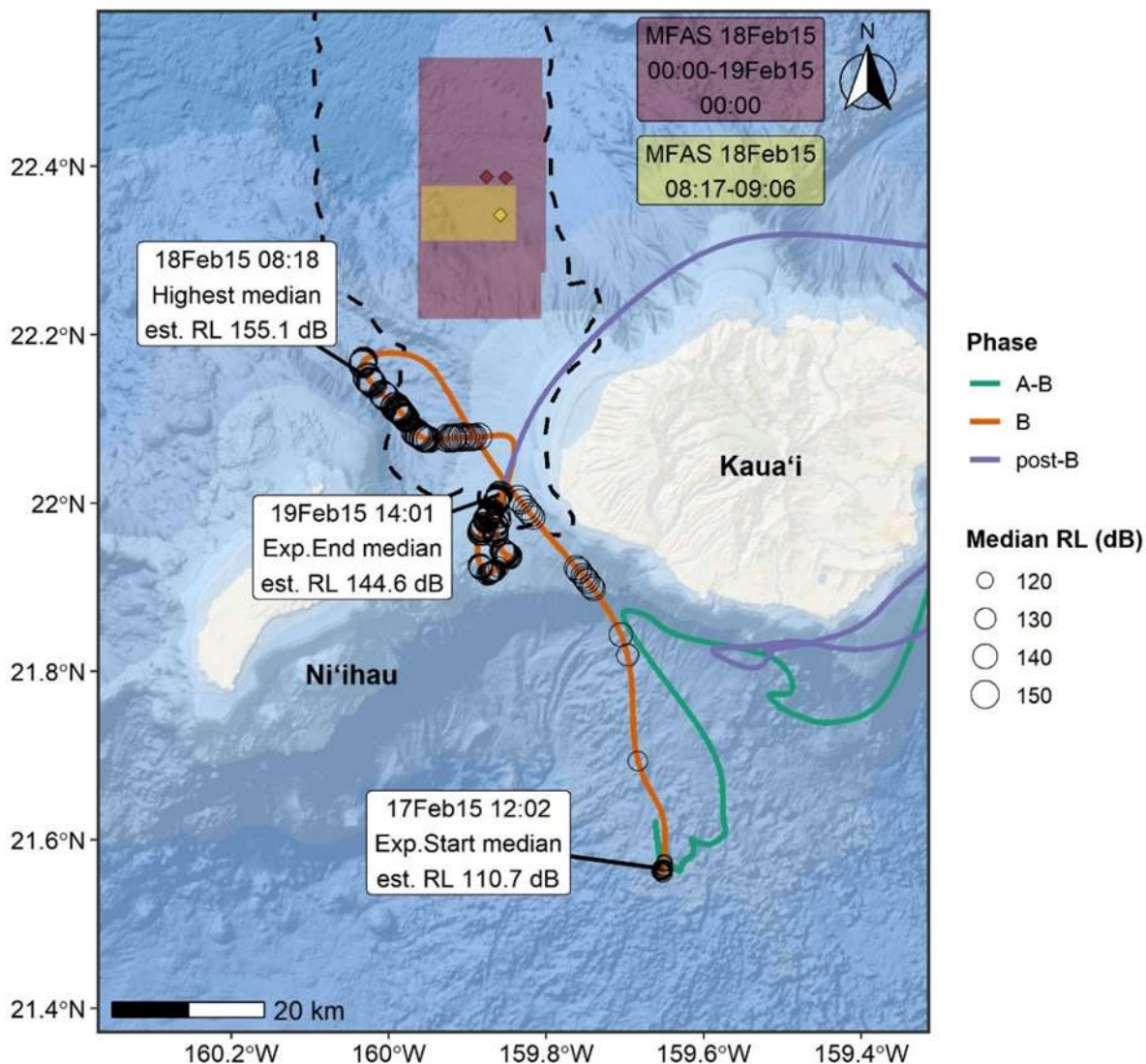
Figure 3.3.2-3. Movements of SbTag015 during the February 2015 SCC event. Crawl tracks are colored by phase; see text for description of phases. Note: only three days of data post-Phase B are plotted, and tracks before Phase A and during Phase A are not shown. Median estimated RLs (RL) are plotted as open circles, with the size of the circle scaled to RL level. Shaded boxes represent area of ship activity (for time periods as specified), and corresponding colored diamond points represent the mean ship position for that time period. For the red-shaded box, the two mean ship position points (red diamonds) correspond to mean positions at 12-hour intervals over that time period. The dashed black line represents the PMRF boundary.

3.3.2.4   TtTag034, TtTag035

SPLASH10 tags were deployed on two bottlenose dolphins encountered during the February 2020 effort (TtTag034, TtTag035) and included in RL estimation in the current study. Both individuals were deployed during the inter-phase period (i.e., prior to Phase B); TtTag034 was tagged on SWTR 3.4 days prior to Phase B and TtTag035 was tagged in the same region 1.8 days prior to the start of Phase B. Information on movements of both individuals were available for all of Phase B (3 days) and several days post-Phase B (7+ days) (Table 3.3.4), and a complete dive record (i.e., dive and surfacing data) was available for both individuals for all of Phase B and at least three days post-Phase B (Table 3.3.6). Although tagged on separate occasions, these dolphins were generally associated throughout their deployment periods (distance apart mean = 3.76 km; median = 2.01 km; maximum = 23.4 km).

Prior to Phase B both individuals occupied nearshore waters of west Kauaʻi, moving between the southwestern and northwestern coasts with brief periods (~1 hour) of movement on the southeastern edge of BARSTUR (Figure 3.3.2-4). During Phase B, these dolphins occupied the same general region along the west side of Kauaʻi (minimal overlap with east BARSTUR) except for brief excursions along the southern coast of Kauaʻi, albeit on separate occasions (i.e., not in concert) (Figure 3.3.2-5). These individuals had similar exposure levels, given they remained largely associated throughout the SCC, although it should be noted that variable proportions of valid TLs were used to derive median estimated RLs for these individuals (range: 2-100%), given their proximity to shore and portions of the location error ellipses overlapping land, where no RLs were estimated. At the start of Phase B, both individuals were off the westernmost point of Kauaʻi. TtTag034 was exposed to its highest estimated median RL of 145.7 dB re 1 µPa (SD=4.11 dB) at the surface following a 172 m dive and preceding at 296 m dive (over 34-minute span, seven total exposures), and TtTag035 was exposed to similar levels (maximum median estimated RL of seven exposures over 34-minute time span: 143.0 dB re 1 µPa SD=4.43 dB, at surface) although not its highest exposure overall. After this exposure, both individuals moved nearshore for a brief period (~5 hours) and then slightly west onto the southeast part of BARSTUR. RL estimates for both individuals generally decreased through the rest of the first day of Phase B, ranging from their first exposure levels (140-145 dB re 1 µPa) to levels around 120-130 dB re 1 µPa primarily at the surface and otherwise at estimated dive depths between 262-488 m for TtTag034 and 121-544 m for TtTag035. During the second day of Phase B both dolphins remained in the same area inshore of west Kauaʻi with short periods (1-2 hours) within or along the southeastern boundary of BARSTUR, and then moved south away from the range (TtTag034 15 km south of BARSTUR; TtTag035 5 km south of BARSTUR), before returning north to inshore waters of west Kauaʻi (over a period of ~15 hours). There were no exposures/RL estimates during this period of movement (20 Feb 2020) for either individual. On the following day, TtTag034 moved northeast along the eastern boundary of BARSTUR (~1 hour on BARSTUR) whereas TtTag035 made an excursion southeast along the southern coast of Kauaʻi (25 km from BARSTUR) before returning back north. Exposure levels during this period ranged from 135.1 dB re 1 µPa (SD=2.77 dB, at surface) to 138.6 dB re 1 µPa (SD=2.70 dB, at surface) for TtTag034 and 123.7 dB re 1 µPa (SD=1.08 dB, at 528 m depth) to 126.2 dB re 1 µPa (SD=3.05 dB, at surface) for TtTag035 (both over 15-minute time span of three exposures), reflecting the latter dolphin's farther distance from the range/source. During the last ~10 hours of Phase B, both individuals moved northeast adjacent to east BARSTUR and closer inshore to Kauaʻi (10 km southeast of BSURE), where exposure levels increased to a maximum median estimated RL of 144.8 dB re 1 µPa (SD=3.11 dB, at surface) for TtTag034 and 145.4 dB re 1 µPa (SD=2.71 dB, at surface, highest overall) for TtTag035 over a 5-minute span (one exposure).

Both dolphins then moved south and RL estimates decreased to around 120-125 dB re 1 μPa for the remainder of Phase B (20-minute span of five exposures). After Phase B, both individuals exhibited movement patterns similar to those of preceding days, moving along the north and south coasts of western Kauaʻi and occupying areas near or within BARSTUR.

Both TtTag034 and TtTag035 were within range of the Kauaʻi Mote for the majority of their deployments and thus had 100 percent dive and surfacing data coverage throughout their deployments, which spanned inter-phase A-B (partial), phase B, and post-phase B periods (Table 3.3.6). The two individuals exhibited similar dive behavior in terms of day-time and night-time patterns (Figure 3.3.2-6, Figure 3.3.2-7, Figure 3.3.2-8), where these dolphins spent long periods at depths <50 m ("surface" periods) during day and night (Table 3.3.6) and dived gradually from deeper to shallower after sunset and shallower to deeper prior to sunrise (Figure 3.3.2-7, Figure 3.3.2-8). For TtTag034, there were significant differences in both night-time and day-time dive depth (Kruskal-Wallis One-way ANOVA; $p < 0.001$ and $p = 0.02$, respectively) and duration (Kruskal-Wallis One-way ANOVA; $p = 0.007$ and $p = 0.004$, respectively) among the three exposure phases when dive data transmitted (Table 3.3.6). Night-time dives were shallower and day-time dives were deeper during phase B and post-phase B periods relative to inter-phase A-B (post-hoc Dunn's Test, night-time: $p < 0.001$ for both; day-time: $p = 0.03$, $p = 0.04$, respectively) (Table 3.3.6, Figure 3.3.2-6). Similarly, night-time dives were shorter and day-time dives longer during phase B and post-phase B periods relative to inter-phase A-B (post-hoc Dunn's Test, night-time: $p = 0.04$, $p = 0.007$, respectively; post-hoc Dunn's Test, day-time: $p = 0.004$, $p = 0.028$ respectively) (Table 3.3.6). Likewise, night-time dive depths and durations for TtTag035 were significantly different among exposure periods (Kruskal-Wallis One-way ANOVA, $p < 0.001$ for both; post-hoc Dunn's Test, $p < 0.05$ for each pairwise comparison, except depth inter-phase A-B and phase B: $p = 0.057$) (Table 3.3.6). In general, TtTag035's night-time dive depths and durations became shallower and shorter, respectively, through phases before, during, and after MFAS use (Figure 3.3.2-8). There was a significant difference in day-time depths among exposure phases for TtTag035 (Kruskal-Wallis One-way ANOVA, $p = 0.014$; Table 3.3.6), where dive depths were deeper after MFAS exposure relative to before exposure (post-hoc Dunn's Test, $p = 0.011$). There was no significant difference in day-time dive durations for TtTag035 ($p > 0.05$, Table 3.3.6), although dive durations were slightly elevated during exposure (i.e., Phase B) relative to before and during Phase B as we might expect given the correlation between dive depth and duration (Figure 3.3.2-8).

Table 3.3.6.Comparison of bottlenose dolphin dive data among SCC phases. Kruskal-Wallis one-way ANOVA significant results (i.e., significant differences among phases were detected) are shown in bold. Pairs of phases where significant differences were detected are listed in the associated post-hoc Dunn's test column (level of significance 0.05).

Dive parameter per individual	Inter-Phase A-B	Phase B	Post-Phase B	Kruskal-Wallis Test p-value*	Post-hoc Dunn's test significant pairs
Night-time dive rate (dives/hour)					
TtTag034	1.66	2.26	1.95		
TtTag035	1.09	1.74	1.53		
% time in surface periods at night					
TtTag034	79.23	74.06	75.93		
TtTag035	82.87	77.24	83.07		
Day-time dive rate (dives/hour)					
TtTag034	1.26	1.21	1.52		
TtTag035	1.16	1.33	1.07		
% time in surface periods during day					
TtTag034	85.81	82.97	80.13		
TtTag035	83.72	83.55	84.16		
Median dive depth night (m)					
TtTag034	**327.5**	**227.5**	**229.5**	**<0.001**	**Inter–B; Inter–Post-B**
TtTag035	**391.5**	**295.5**	**227.5**	**<0.001**	**Inter–Post-B; B–Post-B**
Median dive duration night (min)					
TtTag034	**8.00**	**7.40**	**6.78**	**0.007**	**Inter–B; Inter–Post-B**
TtTag035	**10.20**	**8.12**	**6.80**	**<0.001**	**Inter–B; Inter–Post-B; B–Post-B**
Median dive depth day (m)					
TtTag034	**351.5**	**427.5**	**391.5**	**0.019**	**Inter–B; Inter–Post-B**
TtTag035	**479.5**	**375.5**	**497.5**	**0.014**	**B–Post-B**
Median dive duration day (min)					
TtTag034	**7.48**	**9.13**	**8.53**	**0.004**	**Inter–B; Inter–Post-B**
TtTag035	9.40	9.30	10.40	0.237	NA

*Values for dive rates and percentage time in surface periods represent single values for each individual for each period, thus no statistical testing was undertaken.
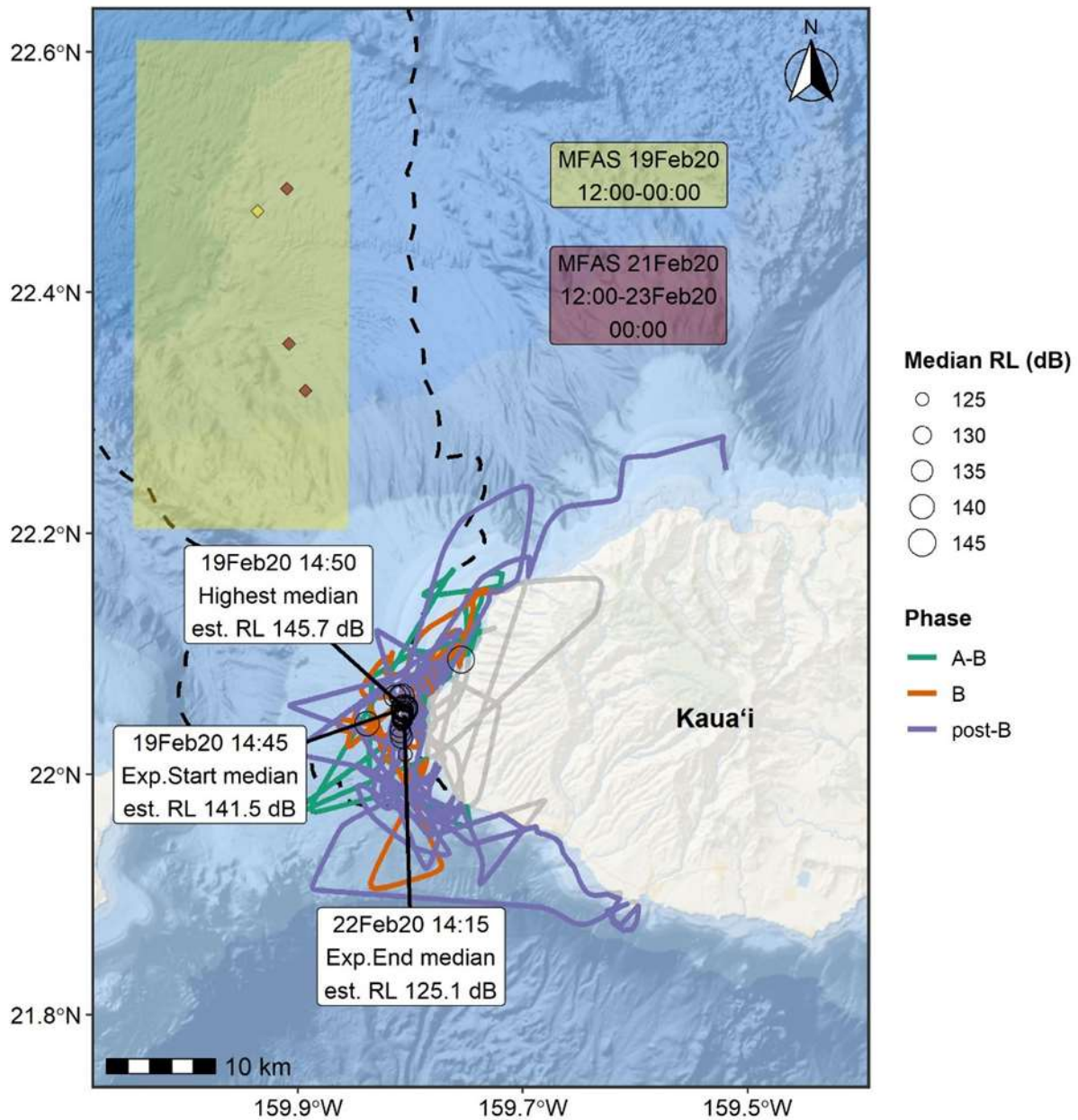
Figure 3.3.2-4. Movements of TtTag034 during the February 2020 SCC. Crawl tracks are colored by phase; see text for description of phases. Gray-shaded tracks show the original crawl track prior to re-routing around land. Median estimated RLs (RL) are plotted as open circles, with the size of the circle scaled to RL level. The shaded box represents area of ship activity for the time period specified, and corresponding colored diamond represents the mean ship location for that time period. The three dark red mean ship position points (red diamonds) correspond to mean positions at 12-hour intervals over that time period. All ship activity boxes for the red-shaded time period fit within the yellow-shaded activity box, and thus, are not plotted. The dashed black line represents the PMRF boundary.
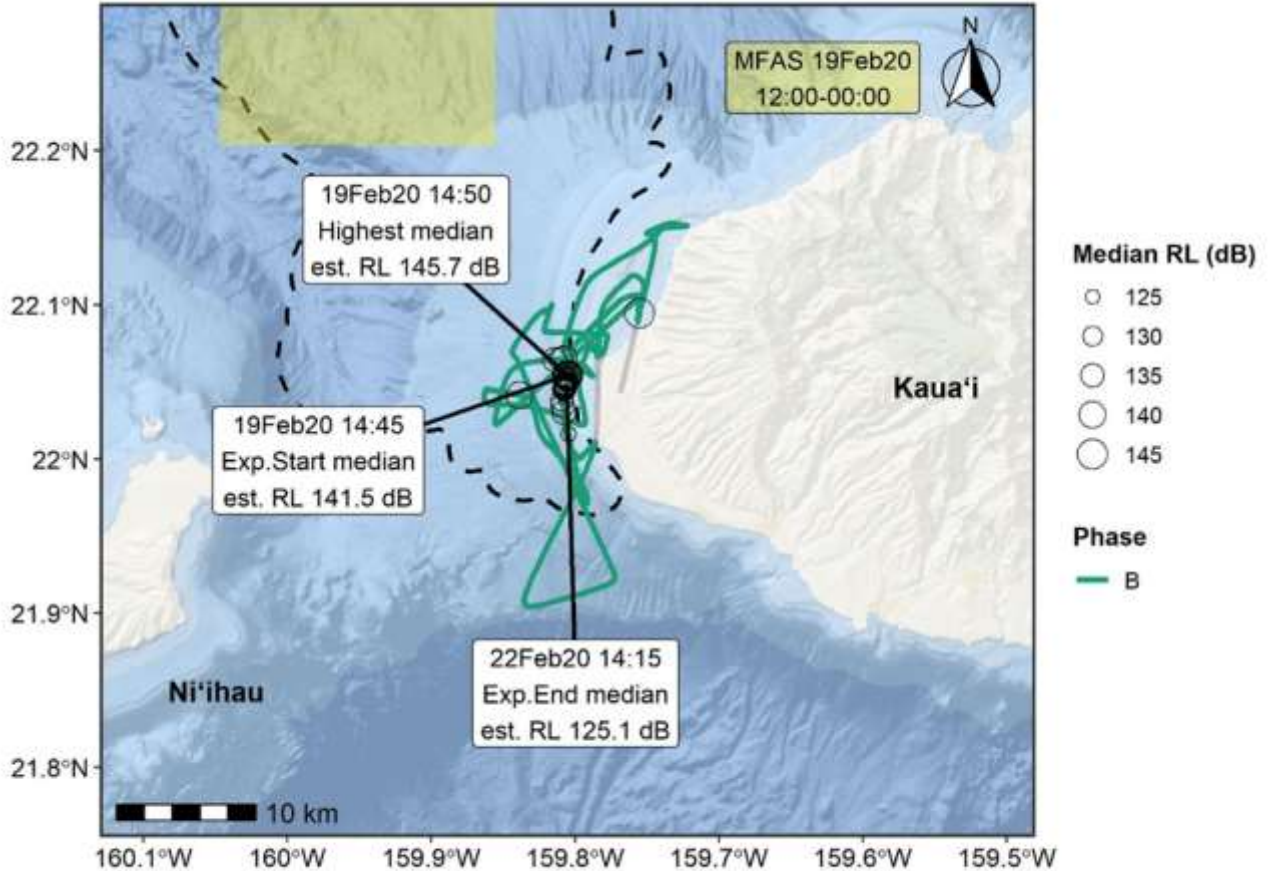
Figure 3.3.2-5. Movements of TtTag034 during Phase B of the February 2020 SCC. Gray-shaded tracks show the original crawl track prior to re-routing around land. Median estimated RLs (RL) are plotted as open circles, with the size of the circle scaled to RL level. The shaded box represents the southernmost area of ship activity for the time period specified (see Figure 3.3.2-4 for more details on ship activity areas). The dashed black line represents the PMRF boundary.
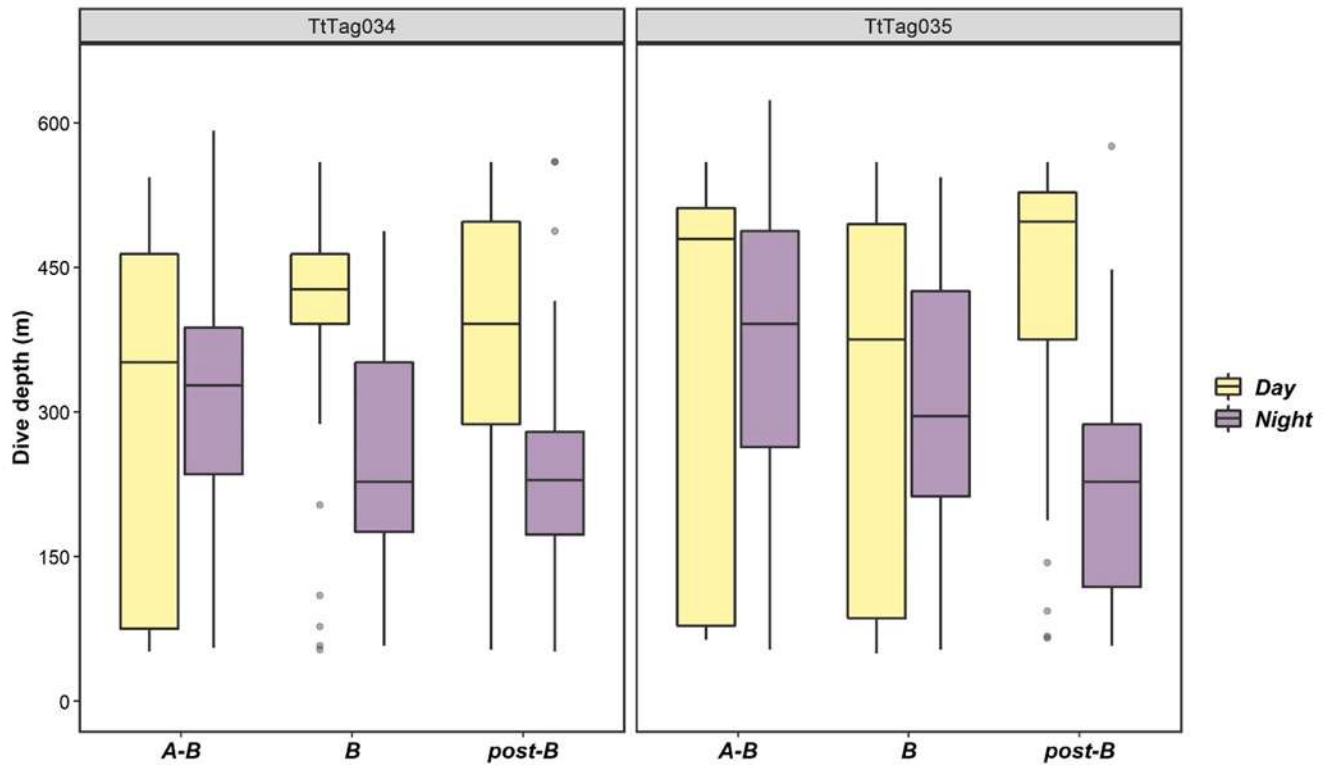
Figure 3.3.2-6. Distribution of dive depths by exposure/SCC phase by day/night, for both bottlenose dolphins tagged during the February 2020 SCC. Lower and upper hinges correspond to the first and third quartiles (25th and 75th percentiles) and the upper and lower whiskers extend from the hinges to +/- 1.5*IQR (interquartile range), respectively. The horizontal line within each box represents the median value, and outliers are shown as gray points.
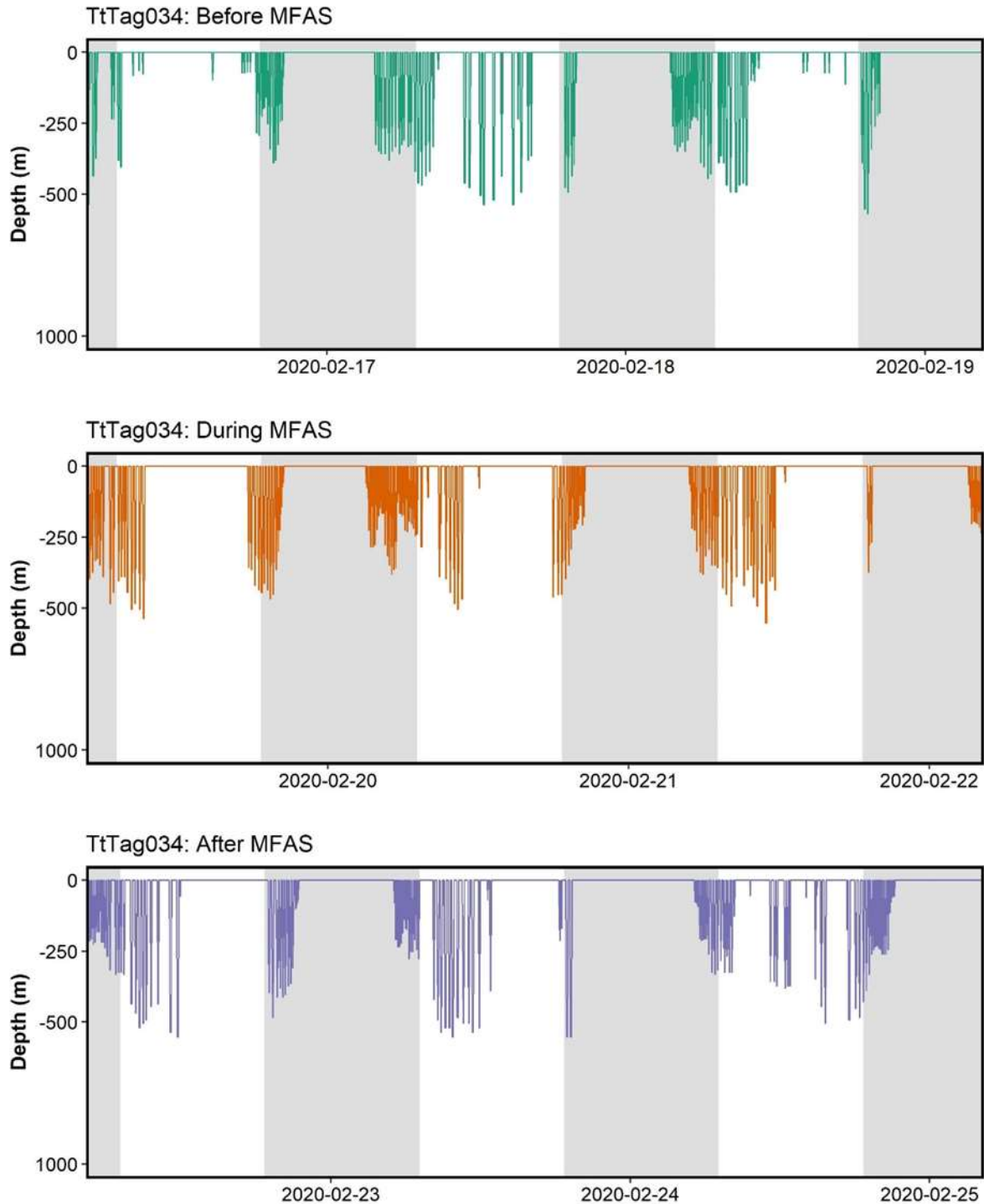
Figure 3.3.2-7. Dive profiles of TtTag034 for the three-day periods before (top, green), during (middle, orange), and after (bottom, purple) the presence of MFAS during the 2020 SCC at PMRF. Note that periods of time where the animal appears to be at the surface may include vertical excursions up to 49 m that were not recorded as dives on the tag.
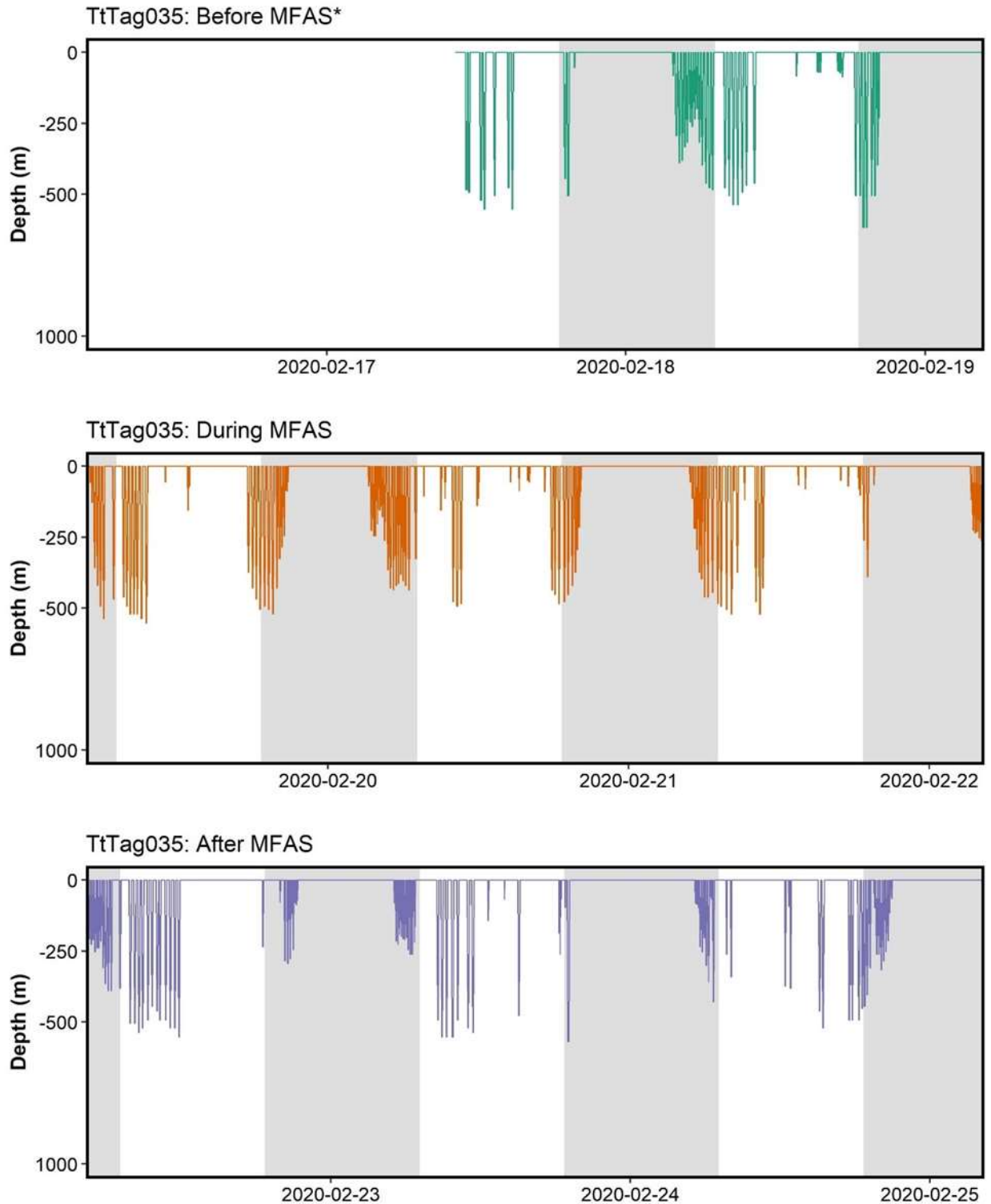
Figure 3.3.2-8. Dive profiles of TtTag035 for the three-day periods before (top, green), during (middle, orange), and after (bottom, purple) the presence of MFAS during the 2020 SCC at PMRF. Note that periods of time where the animal appears to be at the surface may include vertical excursions up to 49 m that were not recorded as dives on the tag.

4 DISCUSSION

The data presented here provide detailed quantitative measurements of behavior, MFAS exposure conditions, and associated probable responses (or lack thereof) in a relatively large number of tagged cetaceans of multiple species on and around PMRF in Hawai'i. These data, particularly for short-finned pilot whales, build on existing samples and are approaching sufficient sample sizes with which to evaluate exposure risk functions for incidentally exposed free-ranging protected species. The results are directly relevant, with an increased degree of resolution, to understanding typical MFAS exposure conditions and responses for protected species in these important habitat areas, as well as identifying those conditions associated with the onset of certain types of behavioral response and those in which no overtly observable responses (with the resolution of the tag sensors utilized) occur.

4.1 UPDATED METHODOLOGIES

The analytical and visualization methods applied here represent a substantial progression in complexity, precision, and data integration from earlier related efforts. Previous analyses from satellite-transmitting tags deployed on odontocetes in Hawai'i (Baird et al., 2014; 2017; 2019b) estimated received noise conditions using increasingly complex methods, though within a 2-D spatial framework. Propagation models were run from estimated point source positions within relatively large regions for Argos location errors to fixed categorical depths based on species-typical "shallow" or "deep" diving conditions. These approaches initially yielded a single point estimate and then many estimated RLs along a specified 2D radial, with which a range and distribution was applied as the approximate exposure 'level.' While this provided some insightful observations, it was clearly recognized that animals move in and are exposed to sonar in three-dimensional space. Also, by limiting estimates of exposure to the infrequent Argos locations, RL estimates could be temporally decoupled from those locations by up to an hour and so occasionally did not provide an accurate assessment of the RLs in time or space.

Additional methods were needed, some of which considered and adapted conceptual aspects of approaches developed in other U.S. Navy monitoring projects (Schick et al., 2019), to begin to apply more sophisticated 3D geospatial methods of incorporating Argos error and other information from satellite-transmitting tags. These new methods allowed us to better predict animal locations (and thus calculate RLs) in three-dimensional space in combination with actual dive data from tagged animals to inform depth selection within that space. A new method that deviates from Schick et al. (2019) was utilized to systematically sample the 3D volume representing the animal's location uncertainty by using multiple azimuthal 2D radials from the source location instead of 100 imputed samples of possible animal locations. The animal's potential x-y locations utilized the 95% CI error ellipses with tag data guiding potential depth locations. While 95% CI error ellipses were utilized for this analysis, other CI's (e.g., 99%) could also be utilized. This method was pursued given the fact that the propagation model has to process from the source to the location of the animal, but when utilizing imputed locations, only the results of the propagation model for the one x-y location at the animal's imputed position, over depth, are utilized. Given the challenges in processing of hundreds to thousands of exposures, utilizing the new method also increases execution speed relative to performing one model run for each of the 100 imputed locations for each exposure. Further, since the RL estimates derived from both methods were very similar, we were confident that the resulting RLs used in this analysis could still be directly compared to the results from the Schick et al. (2019) analysis or other researchers using that method.

Here we applied these enhanced methods to provide a substantially higher spatial and temporal resolution on estimated received noise conditions to evaluate not only recently tagged animals, but also most of the Cascadia-led tag deployments in Hawaii preceding SCC training events between February 2014 and February 2020 (nine pilot whales, four rough-toothed dolphins, and two bottlenose dolphins). The resulting RL estimates occur in higher temporal resolution (5-min intervals) with much greater associated spatial resolution and statistical assessment of associated error, thus providing a better characterization of the actual exposure of individual animals. Additionally, fitting Argos data to a movement model (i.e., *crawl*) based on available spatial error provides a probabilistic basis for possible animal locations that directly considers uncertainty at known points along the track. Finally, by integrating measurements of dive data, we can restrict the possible animal location within a 'cylinder' of three-dimensional space to something more akin to a three-dimensional disk. All of these progressions provide what is strongly believed to be a more precise representation of the range of possible RL conditions for animals moving dynamically in 3D space, with the acknowledgement and in fact direct application of information on possible positional error in the estimation of possible RL conditions. By obtaining a range of possible values and selecting a median estimate with statistical descriptions of variance, we have estimated RLs and possible associated error with far greater confidence and comparability between exposure events than in previous analyses.

It is vital to understand the propagation model results. Propagation models are utilized to effectively provide estimated TLs with long-range propagation and real-world variations in bathymetry and environmental conditions (i.e., range dependent propagation). This effort has highlighted a few cases where the 3D estimated RLs are not Gaussian distributed, which creates challenges in properly conveying the results (e.g., sources located within the animals 95% CI error ellipse with the heavy tail on the right side of the distribution of estimated RLs, and cases with strong multi-modal distributions of the estimated RLs). Other situations also occurred as a result of using this propagation model; for example, we found the modeled RLs close to the seafloor were real, but due to the way the propagation model conducts finer resolution analysis the results were provided in a lower resolution, leading to the modeled RLs near the seafloor often having unrealistically low estimated RLs. Other conditions of complex propagation modeling included the source being located north of the Kaulakahi Channel with the animals to the south. The propagation model interacts with the bathymetry going from deep to shallow (in some cases with only 9 m, or one bin, of depth, available, when a tagged animal was south of Kaua'i), then from shallow back to deep with the animal well south of the channel. The model provided some very limited transmission over the channel, however the model results ended up with estimated RLs values as low as -100 to -200 dB re 1μPa. Understanding these nuances is important, rather than simply removing propagation modeled results below some arbitrary threshold as we have done in the past.

4.2 BROAD-SCALE BEHAVIORAL RESPONSE ASSESSMENT

Our earlier reports (Baird et al. 2014; 2017; 2019b) demonstrated systematic and novel progress in quantifying aspects of exposure and behavioral response to operational MFAS on and around PMRF. However, the systematic and substantial improvement of data integration and modeling methods represented here and applied to both new and previous tags represent major steps forward in the complexity and robustness of describing these important U.S. Pacific Fleet monitoring objectives. Across all species and tagged individuals, with increasing precision in terms of movement, diving, and estimated

RL, we have not observed overtly-evident, strong avoidance responses to the presence of MFAS or other sounds associated with Navy training activity. Subjects have continued to utilize transit and foraging habitat on and around PMRF, including what would be audible exposure conditions during and following known operations. Some species studied here are quite variable in their baseline behavior (e.g., pilot whales), making detection of individual responses, especially on the fine-scales studied with other tag sensors in dedicated behavioral responses, to MFAS more challenging. Some also exhibited discrete diurnal patterns (see discussion of bottlenose dolphins below), which must be considered within the context of interpreting, for instance, changes in diving behavior. Despite these considerations, which are particularly relevant in terms of fine-scale, change-point kinds of response analyses, perhaps the most notable overarching aspect of the results to date now considered with uniform methods across years and species is the relative lack of overt responses such as habitat abandonment. This does not mean that more subtle individual responses such as changes in dive depth and duration may not occur in some individuals (e.g., GmTag081, GmTag231, GmTag152, see Table 3.3.2) or that there may not be some associated non-behavioral concerns regarding intense or repeated exposures (see 4.3 below), but as an overall observation, the absence of habitat abandonment across multiple species is notable in terms of monitoring broad impacts.

It may be tempting to classify the sharp turn by GmTag083 near the onset of MFAS that led to their maximum (median) RL of 176.6 dB re 1 µPa as a behavioral response, and similarly the reversal in travel direction by GmTag115 when they received their maximum (median) RL of 157.5 re 1 µPa. However, one of the benefits of analyzing a dataset of this size is the ability to look at the aggregated movement data of all tagged animals, and sharp changes in direction of travel were observed in the data across individuals of all three species during periods without MFAS or other Navy training activity. Moving forward it may also be beneficial to examine similar movement patterns (e.g., sharp directional changes) from deployments on these species occurring outside of SCC events off Kaua'i and other island areas in Hawai'i, for which substantial sample sizes exist for some species (e.g., short-finned pilot whales). Further, many of the animals remain on or near the range and receive moderate RLs during Phase B. That is not to say those specific changes in direction are not in fact behavioral responses to MFAS, just that an examination of all data can put those movements into a larger context for a behaviorally ephemeral species. Perhaps prey aggregations are a stronger driver of where these animals are located than MFAS, even at moderate to high levels of MFAS exposure. A quantitative version of that is the Mahalanobis distance method, where all data are aggregated, and then anything that occurs outside of the "normal" range of that data is considered significant, and in the case of behavioral response studies is often indicative of a behavioral response (e.g., Antunes et al., 2014). While a similar quantitative method has not yet been developed for satellite tag data (although see Hewitt et al. 2021), methods are being developed, and we hope to apply them to these data to determine whether those changes in direction of travel or other changes in movement behavior might be a behavioral response.

Similarly, although most of the animals that had depth data had significant changes to either their day- or night-time dives, or both, across the different periods of the SCCs, none of those changes seemed to relate only to the presence of MFAS. In fact, several of the changes seem to correspond instead to the lunar cycle and the shift in lunar illumination over the course of the SCC. For example, while GmTag231 was exposed to relatively high median RL estimates during Phase B and there were significant changes in night-time dive depths among the exposure periods (Table 3.3.2), it should also be noted that moon illuminated fraction decreased over GmTag231's deployment period (from third quarter to new moon;

moon illuminated fraction before Phase A = 0.99; 3 days after Phase B = 0.026), such that we would expect to see a decrease in night-time dive depth and duration over time (Owen et al. 2019). This may have contributed to the statistical differences in night-time dive behavior between MFAS use (Phase B) and non-MFAS use periods. Likewise, the moon illuminated fraction increased over the deployments of GmTag153 and GmTag154, and thus we would expect night-time dive depths and durations to increase over time (Owen et al. 2019). Both individuals had increased median night-time dive depths over the exposure phases, but only GmTag152 had increased dive durations (Table 3.3.2). Similar patterns were observed for the rough-toothed and bottlenose dolphins as well. While the variable patterns in dive behavior for SbTag017 and SbTag018 obscure our ability to make inference on dive/surfacing behavioral responses to MFAS use, it is also important to note that lunar phase changed over the duration of these individuals' deployments which could have played a role in their increasing night-time dive depths over the study period (Shaff & Baird, 2021). These results highlight the value of having a baseline understanding of the underlying processes infleuncing behavior when trying to interpret behavior in relation to MFAS.

Finally, the diel diving and surfacing patterns seen in TtTag034 and TtTag035 were generally consistent, although there may have been underlying drivers of variation in their diving behavior that are not well understood. For instance, in Figure 3.3.2-6, there appears to be a bimodal distribution of dive depths during the day that could reflect behavioral patterns at a finer temporal scale (e.g., dawn/day/dusk/night). Thus, variation in diving behavior among exposure periods for these two individuals may be a result of other ecological drivers and not necessarily that of exposure to MFAS. For bottlenose dolphins in Hawaii, potential lunar cycle influences on diving behavior have not been assessed. This species is regularly seen on PMRF and is relatively approachable for tagging, but their near-shore habits often result in Argos-generated locations appearing on land, which complicates both analyses of exposure and assessment of potential responses. Future assessments of this species to MFAS would benefit from the use of SPLASH10-F tags that generate Fastloc-GPS locations, which have much greater location accuracy compared to Argos locations. Of the three species considered here, bottlenose dolphins are the only one whose dive behavior is regularly bottom-limited, i.e., they are often in water where bottom depth is well within reach of their typical dive depths. As such, an assessment of potential changes in dive behavior in response to MFAS should take into account potential movements into or out of shallow water that might limit dive depths.

4.3 POTENTIAL FOR HIGH RECEIVED LEVELS

One of the more notable aspects of some of the exposure events evaluated here is the high RL conditions clearly predicted to have occurred, particularly for one group of pilot whales. For instance, estimated median RLs during multiple exposure events for pilot whales GmTag081, GmTag082, GmTag083 regularly exceed 160 dB re 1 µPa with some approaching 180 dB re 1 µPa. Considering the upper range of possible conditions (+ 2*SDs), some RLs may have exceeded 190 dB re 1 µPa. There is also low probability that these animals may have been exposed to SPLs over 200 dB re 1 µPa if they were located close to the sources when the source was within the animals 95% CI error ellipse. It is notable that these are SPL (rms) estimates of discrete exposures, the effective sound exposure levels (SEL: dB re 1 µPa^2-s) for individual (~1s) pings are identical but the cumulative SELs of multiple exposures which certainly existed would have, at the high end of the possible range, exceeded 200 dB SEL. While, as noted, these are based on upper estimates, even the median estimates, accumulated over multiple

exposures would result in cumulative sound exposure level (cSEL) values of 170-190 dB. The fact that these tagged whales did not exhibit obvious, large scale avoidance of areas up to or following these potentially near-source, high RL conditions are an important observation. Relative to the RLs in many MFAS controlled exposure experiments (see: Southall et al. 2016; 2019) and estimated incidental exposure events for other species (e.g., DeRuiter et al. 2013; Henderson et al. 2014; Moretti et al. 2014), these are among the highest estimated exposure RLs for free-ranging marine mammals exposed to MFAS ever documented. The apparent tolerance of such high RLs, at least for a small number of tagged whales, without overt avoidance responses may reflect a number of factors. A general tolerance of high-level exposures to a towed MFAS source has been observed in long-finned pilot whales (Globicephala melas) off Norway (Antunes et al. 2014). It is important to note that short-finned pilot whales, and all of the species studied here, may be regularly exposed to MFAS given its relatively regular use at PMRF and in surrounding areas. Individuals may simply be highly motivated to remain in important habitat areas for foraging, social, or other reasons, such that they tolerate high-, levels. Their motivations to remain in these areas with potential high-level exposures could be driven by underlying movement mechanisms that are poorly understood in these species. For example, spatial memory has recently gained attention as a prominent factor in shaping movement patterns of several terrestrial species and some marine megafauna (Fagan et al. 2013; Bracis & Mueller 2017; Merkle et al. 2014, 2019; Abrahms et al. 2019). Individuals may rely on their memory (e.g., past experience, positive attributes associated with geographical area) to inform their movement decisions (site fidelity or migration) rather than or in combination with responding to proximate environmental cues within their perceptual range, thus maximizing fitness (Fagan et al. 2013; Bracis & Mueller 2017; Merkle et al. 2014; Abrahms et al. 2019). A recent study also suggested that mule deer were more tolerant of anthropogenic disturbance while participating in memory-based movement behaviors (migration) compared to periods dominated by sensory-based behaviors (foraging) (Sawyer et al. 2020). While these studies primarily concern migratory species, considering the longevity and intellectual capacity of species like short-finned pilot whales, similar memory-based mechanisms likely play a role in where these animals decide to spend their time within their range and how they may perceive and respond to disturbances (Fagan et al. 2013; Wade et al. 2012). Alternately, recent work with captive false killer whales, bottlenose dolphins, beluga whales, and harbor porpoises has demonstrated that animals can self-mitigate the impacts of loud sounds by reducing their hearing sensitivity when a loud sound is preceded by a "warning" signal, and the loud sounds came at regular intervals (Nachtigall et al. 2016a, b; Nachtigall et al. 2018; Nachtigall and Supin 2014; Nachtigall and Supin 2015; Finneran 2018; Finneran 2020). Some bottlenose dolphins also self-mitigated noise impacts by turning their heads and reducing their hearing sensitivity to regularly spaced pile driving sounds without the warning sound (Finneran et al. 2015). However, these self-mitigation responses occurred in the presence of impact sounds, not tonal sounds; they occurred when these sounds were played at rhythmic intervals and the warning signals were temporally close to the loud sound; and they did not occur at the first few exposures of the sounds but were learned over repeated trials. It is possible that marine mammals resident to an area with frequent MFAS occurrence may learn to reduce their hearing sensitivity, but this ability has not yet been tested or demonstrated for tonal signals that have greater temporal separation than the repeated sounds in these studies. Furthermore, a reduction in hearing sensitivity would impact an animal's ability to detect the return echoes from their echolocation clicks and thereby interfere with foraging.

Behavioral responses in MFAS controlled exposure experiments (CEEs) or incidental exposure studies have been observed to occur at various exposure levels, but generally those well below what might begin to raise concern about potential temporary or permanent hearing loss. It is notable that the most current estimated marine mammal noise criteria onset levels for temporary threshold shift (TTS) and permanent threshold shift (PTS) for the group of cetaceans including pilot whales (high frequency cetaceans) for non-impulsive noise (including MFAS) are 178 and 198 dB SEL respectively[1] (Southall et al. 2019). Again, while the exact exposure RLs are unknown, it should be noted that multiple individuals evaluated here likely received MFAS exposures that approached or exceeded estimated TTS levels. The highest individual levels received, particularly if sustained over many minutes or hours could have even reached PTS levels. It should be further noted that such exposure conditions have the potential to result in other kinds of effects such as increases in physiological stress hormones (cortisol) that are not measurable using the tracking methods employed with tags (Thomas et al. 1990; Thomas and Geraci 1986; e.g. Romano et al. 2003). While the absence of overt behavioral responses of some individuals at these very potentially high estimated RLs may indicate a degree of tolerance to MFAS presence in these exposed areas, it does not necessarily mean that non-behavioral kinds of effects that may be of some concern are not occurring.

4.4 FUTURE WORK

This report summarizes an extensive amount of collaborative effort in developing, adapting, and applying much more sophisticated analytical and visualization methods to quantify exposure and evaluate behavioral responses of marine mammals in Hawaii to MFAS associated with Navy training on and around PMRF. While major progress has been made and data from tags spanning nearly a decade of effort analyzed with variable methods have now been evaluated with common and more sophisticated methods, future effort remains in a number of areas. First, three previously tagged pilot whales still need to be analyzed, along with three additional rough-toothed dolphins and one additional bottlenose dolphin, and tag data are also available for two melon-headed whales and one false killer whale exposed to MFAS during SCCs prior to 2021 (Baird et al. 2017, 2019b). During the August 2021 SCC additional tag data were obtained from two Blainville's beaked whales *(Mesoplodon densirostris)*, three melon-headed whales, two bottlenose dolphins, two rough-toothed dolphins, three short-finned pilot whales, and one false killer whale, that are also available for analysis (Cascadia Research Collective, unpublished). We would also note some interesting results from several other delphinid cetaceans, including bottlenose dolphins, from CEEs with simulated and operational helicopter-dipped MFAS sources from ongoing studies off California (Southall et al., 2021). While the context of these exposures differs in geographic location and operational parameter (e.g., number of sources, experimental control), their observations of relatively strong group responses to relatively low levels in these ongoing studies points to the need to sustain research on the responses of related species in other locations, even (or arguably especially) if initial indications in Hawaii suggest less clear response to MFAS.

We have also not yet extended the analysis to evaluate non-53C sonar systems, notably helicopter-dipping MFAS systems (e.g., AN/AQS-22) or active sonar sonobuoys (e.g., AN-SSQ systems), although these are sources that we plan to assess in the future. Furthermore, while we focused on the area of

---

[1] Note: while these are frequency-weighted values, the MFAS frequency range is near or within the flat part of the exposure function (see: Southall et al. 2019, Fig. 12), meaning these are near or at the effective TTS and PTS onset estimates.

activity during Phase B, a similar analysis of the animals' movement relative to the activity during Phase A should be conducted. While the above MFAS sources are not utilized during Phase A, there are other sources of sound associated with Navy training that the animals may respond to, as was observed for Blainville's beaked whales (Henderson et al. 2019; Jacobson et al. 2019) and minke whales (*Balaenoptera acutorostrata*; Harris et al. 2019). Analyses of baseline diving behavior and movement patterns of species other than rough-toothed dolphins and short-finned pilot whales that have or can be used in MFAS exposure analyses (e.g., bottlenose dolphins, melon-headed whales, false killer whales, Blainville's beaked whales) could also be undertaken using existing Cascadia Research Collective datasets. A better understanding of baseline movement and dive behaviors is essential when contextualizing potential responses to anthropogenic activity, as evidenced by the abrupt changes in direction of travel by animals in this study both during and outside of MFAS. Finally, the RL data should also be calculated as SELs and cSELs over each MFAS period, as these metrics are becoming more frequently reported and may even be a more salient metric against which to measure behavioral responses than SPL (e.g. Isojunno et al. 2020).

It should be noted that while these tagging efforts were not designed as an explicit behavioral response study to evaluate fine-scale individual responses in controlled conditions, they provide novel insight with increased resolution and precision to exposure and response to MFAS in realistic training conditions. While additional samples are likely needed for some species (rough-toothed, bottlenose dolphins), given the additional methods here and recent and ongoing advances in statistical methods to identify behavioral change-points in time series data from these kinds of tags, we are confident that sufficient data for at least pilot whales exist to develop a response paper utilizing emerging methods (e.g., being developed in the ONR-funded Double Mocha efforts) considering response probabilities at variable RLs (e.g., behavioral risk function). It is notable that the data and analytical methods applied here include the kinds of 3D geospatial and behaviorally-explicit time series data required for cutting edge behavioral response detection methods such as behavioral state-switching analyses (e.g., Hidden Markov Models) being developed and applied in other contexts using satellite-telemetered data. Finally, sustained field effort strategically directed to increase tag sample sizes for various species or other observation methods (e.g., unmanned aerial systems) for other species on or near PMRF should be continued. These efforts should perhaps be augmented by physiological tissue sampling before and after MFAS events, as possible, to evaluate non-behavioral effects. Such evaluations, in combination with ongoing efforts to continue to better understand and monitor populations of protected species, will allow increasing assessment of the more challenging consequence of MFAS exposure questions specified as an overall goal of the U.S. Navy's monitoring program.

5 REFERENCES

Abrahms, B., E.L. Hazen, E.O. Aikens, M.S. Savoca, J.A. Goldbogen, S.J. Bograd, M.G. Jacox, L.M. Irvine, D.M. Palacios, and B.R. Mate. 2019. Memory and resource tracking drive blue whale migrations. Proceedings of the National Academy of Sciences 116(12):5582-5587.

Albertson, G.R., R.W. Baird, M. Oremus, M.M. Poole, K.K. Martien and C.S. Baker. 2016. Staying close to home? Genetic differentiation of rough-toothed dolphins near oceanic islands in the central Pacific Ocean. Conservation Genetics doi: 10.1007/s10592-016-0880-z.

Antunes, R., P.H., Kvadsheim, F.P.A., Lam, P.L., Tyack, L., Thomas, P.J. Wensveen, and P.J.O., Miller. 2014. High thresholds for avoidance of sonar by free-ranging long-finned pilot whales (Globicephala melas). Marine pollution bulletin, 83(1), pp.165-180.

Baird, R.W. 2016. The lives of Hawai'i's dolphins and whales: natural history and conservation. University of Hawai'i Press, Honolulu, Hawai'i.

Baird, R.W., D.J. McSweeney, D.L. Webster, A.M. Gorgone and A.D. Ligon. 2003a. Studies of odontocete population structure in Hawaiian waters: results of a survey through the main Hawaiian Islands in May and June 2003. Report prepared under Contract No. AB133F-02-CN-0106 from the National Oceanic and Atmospheric Administration, Western Administrative Support Center, 7600 Sand Point Way N.E., Seattle, WA 98115 USA

Baird, R.W., D.J. McSweeney, M.R. Heithaus and G.J. Marshall. 2003b. Short-finned pilot whale diving behavior: deep feeders and day-time socialites. In Abstracts of the 15th Biennial Conference on the Biology of Marine Mammals, Greensboro, NC, December 2003.

Baird, R.W., G.S. Schorr, D.L. Webster, D.J. McSweeney, M.B. Hanson, and R.D. Andrews. 2008a. Multi-species cetacean satellite tagging to examine movements in relation to the 2008 Rim-of-the-Pacific (RIMPAC) naval exercise. A quick look report on the results of tagging efforts undertaken under Order No. D1000115 from the Woods Hole Oceanographic Institution.

Baird, R.W., D.L. Webster, S.D. Mahaffy, D.J. McSweeney, G.S. Schorr and A.D. Ligon. 2008b. Site fidelity and association patterns in a deep-water dolphin: rough-toothed dolphins (*Steno bredanensis*) in the Hawaiian Archipelago. Marine Mammal Science 24:535-553.

Baird, R.W., A.M. Gorgone, D.J. McSweeney, A.D. Ligon, M.H. Deakos, D.L. Webster, G.S. Schorr, K.K. Martien, D.R. Salden, and S.D. Mahaffy. 2009. Population structure of island-associated dolphins: evidence from photo-identification of common bottlenose dolphins (*Tursiops truncatus*) in the main Hawaiian Islands. Marine Mammal Science 25:251-274.

Baird, R.W., G.S. Schorr, D.L. Webster, D.J. McSweeney, M.B. Hanson, and R.D. Andrews. 2010. Movements and habitat use of satellite-tagged false killer whales around the main Hawaiian Islands. Endangered Species Research 10:107-121.

Baird, R.W., D.L. Webster, J.M. Aschettino, G.S. Schorr and D.J. McSweeney. 2013. Odontocete cetaceans around the main Hawaiian Islands: habitat use and relative abundance from small-boat sighting surveys. Aquatic Mammals 39:253-269.

Baird, R.W., S.W. Martin, D.L. Webster, and B.L. Southall. 2014. Assessment of modeled received sound pressure levels and movements of satellite-tagged odontocetes exposed to mid-frequency active sonar at the Pacific Missile Range Facility: February 2011 through February 2013. Prepared for U.S. Pacific Fleet, submitted to NAVFAC PAC by HDR Environmental, Operations and Construction, Inc.

Baird, R.W., S.W. Martin, R. Manzano-Roth, D.L. Webster, and B.L. Southall. 2017. Assessing exposure and response of three species of odontocetes to mid-frequency active sonar during Submarine Commanders Courses at the Pacific Missile Range Facility: August 2013 through February 2015. Prepared for U.S. Pacific Fleet, submitted to NAVFAC PAC by HDR Environmental, Operations and Construction, Inc., Honolulu, Hawai'i.

Baird, R.W., Webster, D.L., Jarvis, S.M., Henderson, E.E., Watwood, S.L., Mahaffy, S.D., Guenther, B.D., Lerma, J.K., Cornforth, C.J., Vanderzee, A.W., and D.B. Anderson. 2019a. Odontocete studies on the Pacific Missile Range Facility in August 2018: satellite-tagging, photo-identification, and passive acoustic monitoring. Prepared for Commander, Pacific Fleet, under Contract No. N62470-15-D-8006 Task Order 6274218F0107 issued to HDR Inc., Honolulu, HI.

Baird, R.W., Henderson, E.E., Martin, S.W., and B.L. Southall. 2019b. Assessing odontocete exposure and response to mid-frequency active sonar during Submarine Command Courses at the Pacific Missile Range Facility: 2016-2018. Prepared for Commander, Pacific Fleet, under Contract No. N62470-15-D-8006 Task Order KB16 issued to HDR, Inc., Honolulu, HI.

Booth, C. G., Donovan, C., Plunkett, R. & J. Harwood. 2014. Using an interim pcod protocol to assess the effects of disturbance associated with US Navy exercises on marine mammal populations: Interim report. Report code smrum–onr–004. Submitted to the Office of Naval Research - Marine Mammal & Biology Program, February 2016.

Boyd J.D., Brightsmith, D.J. 2013. Error Properties of Argos Satellite Telemetry Locations Using Least Squares and Kalman Filtering. PLoS ONE 8(5) doi:10.1371/journal.pone.0063051

Bracis, C., and T. Mueller. 2017. Memory, not just perception, plays an important role in terrestrial mammalian migration. Proceedings of the Royal Society B: Biological Sciences 284:20170449.

Bryant, E. 2007. 2D location accuracy statistics for Fastloc RCores Running Firmware Versions 2.2 & 2.3. Otley, West Yorkshire. United Kingdom: Wildtrack Telemetry Systems Ltd. 1-5pp.

Cioffi, W.R. 2020. Parsegonio: Parse Argos Goniometer log data and convert to prv. R code version 0.1.0. https://github.com/williamcioffi/parsegonio. https://doi.org/10.5281/zenodo.3647697

Cox, T.M., T.J. Ragen, A.J. Read, E. Vos, R.W. Baird, K. Balcomb, J. Barlow, J. Caldwell, T. Cranford, L. Crum, A. D'Amico, G. D'Spain, A. Fernandez, J. Finneran, R. Gentry, W. Gerth, F. Gulland, J. Hildebrand, D. Houser, T. Hullar, P.D. Jepson, D. Ketten, C.D. Macleod, P. Miller, S. Moore, D.C. Moutain, D. Palka, P. Ponganis, S. Rommelo, T. Rowles, B. Taylor, P. Tyack, D. Wartzok, R. Gisiner, J. Meads, and L. Benner. 2006. Understanding the impacts of anthropogenic sound on beaked whales. Journal of Cetacean Research and Management 7(3):177–187.

D'Spain, G. L., D'Amico, A. & Fromm, D. M. 2006. Properties of the underwater sound fields during some well documented beaked whale mass stranding events. Journal of Cetacean Research and Management, 7, 223–238.

Douglas, D.C., Weinzierl, R., Davidson, S.C., Kays, R., Wikelski, M., and G. Bohrer. 2012. Moderating Argos location errors in animal tracking data. Methods in Ecology and Evolution 6:999-1007.

Dujon, A.M., Lindstrom, R.T., and G.C. Hays. 2014. The accuracy of Fastloc-GPS locations and implications for animal tracking. Methods in Ecology and Evolution 5:1162-1169.

Durbach, I., Harris, C., Helble, T.A., Henderson, E. E., Ierley, G., Thomas, L., and S. W. Martin. 2021. Changes in the movement and calling behavior of minke whales (*Balaenoptera acutorostrata*) in response to navy training. Frontiers in Marine Science 8:880.

Fagan, W.F., M.A. Lewis, J. Auger-Méthé, T. Avgar, S. Benhamou, G. Breed, L. LaDage, U.E. Schlägel, W. Tang, Y.P., Papastamatiou, J. Forester, and T. Mueller. 2013. Spatial memory and animal movement. Ecology Letters 16:1316-1329.

Falcone, E.A., Schorr, G.S., Watwood, S.L. DeRuiter, S.L., Zerbini, A.N., Andrews, R.D., Morrissey, R.P., & Moretti, D.J. 2017. Diving behaviour of Cuvier's beaked whales exposed to two types of military sonar. Royal Society Open Science 4:170629.

Filadelfo, R. J., Michlovich, E. S., Wolfanger, J. S. & D'amico, A. 2005. Sonar use and beaked-whale strandings. Arlington, VA: The CNA Corporation.

Finneran, J.J., Schlundt, C.E., Branstetter, B.K., Trickey, J.S., Bowman, V. and Jenkins, K., 2015. Effects of multiple impulses from a seismic air gun on bottlenose dolphin hearing and behavior. The Journal of the Acoustical Society of America, 137(4), pp.1634-1646.

Finneran 2018. Conditioned attenuation of auditory brainstem responses in dolphins warned of an intense noise exposure: Temporal and spectral patterns. The Journal of the Acoustical Society of America. 143: 795-810.

Finneran 2020. Conditioned attenuation of dolphin monaural and binaural auditory evoked potentials after preferential stimulation of one ear. The Journal of the Acoustical Society of America. 147: 2302-2313.

Harris, C. M., Martin, S. W., Martin, C., Helble, T. A., Henderson, E. E., Paxton, C. G. M. & Thomas, L. 2019. Changes in the spatial distribution of acoustically derived minke whale (*Balaenoptera acutorostrata*) tracks in response to navy training. Aquatic Mammals, 45, 661-674.

Hazel, J. 2009. Evaluation of fast-acquisition GPS in stationary tests and fine-scale tracking of green turTLs. Journal of Experimental Marine Biology and Ecology 374:54-68.

Henderson, E. E., Aschettino, J., Deakos, M., Alongi, G. & Leota, T. 2019. Quantifying the behavior of humpback whales (megaptera novaeangliae) and potential responses to sonar. Aquatic Mammals, 45, 612–631.

Henderson, E. E., Aschettino, J., Deakos, M., Alongi, G. and T. Leota. 2019. Blainville's beaked whales reduced foraging dives prior to the onset of hull-mounted MFAS sonar during Navy training

events. 5th International Conference on Effects of Aquatic Noise on Marine Life, Den Haag, 7-12 July 2019.

Hewitt, J., Schick, R.S. & Gelfand, A.E. Continuous-Time Discrete-State Modeling for Deep Whale Dives. JABES 26, 180–199 (2021). https://doi.org/10.1007/s13253-020-00422-2

Hooten, M.B., Johnson, D.S., McClintock, B.T. and J.M. Morales. 2017. Animal movement: Statistical models for telemetry data. Boca Raton, FL: CRC Press

Isojunno, S., Wensveen, P.J., Lam, F.P.A., Kvadsheim, P.H., von Benda-Beckmann, A.M., López, L.M.M., Kleivane, L., Siegal, E.M. and Miller, P.J., 2020. When the noise goes on: received sound energy predicts sperm whale responses to both intermittent and continuous navy sonar. *Journal of Experimental Biology*, *223*(7).

Jacobson, E.K., Henderson, E.E., Oedekoven, C.S., Miller, D.L., Watwood, S.L., Moretti, D.J., and Thomas, L. 2019. Quantifying the response of Blainville's beaked whales to Naval sonar exercises in Hawaii. World Marine Mammal Conference, Barcelona, 9-12 December 2019.

Jeanniard-du-Dot, T., K. Holland, G.S. Schorr, and D. Vo. 2017. Motes enhance data recovery from satellite-relayed biologgers and can facilitate collaborative research into marine habitat utilization. Animal Biotelemetry 5:17 doi:10.1186/s40317-017-0132-0

Johnson, D.S., J.M. London, M.-A. Lea, and J.W. Durban. 2008. Continuous-time correlated random walk model for animal telemetry data. Ecology 89:1208-1215 doi:10.1890/07-1032.1

Johnson, D.S., and J.M. London. 2018. Crawl: An R package for fitting continuous-time correlated random walk models to animal movement data. Zenodo doi:10.5281/zenodo.596464

Kranstauber, B., A. Cameron, R. Weinzierl, T. Fountain, S. Tilak, M. Wikelski, and R. Kays. 2011. The Movebank data model for animal tracking. Environmental Modelling & Software 26(6):834-835 doi:10.1016/j.envsoft.2010.12.005

Lopez, R., J.P. Malardé, P. Danès, and P. Gaspar. 2015. Improving Argos Doppler location using multiple-model smoothing. Animal Biotelemetry 3(32) doi:10.1186/s40317-015-0073-4

Lowther, A.D., C. Lydersen, M.A. Fedak, P. Lovell, and K.M. Kovacs. 2015. The Argos-CLS Kalman Filter: Error structures and state-space modelling relative to Fastloc GPS data. PLoS ONE 10(4):e0124754 doi:10.1371/journal.pone.0124754

Manzano-Roth, R., Henderson, E. E., Martin, S. W., Martin, C. & Matsuyama, B. M. 2016. Impacts of u.S. Navy training events on Blainville's beaked whale (*Mesoplodon densirostris*) foraging dives in Hawaiian waters. Aquatic Mammals, 42, 507–518.

Martin, S. W., Martin, C. R., Matsuyama, B. M. & Henderson, E. E. 2015. Minke whales (*Balaenoptera acutorostrata*) respond to navy training. The Journal of the Acoustical Society of America, 137, 2533–2541.

McClintock, B.T., J.M. London, M.F. Cameron, and P.L. Boveng. 2014. Modelling animal movement using the Argos satellite telemetry location error ellipse. Methods in Ecology and Evolution 6:266-277 doi:10.1111/2041-210X.12311

Merkle, J.A., D. Fortin, and J.M. Morales. 2014. A memory-based foraging tactic reveals an adaptive mechanism for restricted space use. Ecology Letters 17(8):924-031.

Merkle, J.A., H. Sawyer, K.L. Monteith, S.P.H. Dwinnel, G.L. Fralick, and M.J. Kauffman. 2019. Spatial memory shapes migration and its benefits: evidence from a large herbivore. Ecology Letters 22:1797-1805.

Nachtigall, P.E. and Supin, A.Y., 2014. Conditioned hearing sensitivity reduction in a bottlenose dolphin (*Tursiops truncatus*). Journal of Experimental Biology, 217(15):2806-2813.

Nachtigall, P.E. & Supin, A. 2015 Conditioned frequency dependent hearing sensitivity reduction in the bottlenose dolphin (*Tursiops truncatus*) Journal of Experimental Biology, 218: 999 -1005

Nachtigall, P.E., Supin, A.Y., Estaban, J.A. and Pacini, A.F., 2016. Learning and extinction of conditioned hearing sensation change in the beluga whale (*Delphinapterus leucas*). Journal of Comparative Physiology A, 202(2): 105-113.

Nachtigall, P.E., Supin, A.Y., Smith, A.B. and Pacini, A.F., 2016. Expectancy and conditioned hearing levels in the bottlenose dolphin (*Tursiops truncatus*). Journal of Experimental Biology, 219(6): 844-850.

Nachtigall, P.E., Supin, A.Y., Pacini, A.F. and Kastelein, R.A., 2018. Four odontocete species change hearing levels when warned of impending loud sound. Integrative zoology, 13(2)160-165.Owen, K., R.D. Andrews, R.W. Baird, G.S. Schorr, and D.L. Webster. 2019. Lunar cycles influence the diving behavior and habitat use of short-finned pilot whales around the main Hawaiian Islands. Marine Ecology Progress Series doi:10.3354/meps13123

Quick, N.J., Cioffi, W.R., Shearer, J., & Read, A.J. 2019. Mind the gap – optimizing satellite tag settings for time series analysis of foraging dives in Cuvier's beaked whales (*Ziphius cavirostris*). Animal Biotelemetry 7:5.

R Core Team. 2020. R: A language and environment for statistical computing. R Foundation for Statistical Computing, Vienna, Austria. https://www.R-project.org/

Romano, T. A., Keogh, M. J., Kelly, C., Feng, P., Berk, L., Schlundt, C. E., Carder, D. A., & Finneran, J. J. (2004). Anthropogenic sound and marine mammal health: Measures of the nervous and immune systems before and after intense sound exposure. Canadian Journal of Fisheries and Aquatic Sciences, 61, 1124-1134.

Sawyer, H., M.S. Lambert, and J.A. Merkle. 2020. Migratory disturbance thresholds with mule deer and energy development. The Journal of Wildlife Management 84(5):930-937. Schick, R.S., M. Bowers, S. DeRuiter, A. Friedlaender, J. Joseph, T. Margolina, D.P. Nowacek, and B.L. Southall. 2019. Accounting for positional uncertainty when modeling RLs for tagged cetaceans exposed to sonar. Aquatic Mammals 45:675-690 doi:10.1578/AM.45.6.2019.675

Schorr, G.S., R.W. Baird, M.B. Hanson, D.L. Webster, D.J. McSweeny, and R.D. Andrews. 2009. Movements of satellite-tagged Blainville's beaked whales off the island of Hawaiʻi. Endangered Species Research 10:203-213.

Shaff, J.F. and R.W. Baird. 2021. Diel and lunar variation in diving behavior of rough-toothed dolphins (*Steno bredanensis*) off Kauaʻi, Hawaiʻi. Marine Mammal Science 1(16) doi:10.1111/mms.12811

Southall, B.L. 2021. Behavioral and Physiological Response Studies (BPRS) with Social Delphinid Cetaceans Using Operational and Simulated Military Mid-Frequency Active Sonar. ONR annual report, N000014-19-1-2572.

Thomas, J. A., Kastelein, R. A., & Awbrey, F. T. (1990). Behavior and blood catecholamines of captive belugas during playbacks of noise from an oil drilling platform. Zoo Biology, 9, 393-402.

Thomson, C.A., and Geraci, J.R. 1986. Cortisol, aldosterone, and leucocytes in the stress response of bottlenose dolphins, Tursiops truncatus. Can. J. Fish. Aquat. Sci. 43: 1010–1016.

Wade, P.R., R.R. Reeves, and S.L. Mesnick. 2012. Social and behavioural factors in cetacean responses to overexploitation: are odontocetes less "resilient" than mysticetes? Journal of Marine Biology 15:567276.

Witt, M.J., S. Åkesson, A.C. Broderick, M.S. Coyne, J. Ellick, A. Formia, G.C. Hays, P. Luschi, S. Stroud, and B.J. Godley. 2010. Assessing accuracy and utility of satellite-tracking data using Argos-linked Fastloc-GPS. Animal Behavior 80:571-581 doi:10.1016/j.anbehav.2010.05.022

Back Page

NIWC Pacific
San Diego, CA 92152-5001